CONTRIBUTIONS OF SIGNAL TRANSDUCER AND ACTIVATOR OF TRANSCRIPTION 3 TO TUMOR AND IMMUNE CELL FUNCTIONS IN BREAST CANCER

A Dissertation
SUBMITTED TO THE FACULTY OF
UNIVERSITY OF MINNESOTA
BY

PAVLINA DECHKOVA CHUNTOVA

IN PARTIAL FULFILLMENT OF THE REQUIREMENTS
FOR THE DEGREE OF
DOCTOR OF PHILOSOPHY

Under the Advisement of Dr. Kathryn L. (Kaylee) Schwertfeger

October 2016

Acknowledgements

The completion of my thesis work would not have been possible without the support and encouragement of many people who have been there for me, both personally and professionally.

First of all, I would like to thank Kaylee. For the past 6 years, she has been an amazing mentor. She has taught me to persevere through the frustrations and setbacks of science experiments and always try to learn more, reexamine my assumptions, and consider the context of my data. I have learnt how important it is to be able to communicate the value of our results and how finding the story one's data tells can be labor-intensive but very gratifying at the end. Throughout all my years in her lab, I was excited to run into her office and show her new interesting data, and I never doubted that if I asked her advice on an experiment that did not work, our conversation would end with me feeling encouraged and re-energized. Kaylee has always shared in my successes, whether it was great-looking western blots or a notice of a granted award. I am so grateful for all of her patience and leadership, and I hope to be able to pay it forward one day.

The Schwertfeger lab was a fantastic environment to train in, not just only because of Kaylee's mentorship, but also because it has brought together an amazing group of young scientists. Nick Brady – my partner in so many crimes – was my rock throughout graduate school, and I am so thankful for all the science help, fun time at conferences, agreeing to join me as a student rep, all the life advice, and endless explanations of pop-culture references. I can't wait to see the many great things he'll achieve throughout his career, and I am happy and proud to have shared a lab with him. Dr. Laura Bohrer was another member of the lab who has been indispensable in my

growth as a scientist and in my personal life as a friend. Her intelligence, her calm, and her kindness helped me weather many storms – both in the lab and at home, and I am very grateful for her continued friendship and support. Drs. Johanna Reed and Lindsey Bade also helped me tremendously when I first joined the lab, and I appreciate them sharing their knowledge and experience with me. As the lab has evolved throughout the years, I was fortunate enough to be able to learn from and help train many other Schwertfeger lab members – Dr. Mariya Farooqui, TJ Beadnell, Sarah Kemp, Thomas Chaffee, Kelly Aukes, Ally Fuher and Christina Lindemann have all contributed significantly in a number of experiments and have shared in successes and failures during lab lunches at Surly. A special thank you to the three women who are currently in the lab – Patrice Witschen, Emily Irey, and Dr. Chelsea Lassiter – who helped me so much throughout the past year. We have spent so many hours helping each other in lab, but we have also painted in bars, played sports together, and enjoyed numerous dinner parties. Without their support and encouragement, I would not have made it to the finish line.

Next, I would like to thank all the faculty who helped guide me throughout the years. Dr. Devavani Chatterjea who first showed me how challenging, fun, and gratifying science research can be. Dr. Deepali Sachdev who was always around to answer my questions, share a laugh, or give me a late night ride home. And all the members of my thesis committee – Dr. Scott Dehm, Dr, Michael Farrar, and Dr. Tim Starr – who provided welcomed feedback and expertise on my project.

I also would like to thank the many people in my life who did not sign up to get a science degree, but deserve at least partial credit for mine as they spent endless hours listening to my practice talks, mournful stories of failed experiments, and excited babbling of successful data collection. Katie Tholkes, Michaela McDonald, Anna Waugh,

Syreeta Wilkins, and Rebecca Godar formed the core of our Macalester alumni group and kept me sane (and were often responsible for feeding me and reminding me to take care of myself in the midst of long, long science experiments). Julie Storck and the rest of the Grace Trinity gang accepted me and supported me unquestioningly despite my constant tardiness and sometimes foul moods, and cheered me on as I worked on grants, papers, and presentations. I am so grateful for having them in my life.

In addition, I want to extend my gratitude to the people who may not have been here in person, but who made me feel like I always had someone in my corner who believed in me – Amelia Mueller, Lilly Georgieva, and Lilly Andonova cheered me on from afar, reminded me what mattered and why I was doing this, and made me believe that some friendships really do last a lifetime.

Finally, I would like to thank the two families who welcomed me into their homes and into their lives and who often acted as my surrogate parents in moments when I needed them the most. Greg and Cathy Tholkes shared so many amazing meals and game nights, and I am so grateful for their welcoming home. And finally, Mati and Nikolay Platikanovi, who attended all of my school graduations, helped me through numerous dorm and house moves, offered help and advice when needed, and provided a much needed and comforting link to home. I will be eternally grateful to them for all their care and support.

Dedication

I would like to dedicate the work presented here to my parents, Tanya and Dechko, who despite our occasional differences in opinion, have always been there for me and encouraged me to be the best version of myself.

Table of Contents

List of Tables

List of Figures

List of Abbreviations

4-MU.....4-methylumbelliferone

ADAM17.....a disintegrin and metalloprotease domain 17

AFF3..... AF4/FMR2 Family Member 3

Arg1..... Arginase I

Bcl2..... B cell leukemia/lymphoma 2

BMDM.....bone marrow-derived macrophages

BrdU..... 5-bromo-2'-deoxyuridine

Ccl2.....C-C motif chemokine ligand 2

Ccl5.....C-C motif chemokine ligand 5

Cox.....cyclooxygenase-2

Csf1.....colony-stimulating factor 1

Csf1r.....colony-stimulating factor 1 receptor

CX3CL1.....C-X3-C motif chemokine ligand 3

CXCL3.....C-X-C motif chemokine ligand 3

DCIS.....ductal carcinoma *in situ*

ECM.....extracellular matrix

EGF.....epidermal growth factor

ER.....estrogen receptor

FFPE..... formalin-fixed paraffin embedded

FGFR..... fibroblast growth factor receptor

FLT-3.....FMS-like tyrosine kinase 3

FRS2..... fibroblast growth factor receptor substrate 2

gp130..... glycoprotein 130

GRB2..... growth factor receptor bound 2

HA..... hyaluronan

HAS2..... hyaluronan synthase 2

HER2..... human epidermal growth factor receptor 2

HIF-1α ..... hypoxia-inducible factor 1 α

HMW ..... high molecular weight

HR.....hormone receptor

i.p. ..... intraperitoneal

IDC..... invasive ductal carcinoma

IFNγ ..... interferon gamma

IFP .....interstitial fluid pressure

IHC .....immunohistochemistry

IL-10 .....interleukin 10

IL-12 .....interleukin 12

IL-13 .....interleukin 13

IL-1β .....interleukin 1 beta

IL-4 ..... interleukin 4

IL-6 ..... interleukin 6

JAK ..... janus kinase

K8 ..... keratin 8

K14 ..... keratin 14

LIF .....leukemia inhibitory factor

LMW .....low molecular weight

LPS .....lipopolysaccharide

LyzM .....lyzozyme

MAPK .....mitogen-activated protein kinase

MDSCs ..... myeloid-derived suppressor cells

MEFs ..... mouse embryonic fibroblasts

MHCII .....major histocompatibility complex II

MMPs .....matrix metalloproteinases

MMTV-PyMT ..... mouse mammary tumor virus – polyoma middle T

Mrc1 .....mannose receptor 1, type C

NK cells .....natural killer cells

Nos2 .....nitric oxide synthase 2

NT ..... non-targeting

pCR .....pathological complete response

PD-L1 .....programmed death ligand 1

PDA .....pancreatic ductal carcinoma

PDGFR ..... placental-derived growth factor receptor

PI3K ..... phosphatidylinositol 3-kinase

PR ..... progesterone receptor

RHAMM ..... receptor for hyaluronan-mediated motility

SH2 .....Src-holomogy 2

SNPs .....single nucleotide polymorphisms

STAT .....signal transducer and activator of transcription

TAMs .....tumor-associated macrophages

TGFβ .....transforming growth factor beta

Th1 .....T-helper 1

Th2 .....T-helper 2

TICs ..... tumor initiating cells

TILs .....tumor infiltrating lymphocytes

TKIs ..... tyrosine kinase inhibitors

TMA ..... tissue microarray

TNBC .....triple negative breast cancer

VEGF ..... vascular endothelial growth factor

Chapter 1. Introduction

A. Breast Cancer Overview

Despite significantly improved methods of detection and treatment, breast cancer morbidity and mortality remains a substantial health and economic burden among American women. It is estimated that 246,000 women will be diagnosed with breast cancer, and 40,000 patients will die of the disease in 2016 [1]. A significant challenge in the treatment of breast cancer is the molecular heterogeneity exhibited among patients and within individual tumors. The estrogen receptor (ER), progesterone receptor (PR), and human epidermal growth factor receptor 2 (HER2) are the three biological markers that have been used for the clinical diagnosis and treatment of patients [2]. Tumors that stain positive for ER/PR expression are targeted with endocrine therapies, which utilize ER antagonists or inhibitors to the enzyme responsible for estrogen synthesis, aromatase [3]. Amplification of the *HER2* gene, on the other hand, renders tumors susceptible to treatment with monoclonal antibodies and small molecule kinase inhibitors targeting the overexpressed HER2 protein [4]. Tumors that do not fall into the previous two categories are classified as triple negative (TN), and their treatment relies heavily on surgery and chemotherapy [5]. The prognoses and overall survival of ER^+/PR^+ and $HER2^+$ breast cancer patients have improved significantly as endocrine and targeted therapies have advanced, whereas TNBC outcomes have been slower to improve due to the lack of therapeutically defined targets and the aggressive nature of this subtype [2]. Further analyses of tumor tissues have revealed greater subtype heterogeneity among patient populations. Molecular profiling using next-generation sequencing has expanded

the classification of breast tumors describing four major molecular subtypes: Luminal A and B, defined largely by the expression of ER-target genes, the ERBB2$^+$ subtype, largely overlapping with the previously described HER2$^+$ subtype, and the basal subtype, defined by the expression of basal-cellular molecules (such as basal cytokeratins) and representing the most heterogeneous population [6-9]. These subtypes are believed to represent the major intrinsic drivers of breast cancer. However, additional (extrinsic) factors, such as the tumor microenvironment (reviewed later), contribute extensively to the evolution of breast tumors. As a result, breast cancer classification and treatment presents an ongoing challenge in need of further study.

B. FGFR Signaling Contributes to Breast Cancer Development

One signaling pathway that has been implicated in the pathogenesis of all histological subtypes is the fibroblast growth factor receptor (FGFR) pathway. FGFRs represent a family of four membrane-bound tyrosine kinase receptors, which are able to interact with 22 structurally similar FGF ligands to regulate a wide range of cellular functions such as cell proliferation, survival, migration, and differentiation [10]. Aberrant FGFR signaling has been observed in multiple tumor types including prostate, endometrial, and breast cancer [11-14]. Amplification of the genomic locus containing *FGFR1* has been reported in about 10% of human breast tumor samples and has been correlated with early disease relapse and poor overall survival of ER$^+$ breast patients [15-17]. In a 2010 study, Turner and colleagues evaluated two breast cancer cohorts for *FGFR1* copy number variations and FGFR1 expression. The authors reported a strong correlation between *FGFR1* amplification and mRNA overexpression in both patient

series [17]. The same study demonstrated that *FGFR1* amplification is required for anchorage-independent growth of human breast cancer cells that harbor *FGFR1* amplification, and that overexpression of FGFR1 leads to increased ligand-dependent and ligand–independent signaling [17]. Furthermore, Turner *et al.* suggested that *FGFR1* amplification may lead to resistance to endocrine therapy *in vitro* through increased activated mitogen-activated protein kinase (MAPK) activation and production of downstream proliferative signals [17]. In addition to *FGFR1* amplification, a recent study by Wu and colleagues reported a novel interchromosomal in-frame fusion between *FGFR2* and the transcription factor *AF4//FMR2 family member 3* (*AFF3*) in a patient with metastatic breast cancer [18]. This genomic fusion, which was validated by quantitative reverse-transcription polymerase chain reaction (qRT-PCR), retained the *FGFR* tyrosine kinase domains, suggesting that the resulting product can participate in FGF-induced downstream signaling [18]; however, additional studies will need to determine the oncogenic potential of this genomic rearrangement. Fusions involving other *FGFR* members in breast cancer have not been reported, nonetheless, studies examining rare chromosomal aberrations across multiple tumor types are ongoing. These experiments will contribute to the expanding catalogue of targetable genomic alterations that have been linked to breast cancer development.

In addition to genomic abnormalities of FGF receptors, dysregulated FGFR signaling has been observed due to increased expression of FGF ligands, particularly within the TNBC subtype [19, 20]. In a panel of 31 breast cancer cell lines, Sharpe *et al.* demonstrated increased sensitivity of a subset of TNBC cell lines to the selective FGFR inhibitor PD173074 [20]. The authors found increased expression of the ligand FGF2 among cell lines and breast cancer tissue samples belonging to the basal-like subset of TNBC [20]. Inhibition of FGF2 signaling via siRNA or neutralizing antibody inhibited cell

growth *in vitro*, and treatment of xenograft tumors derived from a basal-like cell line with PD173074 substantially reduced tumor growth [20]. These data suggest that FGFR signaling contributes to breast tumorigenesis even in the absence of *FGFR* genomic alterations. Further studies by our lab and others have confirmed the ability of increased FGFR1 signaling to transform mammary epithelial cells through activation of downstream effectors such as protein kinase B (AKT) and MAPK [21-24]. In addition, we and others have shown that FGFR signaling can lead to tumorigenic alterations of the extracellular environment, such as production of matrix metalloproteinases (MMPs), chemokines, cytokines, and extracellular matrix (ECM) components [24-28]. Together, these findings demonstrate the pivotal role of FGFR signaling in breast cancer development.

C. Targeting FGFR activation in the clinical setting

The results of studies such as those outlined above have led to the initiation of clinical trials exploring the safety and efficacy of FGFR inhibition in solid tumors, including breast cancer. The two main classes of drugs in clinical development include non-selective and selective inhibitors. Non-selective FGFR tyrosine kinases inhibitors (TKIs) have shown activity against FGFRs, but also against most commonly vascular endothelial growth factor receptors (VEGFRs), placental derived growth factor receptor (PDGFR), Fms-like tyrosine kinase receptor 3 (FLT-3), and other related tyrosine receptor kinases. TKI258 (i.e. dovitinib) is the most clinically advanced TKI. In a phase II trial of breast cancer patients with metastatic disease, patients were stratified based on *FGFR1* amplification and hormone receptor (HR) status. Among the 81 enrolled patients, greatest treatment benefit was observed among the *FGFR1*$^{+}$/HR+ group, where 25% of

patients had unconfirmed partial response or stable disease at 24 weeks or longer [29]. Dovitinib was tolerated reasonably well in this cohort of heavily pre-treated patients, however there were still severe grade 3 side effects such as gastrointestinal toxicity, liver toxicity, and fatigue, which are common TKI-associated events [29]. Based on this study's results and the previously discussed preclinical data by Turner *et al.* demonstrating FGFR contributions to endocrine resistance, a new phase II clinical trial has been initiated investigating the effects of dovitinib in combination with the ER antagonist fulvestrant (ClinicalTrials.gov, NCT01528345).

In order to avoid adverse effects associated with TKI treatment, selective FGFR inhibitors have also been developed. In a phase I study of the pan-FGFR inhibitor BGJ398 as a single agent in solid tumors, a breast cancer patient with *FGFR1* amplification demonstrated reduction in tumor volume [30]. Adverse events in this study were considered "FGFR-specific" with hyperphosphatemia being the most common [30]. The results of these studies indicate that certain patient populations harboring alterations in *FGFR1* genomic locus or increased FGFs expression will benefit from FGFR-targeted therapies. Careful examination of possible cooperating genetic mutations and changes in the tumor microenvironment will likely increase the chance of success of these therapies. An example of such combination therapy is the phase I trial testing BGJ398 in combination with BYL719, a PI3K inhibitor, which is recruiting breast cancer patients with metastatic disease positive for *FGFR1-3* alterations and *PIK3CA* mutations (ClinicalTrials.gov NCT01928459).

D. FGFR1 Signaling Induces Activation of STAT3

FGFR1 activation regulates numerous signaling pathways and promotes epithelial cell survival, proliferation, and migration [23]. The FGF-FGFR interaction is specified by a variety of mechanisms such as tissue-restricted expression of both FGFs and FGFRs and the formation of an extracellular complex between FGFRs and heparan sulfate proteoglycans (HSPGs), which stabilizes the ligand-receptor interaction [31]. Upon ligand binding, FGFR undergoes dimerization that allows for the autotransphosphorylation of multiple intracellular tyrosine residues (Figure 1.1). These phosphorylated tyrosines provide docking sites for several adapter proteins such as fibroblast growth factor receptor substrate 2 (FRS2) and growth factor receptor-bound 2 (GRB2), which in turn become phosphorylated and commence a signaling cascade that converges on the MAPK and AKT [14, 31, 32]. FGFR activation results in altered gene transcription that affects key cellular processes involved in tumorigenesis, such as cell survival, proliferation, and migration. As a result, in healthy tissues FGFR activation is tightly controlled by receptor internalization and activity of negative regulators such as the Sprouty (Sprty) proteins and the “similar expression to FGF” (SEF) family members [32]. In the context of cancer, ligand and/or receptor overexpression, as well as ligand-independent signaling, override the negative regulation signals and lead to disease.

Our lab and others have reported the ability of FGF ligands to induce expression of various pro-inflammatory molecules, such as interleukin-1β (IL-1β), cyclooxygenase-2 (Cox-2) and chemokine (C-X3-C) ligand 1 (CX3CL1) [26, 27, 33, 34]. As shown in Chapter 2 of this thesis, among the list of FGFR1-induced cytokines is the interleukin-6 (IL-6) family of cytokines. IL-6 is a pro-inflammatory cytokine with well-defined tumorigenic properties [35]. Early studies in breast cancer show a correlation between

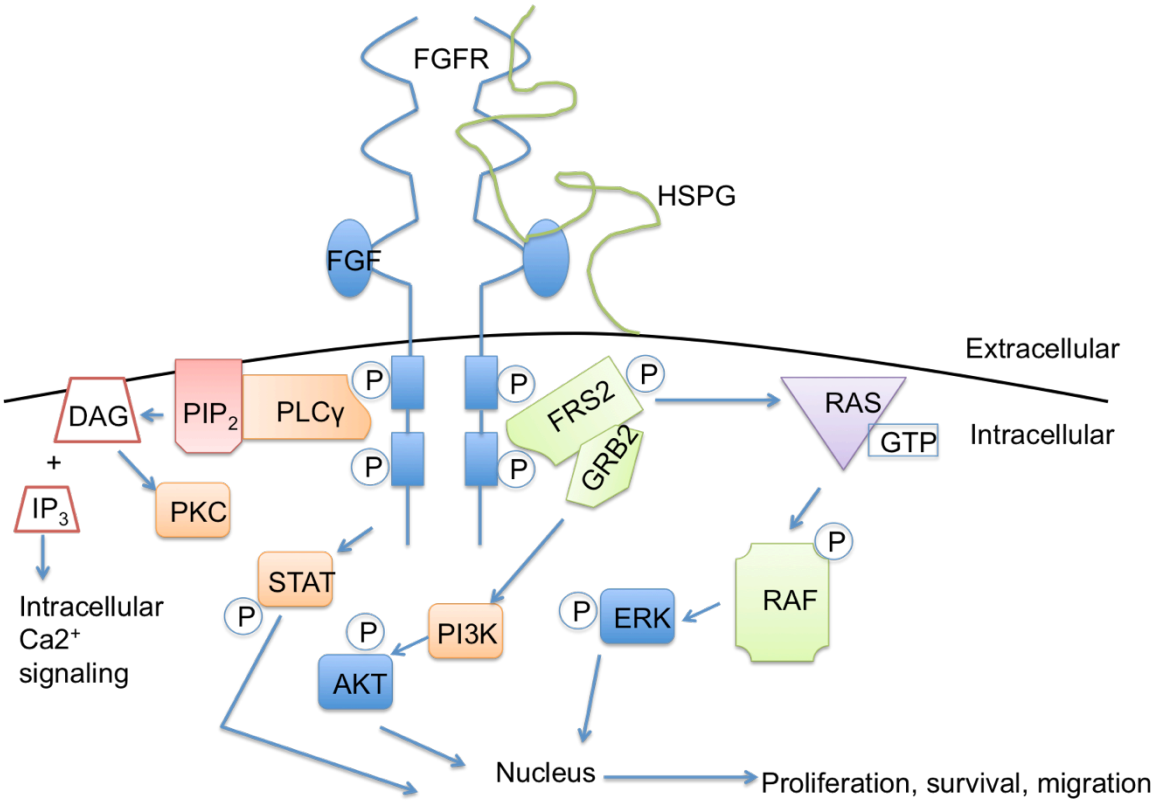

Figure 1.1. FGFR structure and downstream signaling FGFR signaling occurs as a result of a fibroblast growth factor (FGF) binding to a monomeric FGF receptor (FGFR), leading to receptor dimerization and stabilization of the dimer by HSPGs. Dimerization is followed by receptor transautophosphorylation and activation of its kinase domain. The scaffolding proteins FRS2 and GRB2 are then recruited to the receptor's intracellular domain and act to initiate the downstream signaling cascade leading to the activation of RAS GTPase and PLCγ (among others). Together, these act to initiate ERK and AKT signaling, resulting in the cell's increased survival and proliferation, as well as increased migration and invasion potential. HPSG, heparan sulfate proteoglycans; FRS2, fibroblast receptor substrate-2; GBR2, growth factor receptor-bound-2; PI3K, phosphoinositide 3-kinase; PIP2, phosphatidylinositol 4,5-bisphosphate; IP_3, inositol 1,4,5-triphosphate; DAG, diacylglycerol; PKC, protein kinase C; PLCγ = phospholipase C-γ; STAT, signal transducer and activator of transcription [14].

IL-6 serum levels and poor patient prognosis [36, 37]. IL-6 family member receptors are heterodimeric transmembrane molecules that are associated with intracellular Janus kinases (JAKs). Upon ligand binding, receptor –associated JAKs are brought into proximity and thus able to phosphorylate each other and several receptor tyrosine residues [38]. This allows signal transducer and activator of transcription (STAT) molecules to be recruited to the receptor via their SH2-domains and in turn become phosphorylated by JAKs [39]. Phosphorylated STAT molecules are released from the cell surface receptor and are able to homo- and heterodimerize, which allows for nuclear translocation [38]. IL-6 signaling through the IL-6 receptor (IL-6R)/ glycoprotein 130 (gp130) heterodimeric receptor activates JAK1 and results in phosphorylation of STAT3, and to a lesser extent STAT1 [40]. Certain mellatoproteases such as ADAM10 and ADAM17 have been shown to cleave membrane-bound IL-6R (mbIL-6R) and produce soluble IL-6R (sIL-6R) [41]. sIL-6R binds IL-6 with the same affinity as mbIL-6R and can associate with gp130 on the surface of cells that do not normally express IL-6R. This process known as *trans*-signaling allows for amplification of the IL-6 signal as not many cell types express mbIL-6R but gp130 is ubiquitously expressed [42]. Where *classic*-signaling is required for the induction of systemic inflammatory responses, *trans*-signaling occurs mainly at the local site of inflammation [43]. IL-6 signaling in cancer cells has been shown to have pleiotropic effects such as increased cell proliferation, survival, migration, invasion, and altered metabolism, however the contributions of *trans*- versus *classic*-signaling pathways have not been determined [35, 44, 45]. Additionally, IL-6 signaling has been shown to promote tumor angiogenesis and matrix remodeling through increased expression of MMPs and hypoxia inducible factor-1α (HIF-1α) [46, 47]. These data provide strong evidence for the pro-tumor effect of IL-6 and its downstream effectors.

STAT3 is the primary STAT family member activated downstream of IL-6, and its transcriptional activity is cell specific. STAT3 signaling is critical for the maintenance of embryonic stem cells and is sufficient for their self-renewal [48]. However, in healthy mammary epithelium, STAT3 promotes apoptosis during gland involution [49]. In addition, evidence suggests that STAT3 is a potent oncogene, which can promote tumor initiation and support tumor progression [50, 51]. Studies have shown that STAT3 in tumor cells drives expression of genes, such as *Myc, Survivin* and *B-cell lymphoma 2 (Bcl2)*, which increase cell survival and proliferation rates [52, 53]. A recent study by Wei and colleagues showed STAT3 activation in a small critical subpopulation of cells within claudin-low breast cancer cell lines known as tumor-initiation cells (TICs) [54]. The limited dilution transplantation experiments done by Wei *et al.* demonstrated that cells, which were sorted by flow cytometry, containing activated STAT3 ($pSTAT3^{+}$) were consistently more efficient at initiating tumor growth than $pSTAT3^{-}$ cells or mock-sorted populations [54]. This study demonstrates that breast cancer cells with higher levels of STAT3 activity exhibit enhanced tumorigenic potential. We and others have observed activation of STAT3 in approximately 60% of breast tumors, and inhibition of STAT3 in mammary tumor models leads to reduced tumor cell proliferation and reduced tumor burden [28, 55]. Taken together, these studies suggest that STAT3 represents an attractive therapeutic target for breast cancer.

E. Prognostic significance of STAT3

Despite the strong evidence supporting the pro-tumorigenic properties of STAT3 and its downstream targets, its prognostic significance in human breast tumor cohorts

has shown an association of STAT3 overexpression/activation and favorable patient outcome [56-58]. In a study evaluating pSTAT3 presence in a cohort of 286 node-negative breast tumor samples by immunohistochemistry (IHC), Dolled-Filhart *et al.* found pSTAT3 to be a predictive marker for improved overall survival [57]. In a 2013 study, Sonnenblick *et al.* reported similar results in a group of patients with node-positive breast cancer [56]. One possible rationale for these inconsistent findings is the heterogeneity of cell types within human breast tumors and the varying levels of STAT3 activation among different cell types. IHC staining of breast tumor microarray samples often can not distinguish STAT3 staining within tumor epithelium and tumor stroma, making results and conclusions on its role as an oncogene or tumor suppressor difficult to interpret. This provides further rationale for the need to elucidate key downstream effects of STAT3 signaling in different cell types to be used in conjunction with pSTAT3 staining for the characterization of human breast tumors.

F. Breast cancer stroma and contributions of hyaluronan

Even though breast cancer initiates in the epithelial compartment of the breast, ample evidence suggests that the stromal compartment actively contributes to tumor development and progression [59-61]. As the initial neoplastic lesions progress from ductal carcinoma *in situ* (DCIS) to invasive ductal carcinoma (IDC), the transformed epithelial cells acquire the ability to invade through a layer of myoepithelial cells and the basement membrane they have secreted and continue to advance through a dense network of extracellular matrix (ECM) composed primarily of collagens and laminins. The ECM is produced and organized by myoepithelial cells and fibroblasts and acts to provide structural integrity and vital environmental signals to the epithelial cells lining the

mammary ducts. In recent years, studies have shown that the largest change in gene expression during the DCIS to IDC transition is within the stromal compartment, not the transformed epithelial cells, suggesting that the creation of reactive stroma is a pivotal step in early tumor progression [62]. The ECM can be remodeled by a variety of cell types including the tumor cell themselves. Transformed epithelial cells are known to secrete MMPs, which degrade ECM components and release factors driving tumor cell proliferation and migration [63]. Additional physical alterations such as collagen cross-linking by the enzyme lysyl oxidase have been shown to increase integrin and growth factor receptor signaling in tumor cells [64]. In a study by Levental *et al.* inhibition of lysyl oxidase in a mouse breast cancer model resulted in delayed tumor onset and lower tumor burden [64]. These studies point to the critical interactions between tumor cells and their surrounding stroma and the need to elucidate the downstream effects of these interactions throughout the different stages of tumorigenesis.

STAT3 signaling in epithelial cells drives production of molecules implicated in the remodeling of the tumor extracellular matrix [65]. *Hyaluronan synthase 2* (*Has2*) is a STAT3 target gene whose increased expression leads to production and accumulation of hyaluronan (HA) [65, 66]. HA is a major component of the ECM and is synthesized as both part of the normal wound healing response and during cancer development. HA is a glycosaminoglycan that binds cell surface receptors such as CD44 and Receptor for Hyaluronan-Mediated Motility (RHAMM), resulting in increased epithelial cell proliferation, migration, and survival [67, 68]. Numerous studies have implicated HA in regulating breast cancer growth and progression [69, 70]. As HA is produced and modified within the breast cancer microenvironment, its accumulation contributes to the development of a “cancerized” stroma [28, 71]. Detailed analysis of the patterns of HA accumulation within the stroma of breast cancer patients reveals an association between

high-level HA accumulation and poor patient survival [69]. Additional studies comparing HA staining in samples from patients with DCIS, DCIS with microinvasion, and invasive ductal carcinoma show higher HA expression in DCIS lesions associated with microinvasion than in samples of pure DCIS suggesting a link between HA and early progression of breast neoplasias [72]. Collectively, these data support the hypothesis that HA synthesis is an integral step in breast epithelial transformation and tumor progression.

G. Macrophages in the tumor microenvironment

Immunogenicity or the ability of a tumor to evoke a productive immune response has emerged as an important tumor characteristic due to the recent advances in cancer immunotherapy. Historically, breast cancer has not been seen as a highly immunogenic cancer due to studies reporting low numbers of tumor-infiltrating lymphocytes (TILs). For example, in a study of 2009 node-positive breast cancer patients, the median value of TILs was reported to be only 2% [73]. Nonetheless, different subtypes of breast cancer display different levels of immune infiltration, and those levels are predictive of patient outcome [74]. In a 2010 study, Denkert *et al.* showed that patients whose samples revealed high numbers of infiltrating lymphocytes responded significantly better to standard therapy with a pathological complete response rate (pCR) of 31% compared to general pCR of all patients of 12.8% [75]. This observation was expanded in the study by Loi and colleagues, which reported no correlation between quantity and location of TILs in ER+ or $HER2^{+}$ patients, however both intratumoral and stromal lymphocytic

infiltrates in TNBC samples were associated with reduced risk of relapse and death [73]. These data provide evidence for the interaction between tumor and immune cells, and its value in predicting patient outcome, suggesting that addition of immune parameters to the currently accepted methods of tumor characterization might be beneficial to patient care.

Innate immune cells, such as macrophages, represent a large portion of tumor immune infiltrates and these tumor-associated macrophages (TAMs) can also be predictive of patient outcome. Increased macrophage density in pre-treatment biopsies of breast cancer patients correlates with reduced recurrence-free and overall survival [76-78]. Therefore, efforts have focused on understanding the mechanisms through which macrophages contribute to breast cancer growth and progression. Early work by Lin and colleagues demonstrated significant delay in the development of metastasis in a transgenic breast tumor model lacking mature macrophages [79]. Later studies provided further evidence of the ability of TAMs to promote metastasis by visualizing the association between intravasating tumor cells and perivascular macrophages *in vivo* through 2-photon microscopy [80]. Wyckoff *et al.* demonstrated the existence of a paracrine loop between cancer cells and macrophages, where cancer cells secrete colony-stimulating factor 1 (CSF-1) that is necessary for the maturation of macrophages, and macrophages produce epidermal growth factor (EGF), which allows the tumor cells to migrate and intravasate [81]. In addition to EGF, TAMs have also been shown to produce VEGF-A and thus play a role in the initial formation of a high-density blood vessel network that is required for tumor progression, also known as the angiogenic switch [82]. In a study by Lin *et al.*, macrophage-depleted mice developed invasive tumors at the same rate as their wild-type controls only when VEGF-A was expressed in mammary epithelial cells through a transgene construct [83]. In more recent studies

using intravital imaging techniques, Lohela *et al.* demonstrated that prolonged depletion of myeloid-derived cells in a model of breast cancer resulted in delayed tumor growth, decreased angiogenesis, and fewer lung metastases [84]. These data strongly suggest that TAMs promote angiogenesis and tumor metastasis. Furthermore, TAMs are able to remodel the tumor ECM by producing proteinases such as cathepsins, which affect tumor cell response to therapy [85]. In a study of bone marrow derived macrophage (BMDM)-tumor cell co-cultures, Shree *et al.* demonstrated that tumor cells growing alone exhibited over three times higher rates of apoptosis after treatment with the chemotherapeutic agent Taxol than tumor cells in co-culture with BMDM. This effect was largely due to the production of cathepsins B and S by the BMDM [85]. *In vivo* treatment of mammary tumor-bearing mice combining Taxol and the cathepsin inhibitor JPM, significantly inhibited tumor growth [85]. Finally, numerous studies have provided evidence of TAM interacting with cells of the adaptive immune system, mainly $CD4^+$ and $CD8^+$ T lymphocytes. In a 2011 study by DeNardo and colleagues, transgenic mouse mammary tumor virus (MMTV)-polyoma middle T antigen (PyMT) mice were treated with a CSF-1R-signaling antagonist, which prevents generation of mature macrophages, in combination with the chemotherapy agent paclitaxel [86]. Mice receiving combination therapy had significantly smaller tumor burden at study endpoint, which was dependent on the recruitment of cytotoxic $CD8^+$ T cells [86]. Additional studies revealed that $CD4^+$ T cells, on the other hand, cooperated with TAMs to promote tumor progression [87]. Analyses of TAMs derived from *$CD4^{+/-}$/PyMT* and *$CD4^{-/-}$/PyMT* tumors demonstrated that TAMs differentiated in the absence of $CD4^+$ T cells expressed higher levels of pro-inflammatory molecules and lower levels of cytokines associated with immunosuppression suggesting a switch of the tumor microenvironment towards an anti-tumor immune response [87]. These studies demonstrate the ability of TAMs in breast

cancer to influence pro-tumorigenic pathways by contributing to tumor cell migration and invasion, angiogenesis, resistance to chemotherapy and suppression of adaptive immune responses [88-90].

H. Macrophage polarization

Once recruited to the tumor microenvironment, macrophages respond to the plethora of stimuli within the microenvironment and differentiate into various effector subsets. Numerous studies have focused on defining macrophage subsets within the tumor microenvironment. Currently, the most widely accepted classification of macrophage polarization is based on descriptions of classical (M1) versus alternative (M2) polarization, which were developed as a result of initial studies investigating macrophage responses to helper T cells 1 (Th1) and helper T cell 2 (Th2) derived molecules [91]. Classically activated macrophages develop in response to interferon-gamma (IFNγ) and pathogen-derived toll-like receptor ligands [92]. This response is characterized by the production of cytotoxic factors such as reactive oxygen species and nitric oxide, increased rates of phagocytosis and enhanced antigen presentation on the cell surface. Alternatively activated macrophages, on the other hand, develop as part of the wound healing program and as such are thought to antagonize inflammation. M2 macrophages are induced by the Th2 cytokines IL-4 and IL-13, as well as in response to IL-10, immunoglobulins, and glucocorticoids [93]. These cells, in turn, secrete factors that promote angiogenesis, upregulate expression of scavenging receptors, and produce enzymes to remodel the surrounding extracellular matrix.

Based on their functions within the tumor microenvironment, TAMs have been generally characterized as M2-like [94]. Several studies have demonstrated that TAMs express higher levels of scavenging receptors, angiogenic factors and proteases, similar to M2 macrophages. Furthermore, TAM polarization to the M2-like phenotype in the MMTV-PyMT model has been attributed to IL-4-producing Th2 cells within the tumor microenvironment [87]. However, there is evidence that macrophages exhibit different phenotypes during different stages of tumor initiation and progression. During early stages of transformation, recently recruited macrophages are exposed to a wide variety of pro-inflammatory signals derived from the epithelial cells and the surrounding stroma and often express M1-related factors that have pro-tumorigenic properties, such as IL-1β and IL-6 [44]. As a component of the pro-inflammatory response, production of reactive oxygen and nitrogen species could also potentially enhance the rate of epithelial cell mutation and thus accelerate tumorigenesis [95]. In established tumors, macrophages exhibit alternatively activated functions including the production of immunosuppressive factors, such as IL-10 and transforming growth factor β (TGFβ), which are capable of actively suppressing the anti-tumor immune response [87, 90]. These macrophages also produce growth factors and remodel the matrix, supporting tumor cell growth and enhancing invasion. Therefore, TAMs phenotypes are now thought to include a combination of markers typically assigned to the M1 and M2 phenotypes. Thus, as efforts are being made to “re-polarize” macrophages within the tumor microenvironment towards the M1/classically activated phenotype, care must be taken to ensure that the potentially pro-tumorigenic factors produced by these macrophages are suppressed.

Furthermore, detailed analyses of mammary tumor myeloid populations have revealed that individual tumors may contain several different subsets of macrophages that differ in their functions. Movahedi *et al*. reported the presence of two distinct TAM

populations in mammary TS/A tumors, distinguishable most easily by the level of major histocompatibility II (MHCII) expression on their surface, with one population expressing low levels ($MHCII^{lo}$) and the other expressing higher levels ($MHCII^{hi}$) [96]. $MHCII^{lo}$ macrophages were shown to reside mainly in hypoxic tumor regions and expressed markers associated with M2 polarization. The $MHCII^{hi}$ subset, however, expressed M1-signature genes such as *Cox2, Nos2* and *Il12*. These cells were shown to secrete pro-inflammatory cytokines and chemokines such as IL-6, CCL5 and CXCL3, which could in turn serve to further recruit additional pro-inflammatory cells to the tumor margins. However, both macrophage subsets were shown to be poor antigen presenting cells and were able to suppress T cell proliferation, indicating that both subsets might be capable of contributing to pro-tumor immunosuppression. In a recent study examining macrophage localization within human breast tumors, high levels of CD68 staining (a surface marker of human macrophage populations), within gaps of ductal tumor structures correlated with reduced lymph node metastasis [97]. Taken together, these data suggest that TAMs not only represent a macrophage population that is distinct from canonical M2 macrophages in the setting of infection, but there is also most likely a spectrum of TAMs whose phenotype and function depend on tumor type and location within the tumor.

I. STAT3 signaling in tumor-associated macrophages

As described earlier, IL-6 is an important factor secreted in the breast tumor microenvironment. Immune cells that infiltrate breast tumors are exposed to a variety of activating signals, including IL-6. Numerous studies have suggested that the IL-6/STAT3

pathway contribute to immune cell activation and function [98]. STAT3 has been implicated in the maturation and function of myeloid cells. Studies have linked constitutively activated STAT3 with a maturation block in dendritic cells and promotion of pro-tumor activities in myeloid cells. Initial observations by Nefedova *et al.* revealed that immature myeloid cells in the spleens of colon tumor-bearing mice exhibited substantially higher levels of STAT3 DNA-binding activity than those isolated from control mice [99]. In addition, lower rates of dendritic cell differentiation and maturation following exposure to STAT3-activating tumor cell conditioned media were observed *in vitro*. Further *in vivo* studies reported that hematopoietic STAT3 ablation led to increased activation of neutrophils and natural killer (NK) cells in tumor-bearing mice, as well as increased *ex vivo* T cell responses and decreased tumor formation in mice challenged with subcutaneous B16 (melanoma) tumor cells [100]. Evaluation of STAT3 activity in immature myeloid cells and TAMs from B16-bearing mice revealed upregulated expression of pro-angiogenic factors such as VEGF and FGF2 and were able to induce endothelial cell tube formation [101]. Further studies have attempted to perform a more targeted analysis of myeloid cell-specific STAT3 contributions to tumor growth. In a glioma mouse model STAT3 knockdown was achieved via intra-tumoral injection of STAT3-targeting siRNA, which disrupted STAT3 signaling in TAMs at a higher proportion than non-TAM cells and improved animal survival [102]. However, the studies described thus far make use of experimental systems that do not exclusively target tumor myeloid cells. The development of a mouse model that allows for conditional genetic deletion of STAT3 in myeloid cells has revealed the complexity of this signaling pathway and its contributions to tumor development. Deng *et al.* reported development of spontaneous colon tumors in $STAT3^{fl}$ *Csf1r-iCre* mice, establishing a role for macrophage STAT3 in protecting intestinal epithelial cells from the effects of excessive

inflammation [103]. Furthermore, a recent study by Kumar et al., demonstrated downregulation of STAT3 activity in both myeloid-derived suppressor cells (MDSCs) and macrophage populations in several tumor models [104]. Closer examination revealed that STAT3 downregulation was required for TAMs accumulation within mammary tumors, and expression of constitutively active myeloid STAT3 together with depletion of polymorphonuclear-MDSCs inhibited tumor growth [104]. These findings are consistent with data from a mouse medulloblastoma model where $STAT3^{fl}$*LyzM-cre* conditional deletion of myeloid STAT3 reversed the accumulation of granulocyte-MDSCs and enhanced the ratio of effector : regulatory T cells, but overall failed to affect tumor growth [105].

Collectively, these data point to the high degree of complexity observed in the regulation of tumor myeloid functions. The results reported in published studies are highly dependent on the experimental system being tested; however, all studies indicate that STAT3 activity is actively being modulated within the tumor myeloid compartment suggesting its pivotal role in sustaining and promoting tumor growth. As JAK/STAT inhibitors are entering clinical trials and being evaluated for clinical benefit, there are several knowledge gaps regarding the oncogenic properties of STAT3 that need to be addressed. Defining the downstream pathways being affected by STAT3 signaling in both epithelial and immune cells will be critical in the development of targeted breast cancer therapies. As described earlier, several studies have reported on the prognostic value of STAT3 in human breast tumor tissues and delineating whether patient outcome is predominantly affected by STAT3 signaling in epithelial or stromal cells will undoubtedly further our ability to effectively target this pathway.

J. Thesis statement

The overall hypothesis of this thesis is that STAT3 is a major signaling pathway that is activated in tumor and immune cells as a result of FGFR activation and contributes to mammary tumor growth (Figure 1.2).

The specific goals of the studies outlined in the following chapters are:

1. Define the contributions of STAT3 signaling in tumor cells to the generation of pro-tumorigenic stroma.
2. Delineate the effects on mammary tumor growth following inhibition of STAT3 signaling in tumor myeloid cells.

Activation of FGFR signaling results in production of pro-inflammatory mediators that act on neighboring cells through autocrine and paracrine mechanisms. Understanding the complex pathways that are affected in tumor cells, as well as infiltrating immune cells, will help define mechanisms that can be exploited as predictive markers or targeted clinically to improve patient outcome.

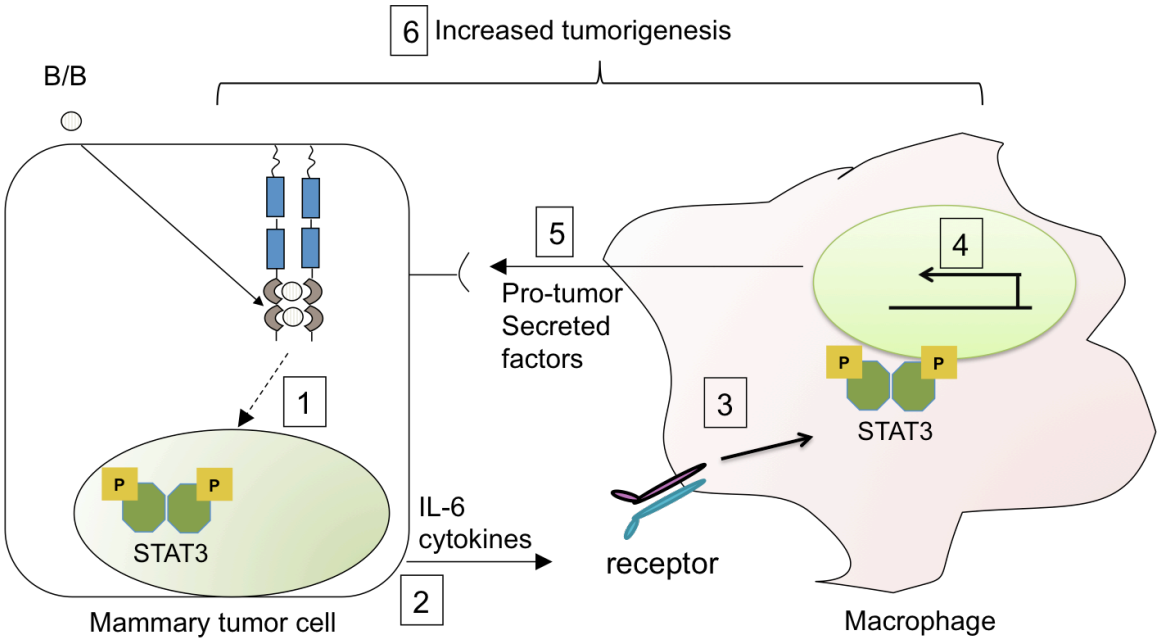

Figure 1.2. Hypothesis Activation of iFGFR1 in mammary tumor cells by induces activation of STAT3 (step 1). STAT3 activation results in increased production pro-inflammatory cytokines and stromal remodeling (step 2). IL-6 family of cytokines activate STAT3 within TAMs (step 3) and affect transcription of pro-inflammatory mediators (step 4) that act in a paracrine fashion (step 5) to affect tumor development (step 6).

Chapter 2. Activation of the FGFR-STAT3 pathway in breast cancer cells induces a hyaluronan-rich microenvironment that licenses tumor formation

Introduction

Recent genomic profiling studies have demonstrated that a number of potentially targetable pathways are aberrantly regulated in breast cancer, including the fibroblast growth factor receptor (FGFR) pathway [106]. Members of the FGFR family, comprised of four *FGFR* genes, are transmembrane receptor tyrosine kinases that are activated by FGFs [107]. Aberrant FGFR activity in breast cancers can occur through a variety of potential mechanisms, including amplification of receptor genes, increased protein expression of both ligands and receptors, single nucleotide polymorphisms (SNPs), gene rearrangements and mutations in FGFRs, all of which have been identified in human breast cancer cell lines and patient samples [18, 32]. Experimental studies have demonstrated that FGFR activation contributes to breast cancer growth and progression [22, 24, 108-112]. Furthermore, a number of clinical trials have been initiated to investigate the safety and efficacy of small molecule FGFR inhibitors in breast and other cancers [32, 108].

To study FGFR1 activation, we use an inducible FGFR1 (iFGFR1) construct containing a dimerization domain that is activated with the synthetic homodimerizer B/B, resulting in sustained activation of FGFR1-induced signaling pathways [22]. Using this inducible model, our studies have focused on the mechanisms through which FGFR1 activation in epithelial and tumor cells contributes to tumor initiation and growth [21, 26, 27, 113, 114]. Specifically, we have shown that aberrant FGFR1 activation in mammary

epithelial cells leads to alterations in the stroma, including the generation of a localized inflammatory response and alterations in the ECM [22, 114]. In the studies described here, we demonstrate that activation of FGFR signaling pathways leads to structural modifications of the ECM component hyaluronan (HA). HA is a glycosaminoglycan that interacts with cancer cells through various receptors including CD44 and receptor for hyaluronan-mediated motility (RHAMM) to promote proliferation and migration. Furthermore, aberrant HA synthesis has been linked to breast cancer growth and progression [67, 69, 70, 115, 116]. We demonstrate here that FGFR activation leads to increased synthesis of HA, which contributes to proliferation, migration and resistance to chemotherapy. Thus these studies link aberrant activation of growth factor receptor signaling pathways in tumor cells to pro-tumorigenic modifications in the surrounding stroma.

Because HA is often associated with an inflammatory environment [117], further studies examined the contribution of FGFR induced inflammatory pathways to HA synthesis. We demonstrate that activation of FGFR leads to increased production of proinflammatory cytokines, including members of the IL-6 family, which activate the signal transducer and activator of transcription 3 (STAT3) pathway. STAT3 is a proinflammatory transcription factor that contributes to breast cancer cell proliferation, migration, invasion and chemotherapeutic resistance [52, 53, 118-120]. In these studies, we demonstrate that FGFR-induced STAT3 activation contributes to HA synthesis and is important for FGFR-driven mammary tumor growth. These studies are the first to identify HA as a downstream target of FGFR activation and suggest that the addition of microenvironment-targeted therapies may enhance the efficacy of FGFR-specific therapies in cancers associated with high levels of FGFR activity.

Materials and Methods

Cell Culture

Generation of HC-11 cells stably expressing the iFGFR1 construct (HC-11/R1 cells) was described previously [23], and cells were obtained from Dr. Jeff Rosen (Baylor College of Medicine, Houston, TX) and maintained as described [23]. Hs578T, MCF-7 and MDA-MB-453 cells were obtained from the American Type Culture Collection (ATCC) and maintained as suggested. For experiments, Hs578T cells were grown on plates coated with 1.2% polyHEMA [poly(2-hydroxyethylmethacrylate)] (Sigma).

Immunoblot analysis

Serum starved cells were treated with B/B (Clontech) or bFGF (Invitrogen). For blocking and inhibitor studies, gp130 blocking antibody (R&D Systems), doxorubicin (Boynton Pharmacy, UMN), Stattic (Sigma) and/or 4-MU (Sigma) were used. ON-TARGETplus SMARTpool STAT3 and non-targeting (NT) siRNA (Thermo Scientific) were used according to manufacturer's instructions. Cells were lysed in RIPA buffer and equal amounts of protein were analyzed by SDS-PAGE. Immunoblot analysis was performed with the following antibodies: pSTAT3^{Ser727} (9134), pSTAT3^{Tyr705} (9131), STAT3 (9132), cleaved caspase-3 (9661), and β-tubulin (2146) (Cell Signaling).

ELISA

Serum starved HC-11/R1 cells were treated with B/B or ethanol as solvent control. Hs578T cells were treated with or without bFGF. At 2,6, and 24 hours, conditioned media was collected and ELISAs for mouse or human LIF, IL-6, and IL-11 were performed according to the manufacturer's protocol (R&D Systems). ON-TARGETplus

SMARTpool-siRNA Has2 or NT siRNA (Thermo Scientific) was transfected into HC-11/R1 cells as described previously [23]. Cells were pretreated with 4-MU for 1 hour prior to addition of B/B. To analyze HA synthesis, conditioned media samples were collected and tumor samples were lysed in RIPA and analyzed using the Hyaluronan ELISA (R&D systems) according to the manufacturer's protocols.

Quantitative reverse transcription-PCR

Cells were treated as described above and qRT-PCR was done as described previously and normalized to *cyclophilin B* levels [25]. The following mouse primers were used: *cyclophilin B* 5'-TGCAGGCAAAGACACCAATG-3' and 5'-GTGCTCTCCACCTCCCGTA-3', *Lif* 5'-GCCTCCCTGACCAATATCACC-3' and 5'-GACGGCAAAGCACATTGCTG-3', *Il-6* 5'-TAGTCCTTCCTACCCCAATTTCC-3' and 5'-TTGGTCCTTAGCCACTCCTTC-3', *Has2* 5'-TGTGAGAGGTTTGTATGTGTCCT-3' and 5'-ACCGTACAGTGGAAATGAGAAGT-3'.

TUNEL assays

Serum starved cells were treated with B/B or ethanol, doxorubicin or saline, and Stattic or DMSO for 20 hours. Cells were fixed and stained using the DeadEnd Fluorometric TUNEL System (Promega) according to the manufacturer's protocol. Five representative pictures were taken of each treatment, and cell counting was performed in a blinded manner.

Mice

3-4 week old Balb/c female mice were purchased from Harlan Laboratories. 250,000 HC-11/R1 cells in 50% Matrigel (BD Biosciences) were injected into the fourth inguinal

mammary fat pads. Mice were given twice weekly intraperitoneal (i.p.) injections of B/B to activate iFGFR1. When tumors reached at least 100 mm^3, mice were given Stattic or solvent control (DMSO) by oral gavage five days a week for three weeks. At least three mice were in each treatment group. For the studies with transgenic mice, MMTV-iFGFR1 mice were treated with B/B and mammary glands were isolated as described previously [114]. All animal care and procedures were approved by the Institutional Animal Care and Use Committee of the University of Minnesota and were in accordance with the procedures detailed in the Guide for Care and Use of Laboratory Animals.

Clinical cohort and TMA construction

Specimens and associated clinical data were obtained from the UMN BioNet core facility (www.bionet.umn.edu) after approval from the UMN Institutional Review Board (IRB). Archival formalin-fixed paraffin-embedded (FFPE) tissues from breast cancer patients treated at the University of Minnesota were collected. Areas of invasive carcinoma were verified by a pathologist. TMA blocks consisting of quadruplicate 1 mm core carcinoma samples were constructed using a manual tissue arrayer (MTA-1, Beecher Inc). Clinical characteristics were abstracted from pathology reports. Coded specimens and data were provided for this study. Patient identifiers were not available to the authors, but rather were held within the BioNet office per the BioNet IRB approval.

Immunohistochemistry

Mammary glands from mice were fixed, sectioned and stained using sodium citrate antigen retrieval as described previously [26, 114]. Antibodies used were $pStat3^{Tyr705}$ (1:200; Cell Signaling, 9145), Has2 (1:50; Santa Cruz, sc-365263), and pFRS2 (1:40; R&D, AF5126). As a control, sections were stained with the biotinylated anti-rabbit only.

For HABP staining, sections were blocked with 3% BSA and then incubated overnight with 2μg/ml biotinylated HABP. Visualization was performed as described above. As a control, tissues were incubated with hyaluronidase before addition of HABP. HABP-positive stromal thickness of at least 50 ducts from three mice per timepoint was quantified using Leica LAS software.

Three-dimensional culture

Primary mammary epithelial cells were isolated from MMTV-iFGFR1 transgenic mice and plated in Matrigel as described previously [121]. 10,000 Hs578T cells were plated per well in Matrigel. 4-MU or DMSO (solvent) was added to the cultures for 8 days. At least 50 acini were measured for each condition using Leica LAS software.

Proliferation Assay

For HC-11/R1 cells, Thiazolyl Blue Tetrazolium Bromide (Sigma, M2128) was used. Serum starved HC-11/R1 cells were treated with B/B, 4-MU or Stattic. MTT reagent was added to the wells and after 2 hours proliferation was determined according to the manufacturer protocol. For Hs578T cells, the CellTiter 96 Aqueous Proliferation Assay (Promega) was used according to manufacturer protocol. Briefly, $1x10^5$ cells/ml were resuspended in serum free media in 96 well plates coated with 1.2% polyHEMA. The next day cells were treated with bFGF and either Stattic or 4-MU. The absorbance was read at 490 nm following 24 and 48 hours of treatment.

Migration Assay

Confluent HC-11/R1 cells were serum starved and wound healing assays were performed as described previously [23] in the presence of B/B and/or 4-MU and/or Stattic. Area of wound closure was quantified following 18 hours using Leica LAS software.

Statistical analysis

Experiments were performed at least three separate times. Statistical analysis was performed using the unpaired student's t-test to compare two means. In all figures, error bars represent the standard error of the mean. For the human samples, the association between pFRS2 and pSTAT3 was evaluated using proportional odds logistic regression with pSTAT3 as the outcome and pFRS2 as a covariate in a univariate regression model and the association between pFRS2 and pSTAT3 was summarized by the odds ratio.

Results

FGFR activation induces synthesis of hyaluronan. We have previously used the MMTV-iFGFR1 transgenic mouse model to identify mechanisms through which FGFR1 activation in mammary epithelial cells contributes to pro-tumorigenic changes within the stroma [21, 23, 26, 27, 114, 121]. It has been previously noted that activation of iFGFR1 in mammary epithelial cells results in alterations in the surrounding ECM [22, 114]. To gain insights into these changes, previously published microarray studies [114] were examined to identify ECM-related genes that are regulated following iFGFR1 activation. Interestingly, *Has2*, which stimulates synthesis of the ECM component HA, was significantly induced following 8 hours of B/B treatment. To verify these findings,

mammary glands from B/B-treated MMTV-iFGFR1 mice were analyzed for HAS2 expression and HA accumulation using immunohistochemical analysis. Following 48 hours of iFGFR1 activation, increased expression of HAS2 was detectable within the aberrant budding epithelial structures (Figure 2.1A). Furthermore, increased accumulation of HA in the surrounding stroma was determined by measuring the thickness of HA-positive stroma (Figure 2.1A,B).

To verify that activation of iFGFR1 leads to increased expression of *Has2* in epithelial cells, HC-11 cells that stably express iFGFR1 (HC-11/R1) [23] were treated with B/B to activate iFGFR1. *Has2* expression increased following iFGFR1 activation as shown by qRT-PCR analysis (Figure 2.1C). Furthermore, increased levels of HA were detected in the media of B/B-treated HC-11/R1 cells using an ELISA-based assay (Figure 2.1D). Analysis of FGF-responsive human breast cancer cell lines, including the estrogen receptor positive (ER^+) cell line MCF-7 and the triple negative cell line Hs578T, demonstrated that basic FGF (bFGF) treatment also led to increased levels of HA in the media (Figure 2.1E,F). To confirm that HAS2 is the primary hyaluronan synthase that contributes to HA synthesis, *Has2* knock-down was performed using siRNA (Figure 2.1G) and resulted in a significant decrease in HA synthesis (Figure 2.1H). Together, these studies demonstrate that FGFR activation induces expression of HAS2, which leads to increased synthesis of HA *in vitro* and *in vivo*.

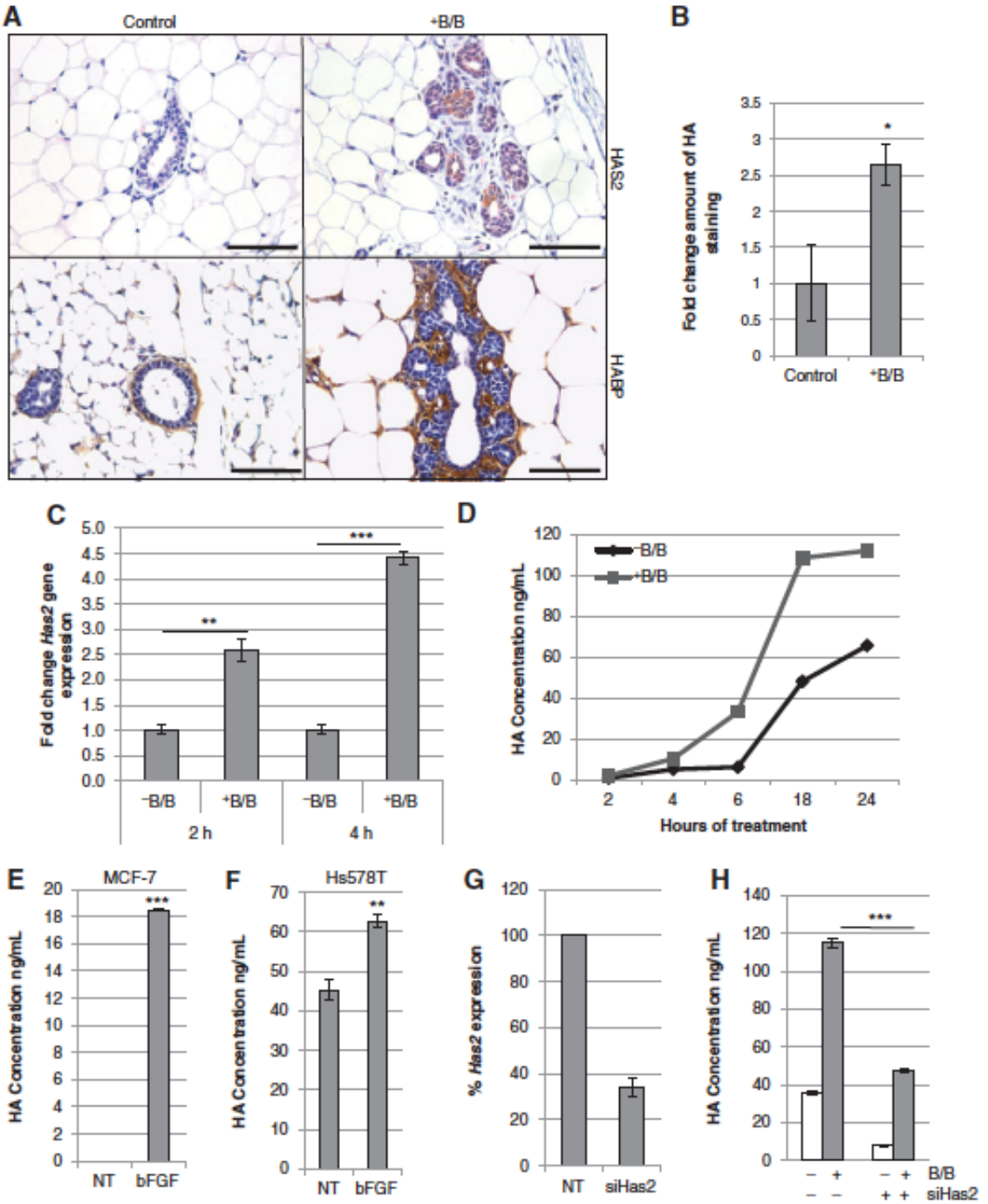

Figure 2.1 FGFR activation leads to increased production of HA. A) MMTV-iFGFR1 transgenic mice were treated with 1mg/kg B/B or solvent for 48 hours. Mammary gland sections were stained with HAS2-specific antibody or HA binding protein (HABP). Magnification bars represent 50μm. B) Quantification of HA-positive stromal thickness in mammary glands from solvent or B/B treated mice. C) HC-11/R1 cells were treated with solvent (-B/B) or 30nM B/B and *Has2* gene expression was analyzed by qRT-PCR. D) HC-11/R1 cells were treated as described in (C) and HA expression in conditioned media was determined by ELISA. E,F) MCF-7 (E) and Hs578T (F) cells were treated with or without 50ng/ml bFGF for 18 hours and HA in the

(*Figure 2.1 continued*)

conditioned media was determined by ELISA. G) HC-11/R1 cells were treated with Has2 siRNA or a non-targeting (NT) control. Expression of *Has2* was measured by qRT-PCR. H) Amount of HA was determined by ELISA. *p<0.05, **p<0.01, ***p<0.001.

Inhibition of HA synthesis leads to decreased proliferation, migration, and chemoresistance. Because HA has been linked to tumor growth and progression [69, 70, 115], further studies were performed to examine the contributions of HA to proliferation and migration. For these studies, cells were treated with 4-methylumbelliferone (4-MU), which inhibits HA synthases including HAS2 [122-124]. As shown in Figure 2.2A, treatment of HC-11/R1 cells with 4-MU effectively inhibited both basal and iFGFR1-induced HA synthesis. Furthermore, treatment of HC-11/R1 cells with 4-MU inhibited iFGFR1-induced migration (Figure 2.2B) and proliferation (Figure 2.2C). In addition, the contribution of HA to iFGFR1-induced survival in response to chemotherapy was examined by analyzing apoptosis following exposure of cells to doxorubicin. Activation of iFGFR1 significantly decreased doxorubicin-induced apoptosis in the HC-11/R1 cells, which was partially reversed by 4-MU, demonstrating that HA contributes to iFGFR1-induced chemoresistance. Similarly, treatment of Hs578T cells with bFGF and 4-MU inhibited bFGF-induced proliferation (Figure 2.2E) and restored apoptosis in response to doxorubicin treatment (Figure 2.2F). Interestingly, we found that treatment of both cell lines with 4-MU had effects on cell behavior independently of FGFR activation, possibly due to the decreased levels in basal HA synthesis (Figure 2.2A). These results suggest that there are likely to be additional mechanisms that regulate HA synthesis in the absence of FGFR activation, which may contribute to the 4-MU induced inhibition of FGFR-induced phenotypes.

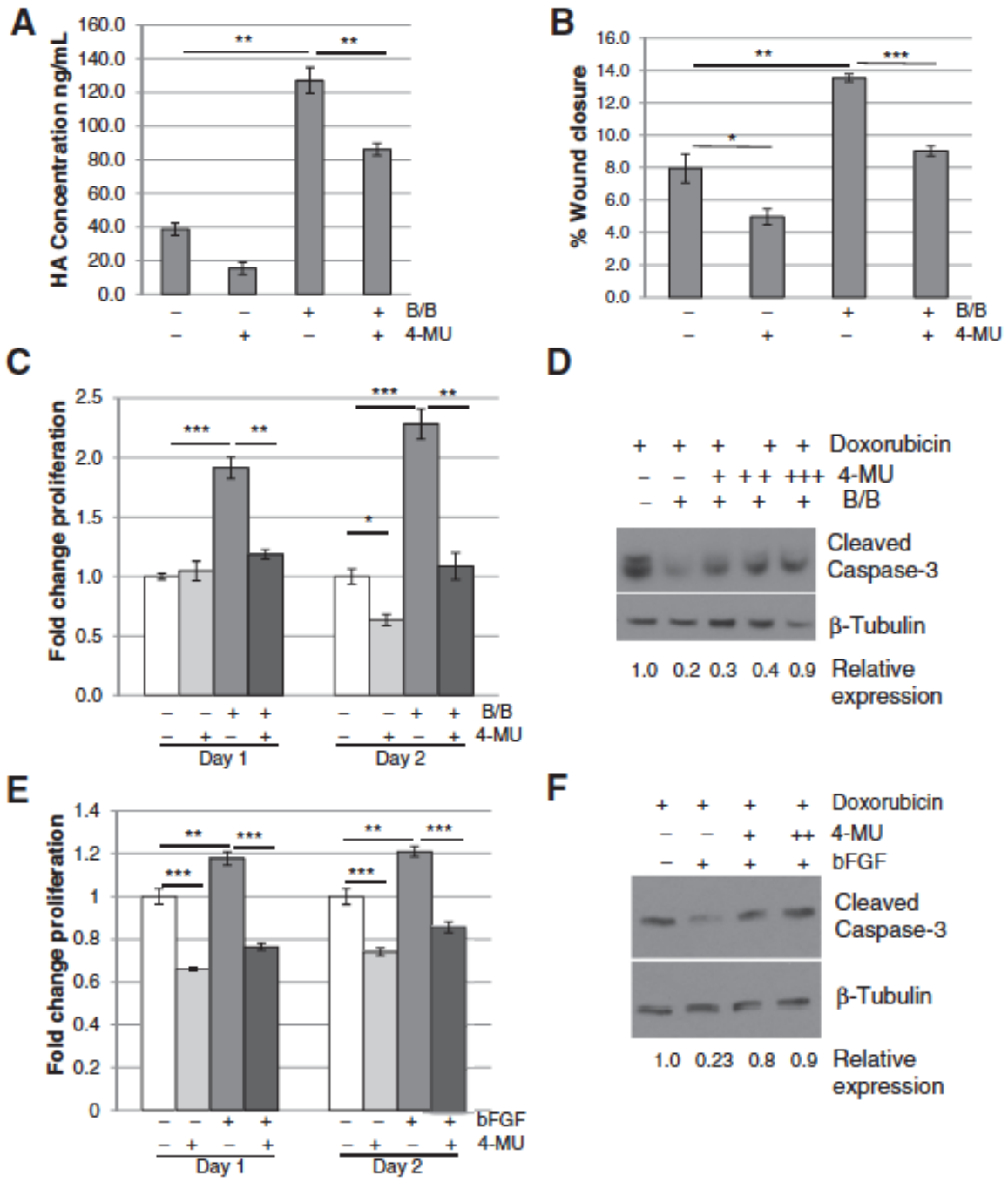

Figure 2.2 Blocking HA synthesis leads to decreased migration, proliferation, and chemoresistance. A) HC-11/R1 cells were treated with 250 μM of the HAS2 inhibitor 4-MU or solvent, followed by the addition of 30nM B/B or solvent. HA was detected in conditioned media by ELISA. B,C) HC-11/R1 cells were treated with B/B, 250μM 4-MU and/or solvent. The change in wound closure was determined at 18 hours (B) and proliferation was measured by an MTT assay (C) at day 1 or 2. D) HC-11/R1 cells were treated with B/B, 4-MU (62.5μM (+), 125μM (++), 250μM 9 (+++)), and 2μM doxorubicin for 24 hours. Levels of cleaved caspase-3 and β-tubulin were examined by immunoblot analysis. E) Hs578T cells were treated with 50ng/ml bFGF and

(*Figure 2.2 continued*)

25μM 4-MU. Proliferation was measured relative to solvent-only treated samples. F) Hs578T cells were treated with bFGF, 4-MU (125μM (+) and 250μM (++)), and doxorubicin and levels of cleaved caspase-3 and β-tubulin were examined. *P<0.05; **p<0.01; and ***p<0.001.

FGFR activation leads to increased phosphorylation of STAT3. Next, we examined the mechanisms involved in mediating FGFR-induced HA synthesis. Because HA is involved in inflammation [117, 125], our initial studies focused on examining inflammatory mediators such as STAT3, which regulates inflammation-related genes including *Has2* [65]. To examine STAT3 activation in the iFGFR1 model, HC-11/R1 cells were treated with B/B and phosphorylation of $STAT3^{Ser727}$ and $STAT3^{Tyr705}$ was assessed by immunoblot analysis. Similar to what has been shown previously [126], $STAT3^{Ser727}$ was phosphorylated within 15 minutes of iFGFR1 activation, although $pSTAT3^{Tyr705}$ was not detected at these timepoints (Fig. 2.3A). However, analysis of later timepoints demonstrated that $pSTAT3^{Tyr705}$ was detectable following 2 hours of iFGFR1 activation and remained elevated throughout the 24-hour time course (Figure 2.3B).

The timing of $STAT3^{Tyr705}$ phosphorylation led to the hypothesis that FGFR induces $STAT3^{Tyr705}$ phosphorylation indirectly through inducing production of soluble factors that activate STAT3. To address this possibility, HC-11/R1 cells were treated with B/B for 18 hours, and conditioned media were used to stimulate parental HC-11 cells. $pSTAT3^{Tyr705}$ was elevated in the HC-11 cells as early as 5 minutes after treatment with conditioned media (Figure 2.3C), consistent with the hypothesis that soluble factors produced by the cells following iFGFR1 activation contribute to STAT3 activation.

Further studies were performed to identify soluble factors that induce $STAT3^{Tyr705}$ phosphorylation in our system. Because STAT3 is a well-established downstream target of IL-6 family cytokines [127], the ability of iFGFR1 to induce expression of genes in the IL-6 family was assessed. Initial screening of HC-11/R1 cells demonstrated that iFGFR1 activation led to increased gene expression of *Il-6, Lif* and *Il-11* (Figure 2.3D,E and data not shown). ELISA analysis of conditioned media confirmed that soluble LIF was detectable within 2 hours of iFGFR1 activation (Figure 2.3F) and soluble IL-6 was

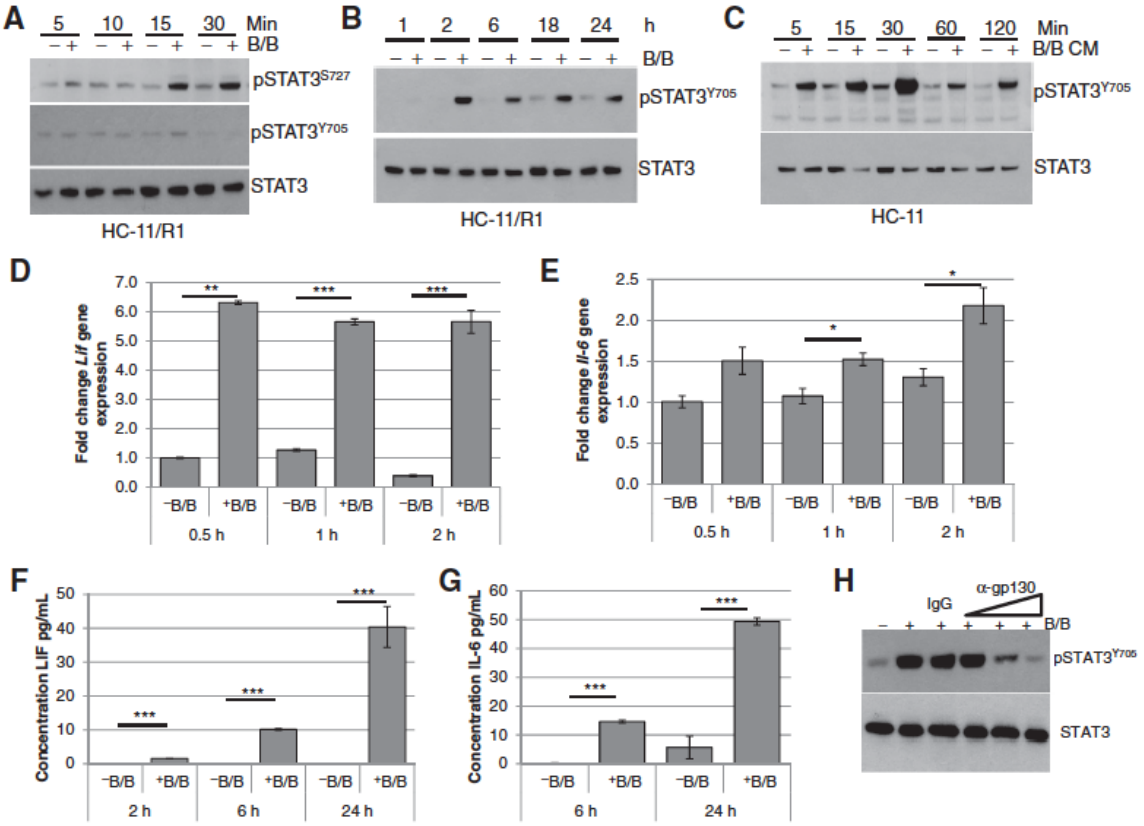

Figure 2.3 Activation of iFGFR1 leads to increased pSTAT3^{Tyr705} in a gp130-dependent manner. HC-11/R1 cells were stimulated with solvent (-B/B) or 30nM B/B, followed by protein and RNA extraction or collection of conditioned media. A, B) pSTAT3^{S727}, pSTAT3^{Y705}, and STAT3 (loading control) were examined using immunoblot analysis. C) Conditioned media (CM) samples from treated HC-11/R1 cells were collected and added to HC-11 cells. pSTAT3^{Y705} and STAT3 was examined using immunoblot analysis. D,E) qRT-PCR analysis was performed to assess *Lif* or *Il-6* gene expression. F,G) LIF and IL-6 expression in conditioned media was assessed by ELISA. H) HC-11/R1 were treated as above with the addition of IgG control or gp130 blocking antibody (0.05, 0.5, 5 µg/ml) for 6 hours. Expression of pSTAT3^{Y705} and STAT3 was examined by immunoblot analysis. *p<0.05, **p<0.01, ***p<0.001.

detectable within 6 hours (Figure 2.3G). However, increased IL-11 was not found in the media at any timepoint (data not shown), suggesting that IL-6 and LIF are the primary IL-6 family cytokines produced by HC-11/R1 cells in response to iFGFR1 activation. Initial studies using cytokine-specific blocking antibodies demonstrated that blocking a single cytokine was unable to completely abolish STAT3 phosphorylation (data not shown), possibly due to ligand redundancy. IL-6 family cytokines utilize the common receptor subunit gp130 to transmit their signals [39]. As shown in Figure 2.3H, treatment of HC-11/R1 cell with a gp130-blocking antibody prior to activation of iFGFR1 led to a dose-dependent reduction of $STAT3^{Tyr705}$ phosphorylation. These results demonstrate that activation of FGFR1 leads to production of IL-6 family cytokines, which act through gp130 to induce phosphorylation of $STAT3^{Tyr705}$.

FGFR activation induces expression of IL-6 family cytokines and STAT3 activation in human breast cancer cells. Further studies focused on validating FGFR-induced $STAT3^{Tyr705}$ phosphorylation in other FGF-responsive cell lines including MCF-7, MDA-MB-453 and Hs578T [20, 21, 128]. Following treatment of cells with bFGF, $pSTAT3^{Tyr705}$ was observed at later time points, including 2 and 6 hours post-treatment, in all cell types (Figure 2.4A-C), similar to what was observed with the HC-11/R1 cells. Furthermore, bFGF treatment of Hs578T cells led to increased production of IL-6 family cytokines, including IL-6 (Figure 2.4D) and IL-11 (Figure 2.4E), although LIF was not induced in these cells (data not shown). Finally, treatment of cells with a gp130-blocking antibody led to decreased $pSTAT3^{Tyr705}$ in a dose dependent manner (Figure 2.4F). These results verify our findings from the HC-11/R1 model that activation of endogenous FGFR induces expression of IL-6 family cytokines, which contribute to phosphorylation of $pSTAT3^{Tyr705}$

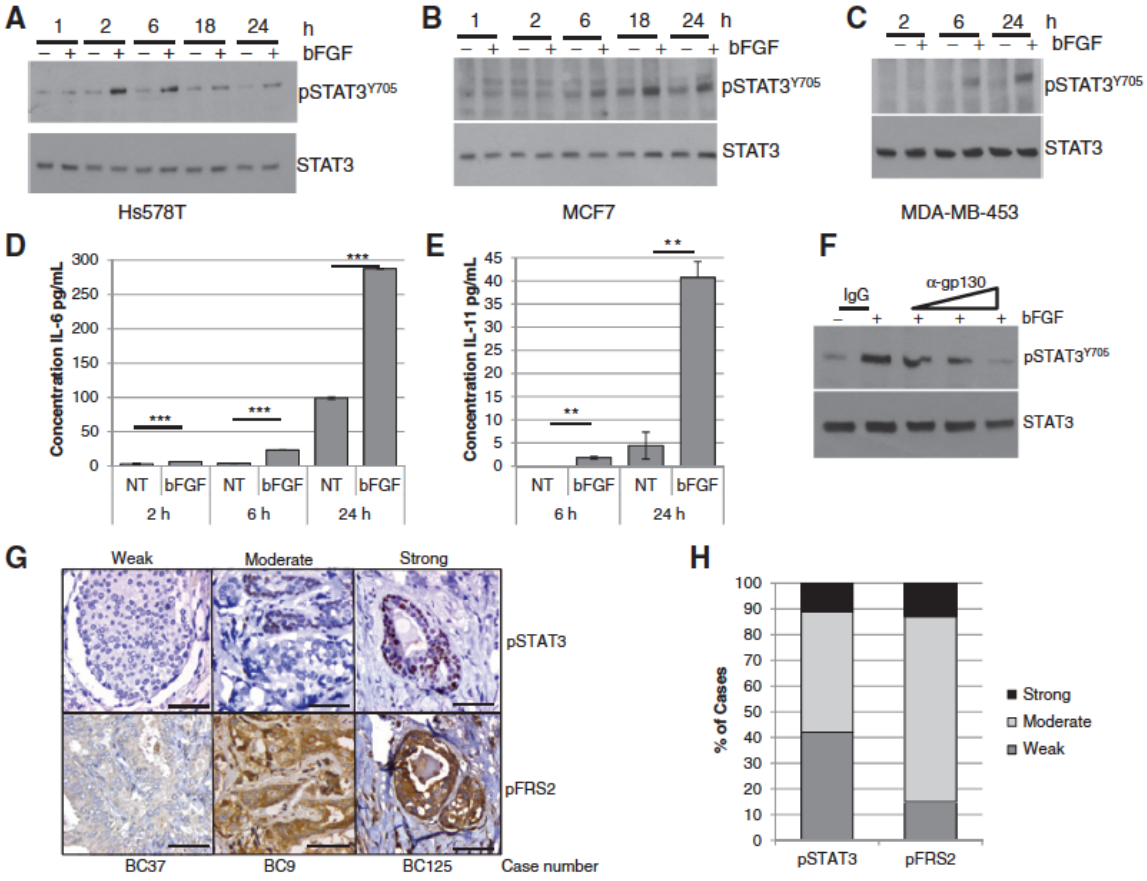

Figure 2.4 FGFR activation leads to pSTAT3^{Tyr705} in human breast cancer cells. Hs578T (A), MCF7 (B), and MDA-MB-453 (C) were treated with or without 50ng/ml bFGF and expression of pSTAT3^{Y705} and STAT3 was examined by immunoblot analysis. D,E) Hs578T cells were treated as described above for the indicated times, and conditioned media samples were collected to examine protein expression of IL-6 (D) or IL-11 (E) by ELISA. F) Hs578T cells were treated as above with the addition of IgG control or gp130 blocking antibody (0.1, 1, 10 μg/ml) for 6 hours. G,H) A human breast cancer tissue microarray was stained for pSTAT3^{Tyr705} and pFRS2 using IHC. G) Representative images of weak, moderate, or strong staining intensity are shown. Magnification bars represent 50μm. H) Percentage of cases based on staining intensity. **p<0.01 and ***p<0.001.

To determine whether the FGFR and STAT3 signaling pathways are correlated in human breast cancers, a tissue microarray (TMA) was generated (Table 2.1) and stained with antibodies that recognize pSTAT3^{Tyr705} and phosphorylated fibroblast growth factor receptor substrate 2 (pFRS2), which is indicative of activated FGFR [11]. As control, tissues were stained with secondary antibody only and positive staining was not detected (Figure 2.5A). Both sets of samples were scored for weak, moderate and strong staining (Figure 2.4G). Similar to previously published results [39, 52, 57], pSTAT3^{Tyr705} was observed at moderate to strong levels in approximately 60% of breast cancers (Figure 2.4H). pFRS2 staining was found to be detectable at some level in all samples, with approximately 85% of tumors expressing moderate to high levels of staining (Figure 2.4H), suggesting that FGFR activity is present in a large percentage of breast cancer samples. Analysis of all samples revealed a significant association between pFRS2 and pSTAT3 (odds ratio=4.8, 95% CI: 1.91, 12.05, $p<0.001$), demonstrating a correlation between FGFR activation and STAT3^{Tyr705} phosphorylation in a proportion of breast cancers (Table 2.1).

STAT3 contributes to FGFR-induced migration, proliferation and resistance to chemotherapy. To assess the functional contributions of STAT3 activation to FGFR-induced tumorigenic phenotypes, we used the pharmacological inhibitor Stattic [129]. Inhibition of STAT3 in HC-11/R1 cells led to decreased iFGFR1-induced migration (Figure 2.6A) and proliferation (Figure 2.6B). Because STAT3 has also been linked to resistance to chemotherapy [130], the contribution of STAT3 activation to FGFR-induced chemoresistance was examined. Stattic restored the sensitivity of HC-11/R1 cells to doxorubicin, suggesting that STAT3 contributes to iFGFR1-induced chemoresistance (Figure 2.6C).

Table 2.1 Proportional odds logistic regression results evaluating the association between pSTAT3 and pFRS2 in all subjects and stratified by ER status, HER2 status, node status and triple negative status.

	N	OR	95% CI	p-value
All samples	85	4.8	(1.91,12.05)	< 0.001[1]
by ER status				
ER-	18	4.28	(0.69,26.7)	0.861[2]
ER+	65	5.23	(1.78,15.43)	
by Her2 status				
HER2-	52	10.98	(2.97,40.54)	0.060[2]
HER2+	30	1.7	(0.39,7.46)	
by node status				
Node -	40	4.34	(1.16,16.31)	0.562[2]
Node +	36	8.09	(1.61,40.62)	
by triple-negative status				
All others	75	4.73	(1.73, 12.91)	0.655[2]
TN	8	7.67	(0.65, 90.97)	

[1]: p-value testing whether the odds ratio is significantly different than 1

[2]: p-value testing whether the two odds ratios are significantly different (i.e. OR for ER- vs. OR for ER+)

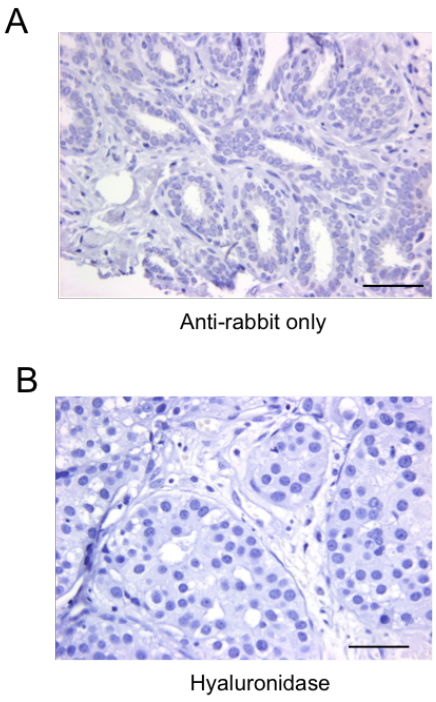

Figure 2.5 A) Representative image of biotinylated anti-rabbit stained section of human breast cancers. B) Representative image of a human breast cancer section treated with hyaluronidase before addition of HABP. Magnification bars represent 50 μm.

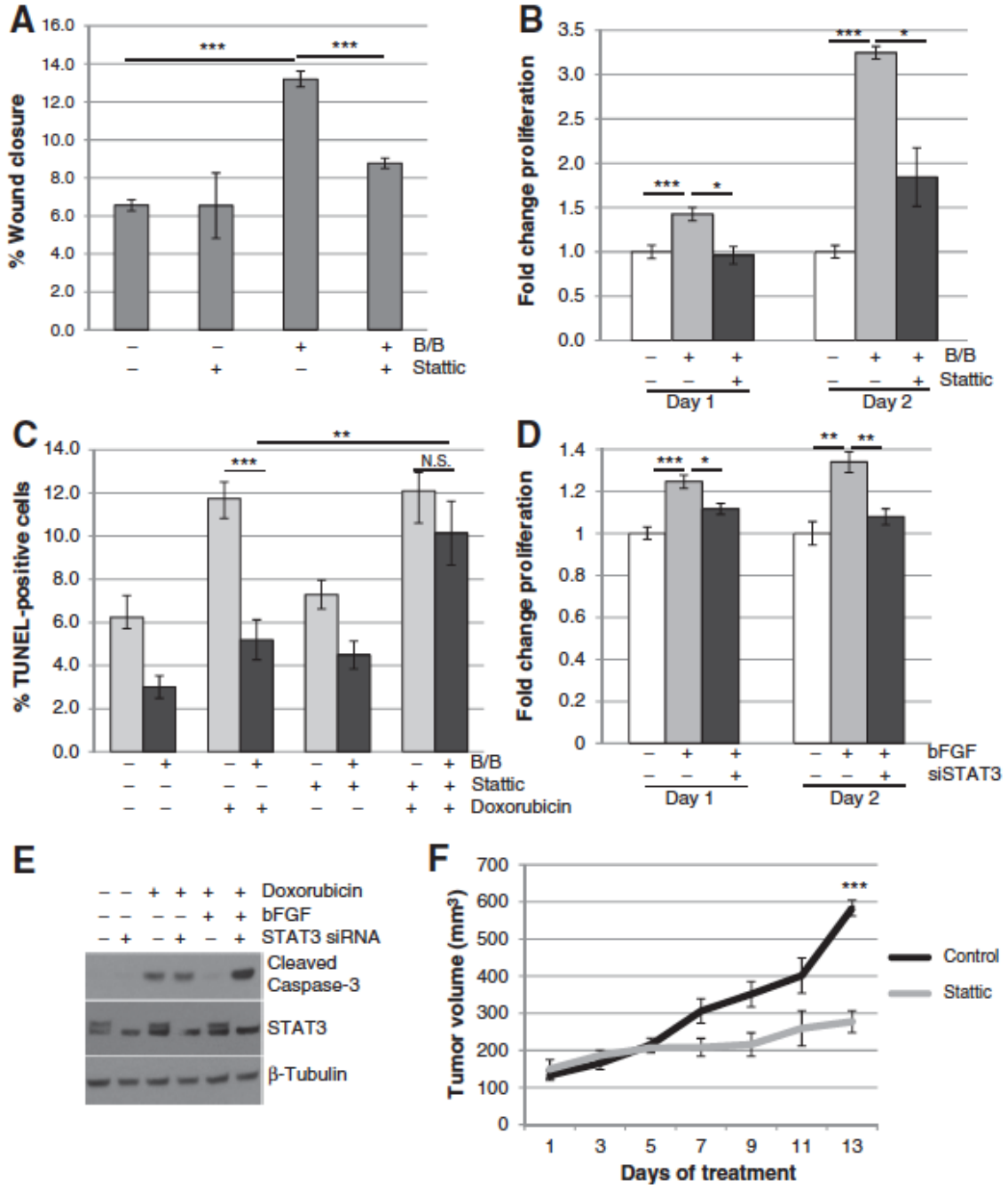

Figure 2.6 STAT3 promotes FGFR-induced migration, proliferation, and chemoresistance. A) HC-11/R1 cells were treated with solvent or 30nM B/B in the presence of 1μM Stattic or DMSO, and wound closure was measured after 18 hours. B) HC-11/R1 cells were treated with B/B, 2μM Stattic or solvent for 1 or 2 days. Proliferation rate was calculated by MTT assay and given relative to the solvent treated samples. C) Apoptosis was determined by TUNEL assay for HC-11/R1 cells treated with B/B, 4μM Stattic, or 2μM doxorubicin for 24 hours. D) Hs578T cells were treated with NT or STAT3 siRNA for 24 hours, followed by 1 or 2 days treatment with 50ng/ml bFGF, and proliferation was calculated relative to solvent treated samples. E) Hs578T cells were treated as described above, and 2μM doxorubicin was added to the indicated groups

(*Figure 2.6 continued*)

for 24 hours. Expression levels of cleaved caspase-3 and β-tubulin were examined by immunoblotting. F) HC-11/R1 cells were injected into the fat pads of Balb/c mice. Mice were given twice weekly injections of 1mg/kg B/B. Once tumors reached a size of 100 mm^3, mice received either DMSO or 20mg/kg Stattic and tumor growth was assessed. *p<0.05, **p<0.01, ***p<0.001.

To verify the contribution of STAT3 to proliferation and chemotherapeutic resistance following endogenous FGFR activation, these processes were assessed in Hs578T cells. Consistent with the results from the HC-11/R1 cells, treatment of Hs578T cells with bFGF in the presence of Stattic decreased bFGF-induced proliferation and reversed resistance to doxorubicin-induced apoptosis (Figure 2.7). To demonstrate that these effects are due to loss of STAT3 activity and not due to off-target effects of Stattic, STAT3 expression was decreased using siRNA. As shown in Figure 2.6E, STAT3 siRNA decreased expression of STAT3α, while leaving the STAT3β splice variant intact. Loss of STAT3α expression correlated with decreased bFGF-induced proliferation of Hs578T cells (Figure 2.6D) and restoration of chemosensitivity as shown by an increase in cleaved caspase-3 (Figure 2.6E).

A novel orthotopic mammary tumor model was used to evaluate the contribution of STAT3 activation to FGFR-induced tumor growth *in vivo*. HC-11/R1 cells were injected into fat pads of Balb/c mice and the mice were administered B/B to induce tumor growth. Average time to tumor growth in this model is 5.5 weeks, compared with parental HC-11 cells, which do not form palpable tumors within this timeframe (Figure 2.8). To determine the effects of STAT3 inhibition on iFGFR1-induced tumor growth, mice bearing 100 mm^3 tumors were treated with either Stattic or solvent control. Treatment of mice with Stattic led to tumor stabilization, resulting in a significant ($p<0.001$) reduction in the size of end stage tumors (Figure 2.6F). Together, these results demonstrate that STAT3 is an important mediator of FGFR-induced proliferation, migration, therapeutic resistance and tumor growth.

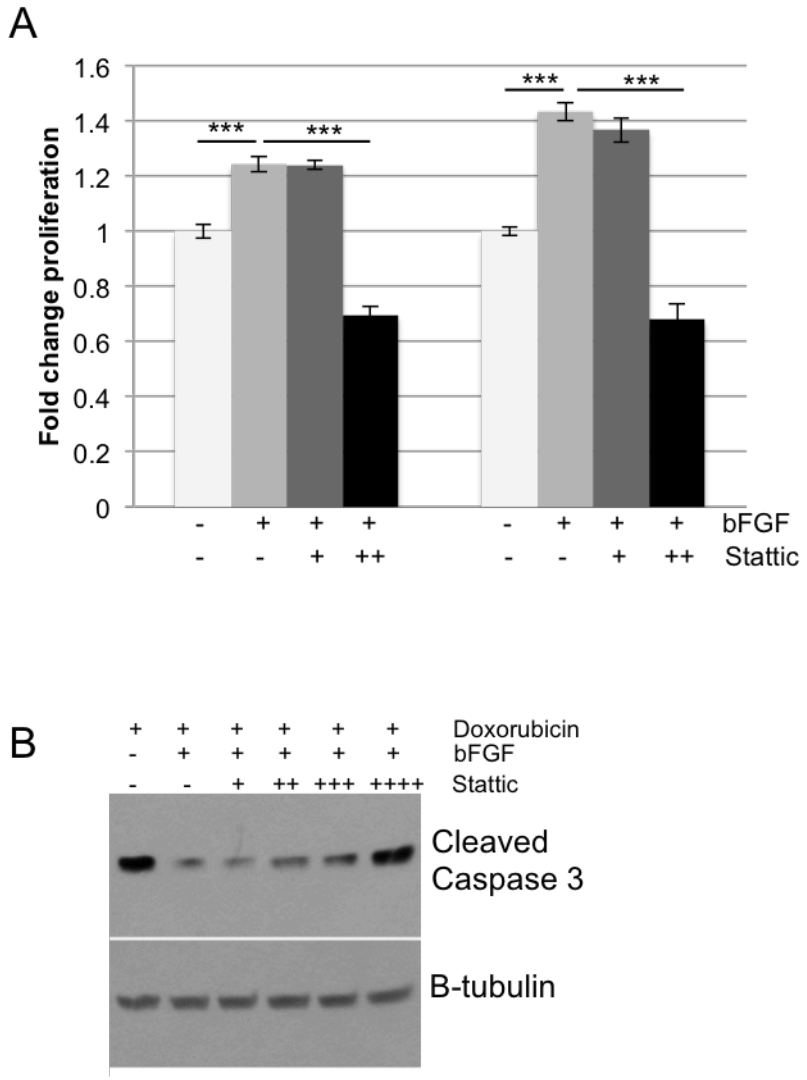

Figure 2.7 A) Hs578T cells were treated with or without bFGF in the presence of 1 μM (+) or 4 μM (++) Stattic or solvent control (DMSO) for 1 or 2 days. Proliferation was calculated relative to solvent-only treated samples. ***p<0.001. B) Hs578T cells were treated with 2 μM doxorubicin, with or without bFGF, and with solvent control (DMSO) or 1 μM (+), 2 μM (++), 4 μM (+++), or 8 μM (++++) Stattic. Expression levels of cleaved caspase-3 and the loading control β-tubulin were examined by immunoblotting.

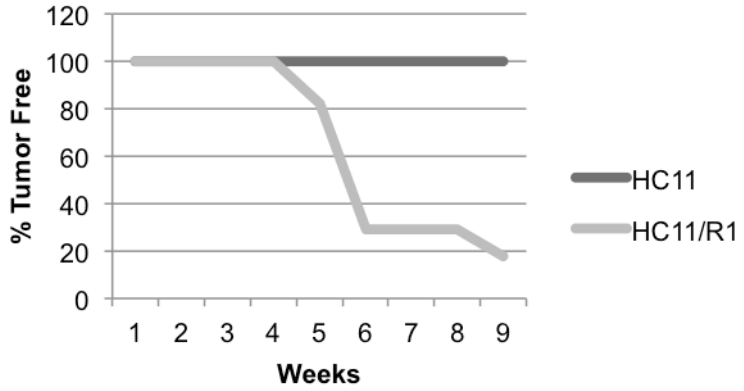

Figure 2.8 HC-11 or HC-11/R1 cells were injected into the mammary fat pads of Balb/c mice. Mice were palpated to determine the % tumor free.

FGFR activation induces HA accumulation in a STAT3-dependent manner.

Because *HAS2* was previously identified as a STAT3 target gene [65], we determined the contribution of STAT3 to iFGFR1-mediated *Has2* expression and HA synthesis. As shown in Figure 2.9A, treatment of HC-11/R1 cells with Stattic led to decreased *Has2* gene expression within 2 hours of B/B treatment. Furthermore, inhibition of STAT3 also led to decreased HA synthesis following iFGFR1 activation (Figure 2.9B). To verify the link between FGFR, STAT3 and HA in human breast cancer cells, Hs578T cells were treated with bFGF in the presence or absence of Stattic and HA synthesis was analyzed. Although Hs578T cells already express high basal levels of HA [68], inhibition of STAT3 activity led to a decrease in bFGF-induced HA synthesis (Figure 2.9C).

To confirm these findings *in vivo*, immunohistochemical analysis was performed on HC-11/R1-derived tumors (Figure 2.6F). Both pSTAT3^{Tyr705} and HAS2 staining were observed in the tumors from solvent-treated mice (Figure 2.9D). Analysis of serial sections of tumors from Stattic-treated mice revealed decreased pSTAT3^{Tyr705} and HAS2 staining in the same areas within the tumor. Furthermore, analysis of tumor-associated HA by ELISA revealed decreased HA levels in tumors from mice treated with Stattic (Figure 2.9E), consistent with the observed decrease in HAS2 expression.

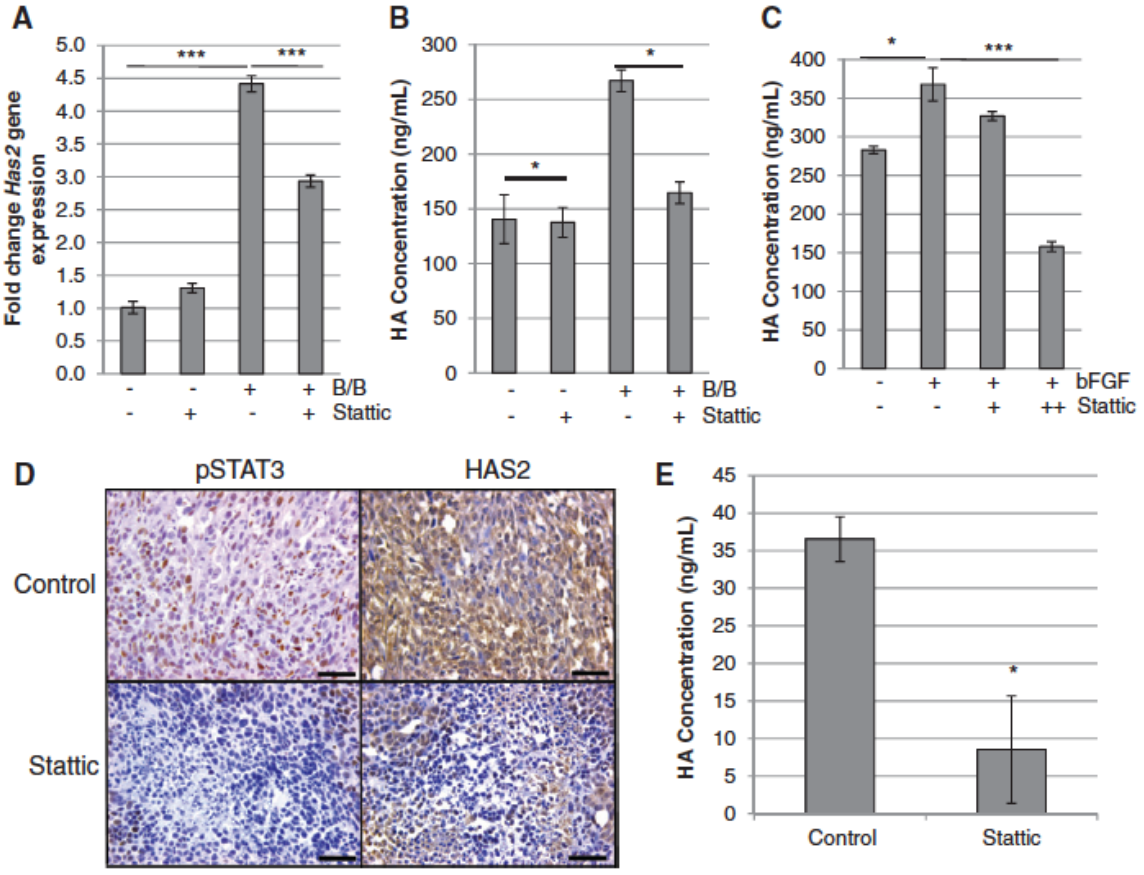

Figure 2.9 STAT3 regulates expression of HAS2 and production of HA. A) HC-11/R1 cells were treated with 30nM B/B, 4μM Stattic or solvent for 2 hours. RNA was collected to examine expression of *Has2* by qRT-PCR. B) HC-11/R1 cells were treated as in (A) for 18 hours. Conditioned media was collected to examine expression of HA by ELISA. C) Hs578T cells were treated with 50ng/ml bFGF and Stattic (2μM (+) or 4μM (++)) or solvent for 18 hours, and levels of HA in the conditioned media were determined by ELISA. D) Serial tumor sections from mice treated with solvent or 20mg/kg Stattic were stained for pSTAT3^{Tyr705} and HAS2. E) Amount of HA in tumors from mice in D) was assessed by ELISA. *p<0.05, **p<0.01, ***p<0.001.

Inhibition of HA synthesis decreases acinar growth in three-dimensional culture. Further studies were performed to determine the effects of inhibiting HA synthesis using three-dimensional (3D) culture models, which provide a more relevant environment than cells in traditional two-dimensional culture [131]. We have previously demonstrated that primary mammary epithelial cells isolated from MMTV-iFGFR1 transgenic mice form large acinar structures in 3D culture upon iFGFR1 activation [121]. To assess effects HA inhibition on acinar growth, 4-MU was added to the 3D culture at the same time as activating iFGFR1, which led to inhibition of iFGFR1-induced acinar growth (Figure 2.10A,B). Furthermore, treatment of established structures with 4-MU led to inhibition of further acinar growth (Figure 2.10C,D). These studies demonstrate that blocking HA synthesis leads to inhibition of iFGFR1-dependent growth of both developing and established acinar structures.

Further studies were performed using the Hs578T cells, which exhibit high levels of both FGFR activation [20] and high levels of HA synthesis [68]. The cells were plated in 3D culture and structures were treated with either PD173074 to inhibit FGFR activation, 4-MU to inhibit HA synthesis or both for 6 days, and proliferation was assessed using phospho-histone H3 staining. Surprisingly, treatment of cells with either PD173074 or 4-MU alone did not affect proliferation (Figure 2.10E,F). However, when treated with both inhibitors together, proliferation was significantly decreased (Figure 2.10E,F). Taken together, the 3D culture studies suggest that HA inhibition may be a relevant approach for targeting both FGFR-driven cancers and cancers that have high levels of FGFR activation, but are not necessarily FGFR-driven. To assess whether high levels of FGFR activation and HA co-exist in human patient samples, the TMA described above was stained for HA. No staining was observed in hyaluronidase treated samples, demonstrating specificity for the staining (Figure 2.5B). HA was found in all samples and

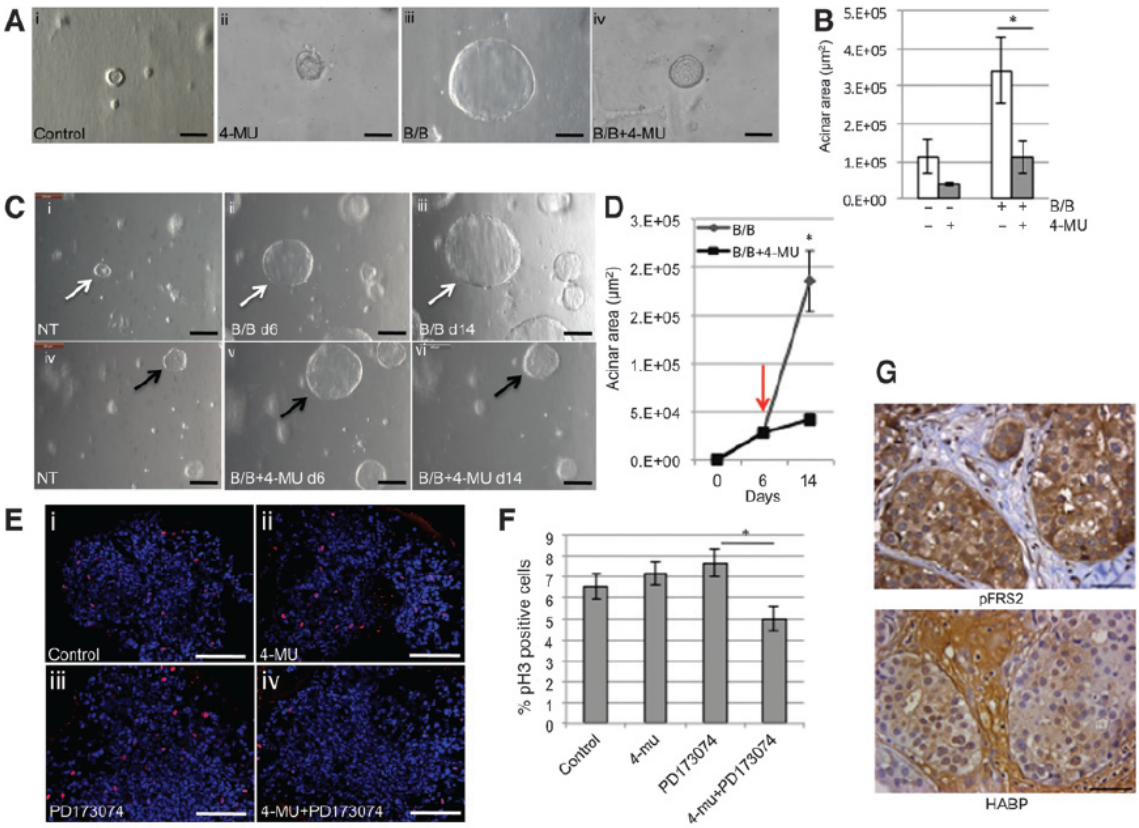

Figure 2.10 Inhibition of HA synthesis leads to decreased FGFR-induced growth in 3D culture. A) Primary mammary epithelial cells were isolated from MMTV-iFGFR1 transgenic mice and plated in 3D culture. Cells were treated with 30nM B/B,10μM 4-MU or solvent. Light microscopy images were obtained after 10 days in culture. B) Quantification of acinar area. C) Structures were treated with B/B to activate iFGFR1 for 6 days, followed by treatment with solvent or 4-MU for 8 days. Images were obtained from the same structures. D) Quantification of acinar area. Red arrow indicates addition of 4-MU. E) Hs578T cells were plated in Matrigel. The cells were treated with solvent (Control), 10μM 4-MU, 1μM PD173074 or both for 6 days. The cultures were stained with phospho-histone H3 and analyzed by confocal microscopy. F) Quantification of phospho-histone H3 positive cells. *p<0.05. G) Representative images of pFRS2 and HABP-stained sections of human breast cancers. Magnification bars represent 50μm.

was therefore present in all breast cancer samples exhibiting high levels of pFRS2 (Figure 2.10G). Therefore, combination therapies targeting both FGFR activity and HA synthesis may be considered for patients with high levels of FGFR activation.

Discussion

The results from these studies reveal a novel link between FGFR activation and synthesis of HA by tumor cells, thus linking intracellular signaling to alterations in the microenvironment (Figure 2.11). HA is an important component of the ECM that is normally involved in a number of physiological processes including maintenance of tissue integrity, morphogenesis, wound healing and inflammation [117, 125]. HA is a prevalent component of the normal human breast ECM and alterations in HA contribute to breast cancer growth and progression [69, 70, 115]. Tumor-associated HA alterations are complex and can include increased HA synthesis, changes in HA localization and increased HA fragmentation [132, 133]. High levels of HA accumulate in breast cancer, in part due to increased HA synthesis by HAS enzymes including HAS2; these high levels of HA are associated with reduced survival and poor response to therapy [134, 135]. HA is typically produced in a high molecular weight form and can be cleaved into lower molecular weight fragments by hyaluronidases or reactive oxygen species under specific conditions, such as during inflammation and within the tumor microenvironment [136-138]. While high molecular weight HA inhibits tumor formation [139], low molecular weight forms have been shown to stimulate cancer cell migration and invasion possibly through differential interactions with its receptors, such as CD44 and RHAMM [132, 133, 140]. While our current studies have not specifically assessed HA fragmentation, they

demonstrate that FGFR can increase the levels of HA within the tumor microenvironment creating the necessary substrate for HA fragment production.

Because changes in HA are often associated with inflammation, further studies focused on the contributions of inflammatory pathways to FGFR-mediated changes in HA, specifically the transcription factor STAT3. In our current studies, we found differences in the kinetics of the two STAT3 phosphorylation sites, Ser727 and Tyr705, following FGFR activation. Phosphorylation at Ser727 has been previously identified as a rapid site of phosphorylation following FGFR activation [126]. However, the observation of cytokine mediated indirect phosphorylation at Tyr705 at later time points is novel and provides a potential feed forward mechanism through which FGFR activation induces inflammation in breast cancer. Although initially thought to be secondary to phosphorylation of Tyr705 and involved in maximal STAT3 activation, recent studies have suggested that $pSTAT3^{Ser727}$ may have different functions than $pSTAT3^{Tyr705}$ [141]. Interestingly, $pSTAT3^{Ser727}$ has been identified in early stage tumors in melanoma, whereas $pSTAT3^{Tyr705}$ has been associated with later stage cancer [141]. Further studies are required to elucidate whether these two phosphorylation sites have different roles in mediating FGFR-driven tumor growth.

Further analysis of the mechanisms driving STAT3 phosphorylation demonstrated that FGFR activation induces various IL-6 family members, which contributed to phosphorylation of $STAT3^{Tyr705}$. While these studies focused on actions of IL-6-mediated signaling in the tumor cells, it is likely that the IL-6 family members also act on neighboring epithelial cells (Figure 2.11) and cells within the tumor reactive stroma, including infiltrating inflammatory cells, to promote tumor growth and progression. Further studies are in progress to determine the relative contributions of IL-

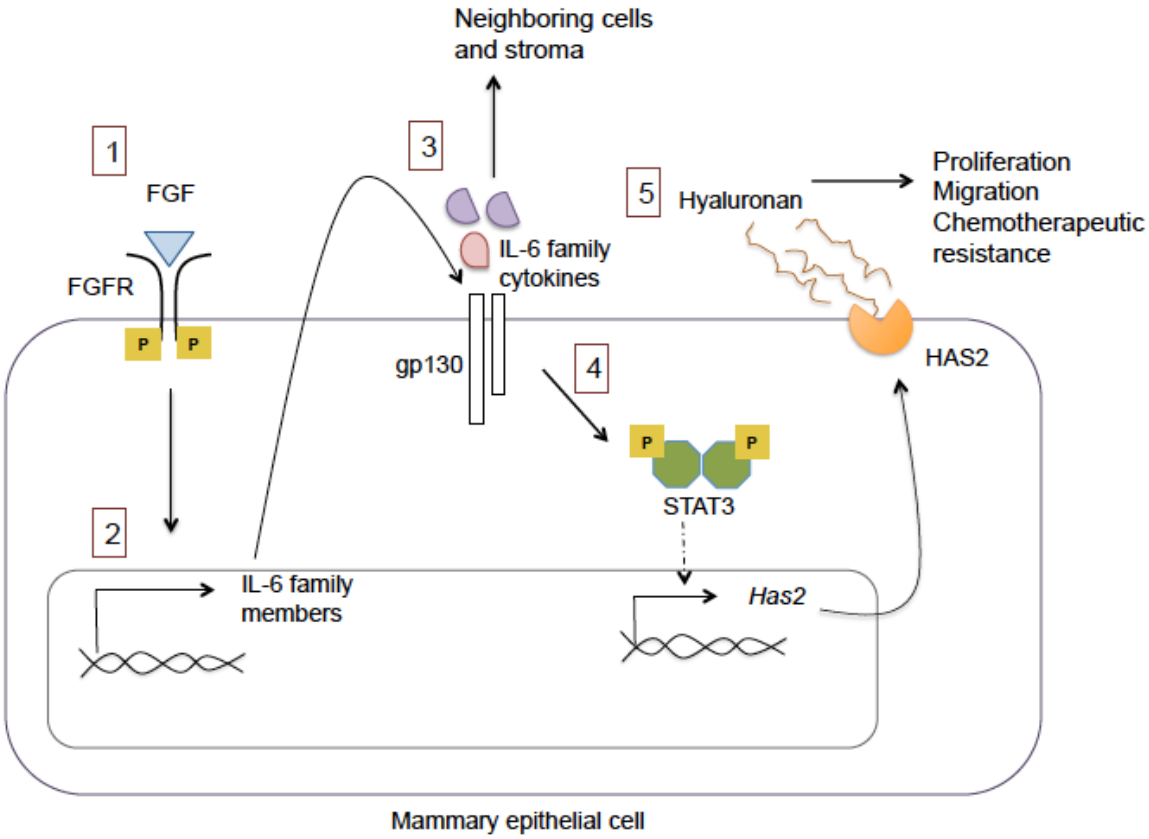

Figure 2.11 Activation of FGFR (1) leads to increased gene expression and secretion of IL-6 family members (2). These bind to the gp130 receptor (3) which activates STAT3 (4). Phosphorylated STAT3 regulates HAS2 expression (5). HAS2 stimulates production of hyaluronan (6), which is then secreted and contributes to induced proliferation, migration and chemoresistance.

6 family cytokine-induced signaling in tumor cells compared with other cell types in the microenvironment.

These studies raise the possibility that patients with high levels of FGFR activity and tumor-associated HA may be candidates for combinatorial therapies targeting both of these molecules. Consistent with this, our 3D culture studies suggest that while inhibition of FGFR in FGF-responsive cells alone does not affect cell proliferation, combinatorial treatment inhibiting both FGFR and HA synthesis leads to decreased proliferation. Whether this is due to cooperative effects of decreased signaling of both pathways or due to removal of HA surrounding the tumor cell and thus providing access of the drug to the cells, which has been demonstrated in other models [142], remains to be determined. Regardless of the mechanism, these findings provide an example of the potential therapeutic impact of designing therapeutic strategies that target both tumor cell-specific oncogenic pathways and the pro-tumorigenic microenvironment.

In conclusion, these studies define a novel pathway involving FGFR, STAT3 and HA synthesis that contribute to tumor growth. Because all of the components of these pathways are known to contribute to other tumor types as well as inflammation-related diseases, this pathway likely represents a general mechanism that can be applied more broadly than just breast cancer. Finally, these results provide important insights into the potential need for targeting growth factor driven signaling pathways within the tumor cells in combination with inhibiting HA/tumor cell interaction to more effectively treat breast cancer in patients.

Chapter 3. Disruption of STAT3 signaling in mammary tumor myeloid cells promotes tumor growth.

Introduction

Tumors arise in the complex environment of intrinsic and extrinsic drivers, and inflammation has been recognized as a critical factor contributing to tumor development [143, 144]. Abundant evidence suggests that tumor infiltrating immune cells are co-opted to aid tumor growth by secreting growth factors, remodeling the extracellular matrix, and shielding the tumor from an effective immune response [145, 146]. Infiltration of different types of immune cells into the tumor microenvironment is associated with differing patient outcomes. For example, increased percentages of tumor infiltrating $CD8^+$ T lymphocytes in breast cancers are associated with better prognosis [147]. In contrast, increased numbers of tumor infiltrating myeloid cells such as myeloid-derived suppressor cells (MDSC) and macrophages have been associated with poor patient prognosis, and depleting or "re-educating" these populations as a means to control tumor progression has been an active field of investigation [76, 143, 148-151]. Tumor-associated macrophages (TAMs) contribute to breast cancer progression through a variety of mechanisms such as production of angiogenic and growth factors, matrix-remodeling enzymes, and molecules that interfere with a productive anti-tumor immune response [152-154]. As current standards of care target primarily the epithelial compartment of breast tumors, development of novel therapeutic strategies that address the critical contributions of tumor infiltrating immune cells is warranted.

Macrophage polarization within the tumor microenvironment is thought to play a key role in tumor progression [155]. Conventionally, macrophages are thought to

assume the M1 (classical) phenotype in response to interferon-gamma (IFNγ) and pathogen-derived toll-like receptor ligands such as lipopolysaccharide (LPS). Alternatively activated macrophages (M2) are induced by the cytokines IL-4 and IL-13, as well as in response to IL-10, immunoglobulins, and glucocorticoids [94]. The two phenotypes are critical in response to infection where M1 macrophages respond initially and drive the pro-inflammatory protective cascade, while M2 macrophages develop to antagonize inflammation and orchestrate the wound-healing response. TAM polarization is often associated with an M2-like phenotype and efforts are being made to repolarize TAMs to an anti-tumor M1-like phenotype. However, more recent studies have suggested that TAMs can reside along a spectrum of the M1/M2 continuum and can express markers associated with both polarization states depending on tumor type and stage [96, 156]. Understanding how macrophages respond to the microenvironment and delineating the mechanisms that regulate their function is critical for developing therapeutic approaches that act on macrophages to control tumor growth and progression.

Signal transducer and activator of transcription (STAT) factors are thought to be important mediators of macrophage polarization. IFNγ-activated STAT1 has been linked to M1 polarization while STAT6 and STAT3, activated by IL-4/IL-13 and IL-10 respectively, have been linked to M2 polarization. Activated STAT3 has been observed in up to 30% of myeloid cells in human breast cancers and has been implicated in regulating myeloid cell function in tumors [157]. Genetic studies have suggested that myeloid-specific STAT3 activation contributes to an immunosuppressive phenotype and that ablation of STAT3 in myeloid cells leads to enhanced anti-tumor T cell responses in mouse models of melanoma and urothelial carcinoma [100]. In contrast, deletion of STAT3 in myeloid cells has also been found to enhance colitis and promote the

formation of colon tumors, possibly as a result of increased chronic inflammation that results upon deletion of STAT3, which is known to constrain pro-inflammatory responses [103]. These studies highlight the potential complexities of STAT3 function within the myeloid compartment during tumor initiation and growth.

Although STAT3 is activated in myeloid cells associated with breast cancer, the contributions of STAT3 to immune cell function during mammary tumor growth have not been investigated using conditional genetic deletion approaches. We previously developed an orthotopic transplant model dependent upon fibroblast growth factor receptor 1 (FGFR1) activation to study the contributions of the IL-6/STAT3 pathway to mammary tumor initiation and growth [28]. Activation of inducible FGFR1 led to a significant increase in STAT3-activating cytokines, such as IL-6. We demonstrate here that these soluble factors also activate STAT3 in macrophages *in vitro*, and that 20% of tumor associated macrophages exhibit activated STAT3 *in vivo*. Surprisingly, injection of tumor cells into STAT3-floxed x c-*fms-iCre* mice, in which STAT3 is efficiently deleted in macrophages and partially deleted in other myeloid and lymphoid lineages [103], led to significantly increased tumor incidence and decreased tumor latency. These phenotypes were not observed in a polyoma middle T (PyMT)-derived model in which the tumor associated macrophages exhibited lower levels of activated STAT3. $STAT3^{\Delta/\Delta}$ bone marrow derived macrophages (BMDMs) displayed an enhanced pro-inflammatory phenotype in the presence of LPS and IFNγ, consistent with published studies demonstrating that STAT3 constrains pro-inflammatory responses [103, 158]. Furthermore, we found that STAT3 deletion in BMDMs led to prolonged activation of STAT1 as well as increased expression of canonical STAT1 target genes including the immune checkpoint inhibitor molecule programmed death ligand 1 (PD-L1) both *in vitro* and within mammary TAM populations. Finally, we demonstrate that secreted factors

from the human breast cancer cell line MDA-MB-231 were able to enhance STAT1 signaling in $STAT3^{\Delta/\Delta}$ macrophages. Taken together, our results demonstrate that conditional deletion of STAT3 in immune cells leads to enhanced mammary tumor initiation and growth. Because STAT3 has oncogenic functions in breast cancer cells and is considered as a potential therapeutic target, our findings highlight the importance of understanding of STAT3 function in non-tumor cells.

Materials and Methods

Animals

B6.129S1-$STAT3^{flox/flox}$ ($STAT3^{tm1Xyfu}$) mice were purchased from The Jackson Laboratory (Bar Harbor, ME). FVB *cfms-icre* Tg(Csf1r-icre)1Jwp/J mice were provided by Dr. Elaine Lin [103]. All mice were backcrossed to the BALB/c and FVB backgrounds via the speed congenic technology provided by IDEXX RADIL (Columbia, MO). The $STAT3^{flox/flox}$ and *cfms-iCre* mice were then crossed to generate the mice lacking STAT3 expression in myeloid cells. $STAT3^{fl/fl}$/*cfms-iCre* mice are referred to as conditional-$STAT3^{\Delta/\Delta}$, while $STAT3^{fl/fl}$ littermates, which lack *cfms-iCre*, are used as controls. All experiments were performed with 6-8 week-old female mice. All animal care and procedures were approved by the Institutional Animal Care and Use Committee of the University of Minnesota and were in accordance with the procedures detailed in the Guide for Care and Use of Laboratory Animals.

Mouse treatments

For BALB/c tumor induction, $1x10^6$ HC-11/R1 cells in 50% Matrigel (BD Biosciences) were injected into the inguinal mammary fat pads of conditional-$STAT3^{\Delta/\Delta}$ and $STAT3^{fl/fl}$ mice, and mice were treated as described previously [28]. For FVB tumors, $0.5x10^6$ MMTV-PyMT tumor derived cells were injected into FVB recipient mice of the indicated genotype. All mice were examined for tumor development by palpation and were considered tumor-bearing once tumor size reached approximately 100 mm^3. Tumor growth was measured using calipers, and tumor volume was calculated using the following equation: $V=(LxW^2)/2$. All mice were injected with 30 mg/kg 5-bromo-2'-deoxyuridine (BrdU) intraperitoneally 2 hours prior to sacrifice.

Cell culture

HC-11/R1 cells were generated and maintained as described previously [22]. Bone marrow derived macrophages (BMDMs) were obtained as described previously [25]. PyMT cells, isolated from tumors generated in transgenic MMTV-PyMT mice, were provided by Dr. Felicite Noubissi and Dr. Brenda Ogle and grown in DMEM/F12, 5 µg/ml insulin (Akron Biotech) and 1 µg/ml hydrocortisone (Sigma-Aldrich), 5 µg/ml EGF (Life Technologies), 5% fetal bovine serum and 1% penicillin-streptomycin (Life Technologies). MDA-MB-231 cells were obtained from ATCC and maintained in DMEM supplemented with 10% FBS and 1% Pen/Strep (Invitrogen). All cells were grown at 37°C and 5% CO_2.

Cell stimulation

Serum-starved HC-11/R1 cells were treated with B/B (Clonetech) or vehicle ethanol for 24 hours, and conditioned medium (B/B CM) was collected, filtered, and used to stimulate BMDMs, previously serum-starved for 4 hours. For inhibitor treatments,

BMDMs were pre-treated with 50μM SC144 (Sigma-Aldrich) or solvent DMSO for 1 hour. 50μM SC144 or equivalent amount of DMSO were then added to the treatment as indicated.

Immunoblot analysis

Cell were lysed in RIPA buffer containing protease inhibitors as previously described [28]. Immunoblot analysis was performed by incubating PVDF membranes overnight at 4ºC with the following antibodies: pSTAT3 (Cell Signaling #9131, 1:1000), STAT3 (Cell Signaling #12460, 1:1000), GAPDH (Cell Signaling #2118, 1:10000), pSTAT1 (Cell Signaling #9167, 1:1000), STAT1 (Cell Signaling #9172, 1:2000), β-tubulin (Cell Signaling #2146, 1:1000).

Flow cytometry

Tumors were harvested by blunt dissection and single-cell suspensions were made by mechanical disruption at room temperature, followed by 30' incubation at 37˚C in 24μg/ml Liberase TL (Roche, #05401020001) and 0.15mg/ml DNAse I (Sigma-Aldrich, #DN-25). Digestion was halted by addition of DMEM+10% FBS and centrifugation, followed by passing the cell suspension through a 70μm strainer (Falcon, #352350). Red blood cells were lysed using ACK Lysing Buffer (Lonza, #10-548E) following manufacturer's instructions. Following addition of ice-cold PBS, cell were centrifuged at 4˚C for 5' at 1500 rpm, and remaining cells were resuspended in pre-chilled FACS buffer (0.5% FBS, 10mM EDTA, 1X PBS). Samples were analyzed with LSRII (Becton Dickinson) after staining with the following antibodies: purified CD16/32 (eBioscience, #14-0161), CD3-APC (Tonbo Biosciences, #20-0031), CD4-BV605 (BioLegend, #100547), CD8-PerCP (BioLegend, #100732), F4/80-FITC (BioLegend, #123107), PD-

L1-PeCy7 (BioLegend, #124313). Fixable Viability Dye eFluor 780 was added to all samples to exclude dead cells (eBioscience, #65-0865-14). All flow data was analyzed in FlowJo software (Tree Star v.10).

Quantitative reverse transcription-PCR

RNA was extracted from cells using TriPure (Roche) and cDNA was prepared using the qScript cDNA synthesis kit (Quanta Biosciences) according to the manufacturers' protocols. Quantitative RT-PCR (qRT-PCR) was performed using PerfeCTa SYBR Green (Quanta Biosciences) and the Bio-Rad iQ5 system. The $2^{-\Delta\Delta Ct}$ method [159] was used to determine relative quantification of gene expression and normalized to *cyclophilin B (CYBP)*. Primer sequences are provided in Supplementary Table 3.1

Tissue analysis

For analysis of frozen sections, BALB/c and FVB tumors were snap frozen in OCT; 5μm thick sections were cut and fixed in acetone for 5 minutes at room temperature. Tissues were permeabilized for 10 minutes at -20˚C in pre-chilled methanol. Following an hour block in 10% normal goat serum, sections were stained for F4/80 (1:100, BioRad, #MCA49RT) and pSTAT3 (1:200, Cell Signaling, #9145) at 4˚C overnight. Secondary antibodies goat α-rat and goat α-rabbit, respectively, were incubated for 1 hour at room temperature (1:250, Invitrogen, #A11007 and #A11008), and tissues were coverslipped with ProLong Gold Antifade DAPI (Invitrogen, #P36931). For analysis of paraffin embedded sections, BALB/c tumors were fixed in 4% paraformaldehyde and paraffin embedded. 5μm thick sections were stained with hematoxylin and eosin (H&E), F4/80 (1:100, no antigen retrieval, BioRad, #MCA49RT), Keratin 8 (1:250, Developmental Studies Hybridoma Bank, TROMA-1), Keratin 14 (1:500, Covance, #PRB 155-P) and

BrdU (1:200, Abcam, #ab6326) as previously described [27, 160]. For statistical purposes, 5 images of at least 3 representative tumors were analyzed.

Statistical analysis

Experiments were performed at least three times. Statistical analysis was performed using the unpaired two-tailed Student *t*-test, one-way ANOVA, tailed Mann-Whitney test or Kaplan-Meier survival plotter (GraphPad PRISM v6) as indicated in figure legends. Differences were considered significant if the *p* value was ≤ 0.05 (*$p \leq 0.05$, **$p \leq 0.01$, ***$p \leq 0.001$).

Error bars represent mean ± SEM.

Results

STAT3 is activated in mammary tumor-associated macrophages. Activation of STAT3 in approximately 60% of breast cancer cases has been well-documented [28, 52]. However the contributions of STAT3 signaling in the tumor epithelial versus myeloid compartment have not been thoroughly evaluated in breast cancer models. To examine STAT3 activation in immune cell populations, we chose a mammary tumor model that we have previously demonstrated expresses high levels of IL-6 [28]. HC-11/R1 cells, which have been previously characterized, express an inducible FGFR1 that can be activated by treating cells with the B/B homodimerizer [22]. Activation of inducible FGFR1 in these cells leads to increased production of IL-6 family cytokines, which activates STAT3 in an autocrine manner, contributing to tumor cell proliferation and migration [28]. As shown previously, activation of inducible FGFR1 in mammary

epithelial cells leads to macrophage recruitment and activation [25]. Therefore, further studies were performed to determine whether soluble factors produced following iFGFR1 activation were capable of activating STAT3 in macrophages *in vitro*. Serum starved HC-11/R1 cells were treated with solvent control or B/B overnight, and conditioned medium (B/B CM) was collected for treatment of primary BMDM. Levels of pSTAT3 were examined using immunoblot analysis (Figure 3.1A). Activation of STAT3 in BMDMs was observed within 10 minutes of exposure to B/B CM, and returned to baseline levels at approximately 90 minutes post-treatment. As we have previously established the high level of IL-6 family of cytokines secreted following activation of the FGFR pathway, we sought to determine their contribution to STAT3 activation in macrophages [28]. As shown in Figure 3.1B, treatment of BMDM with the inhibitor of the IL-6 family common receptor subunit gp130 SC144 lead to reduced STAT3 phosphorylation, indicating that IL-6 family of cytokines contribute significantly to STAT3 activation.

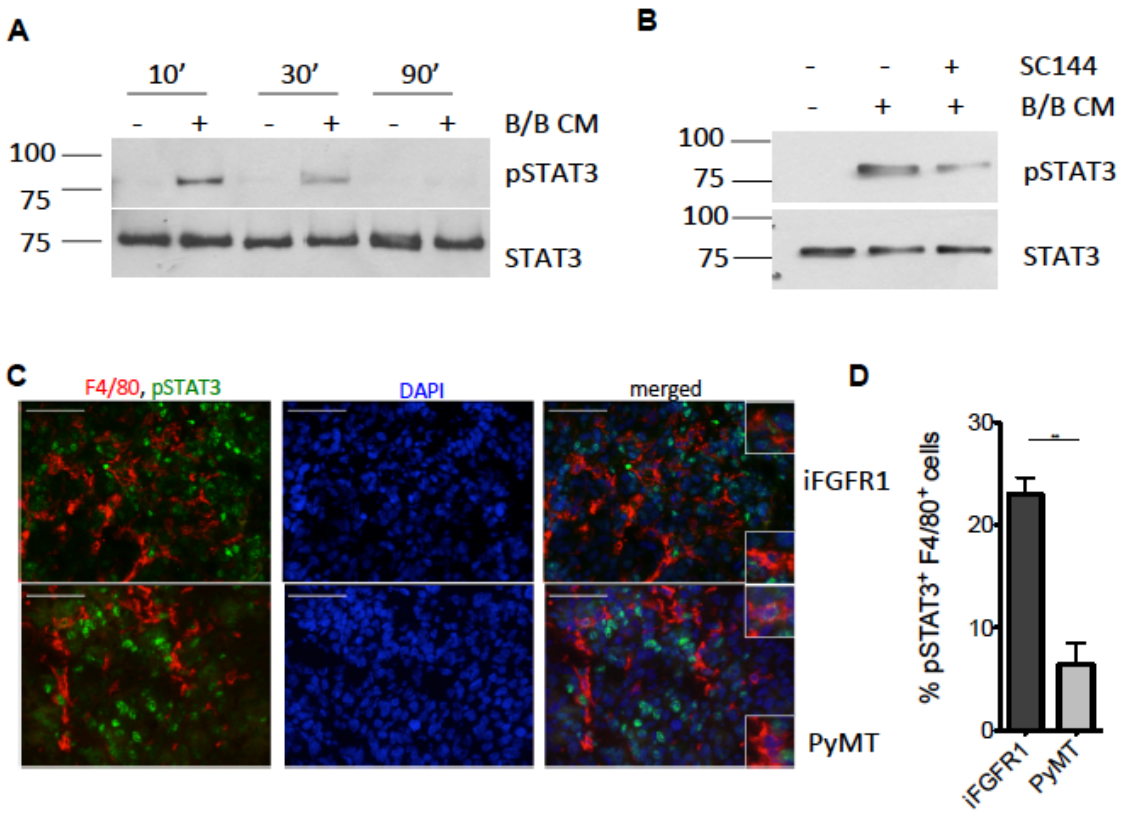

Figure 3.1. STAT3 is activated in mammary tumor-associated macrophages. A. Confluent, serum-starved HC-11/R1 cells were treated with B/B to activate iFGFR1 for 24 hours, and their media was collected and used to treat BMDMs for 10, 30, and 90 minutes. Immunoblot analysis was performed to detect levels of phosphorylated STAT3 (pSTAT3). Levels of total STAT3 are shown as to indicate equal protein loading. **B.** Conditioned media (B/B CM) was collected as described in A. BMDM were serum-starved and pre-treated for 1 hour with 50μM SC144 or solvent control DMSO, at which point B/B CM and SC144 were added for 30 minutes, and levels of pSTAT3 were examined by immunoblot. **C.** 6-week-old mice were injected orthotopically with either iFGFR1 or PyMT and tumors were allowed to develop. 5μM frozen sections were stained for F4/80 (red), pSTAT3 (green), or DAPI (blue) and analyzed using fluorescence microscopy. Scale bar represents 50μm. **D.** Images generated in **C** were used to count total number of macrophages (F4/80+) and the number of macrophages with positive nuclear pSTAT3 signal (pSTAT3+/F4/80+). At least five images from three separate animals were analyzed and results were compared using unpaired Student *t*-test.

Tumor-associated myeloid cells deficient in STAT3 promote growth in FGFR1 dependent tumors. Based on the observation that STAT3 is activated in a subset of mammary TAMs, further studies were performed to determine whether STAT3 signaling in myeloid cells contributes to tumorigenesis. HC-11/R1 were injected into the mammary fat pads of either $STAT3^{fl/fl}$ or conditional-$STAT3^{\Delta/\Delta}$ Balb/c mice. The mice were evaluated for tumor onset and tumor growth rate. Conditional-$STAT3^{\Delta/\Delta}$ mice developed tumors significantly sooner than the control $STAT3^{fl/fl}$ group, and tumors grew at a significantly faster rate (Figure 3.2A, B). In parallel experiments, PyMT cells were injected into $STAT3^{fl/fl}$ or conditional-$STAT3^{\Delta/\Delta}$ FVB mice. We observed no difference in either tumor latency or tumor growth rate in the mice injected with PyMT cells (Figure 3.2C, D). In order to further characterize the HC-11/R1-derived tumors, we performed H&E staining (Figure 3.3A). The tumors appeared histologically similar after H&E staining. Tumor sections were stained for nuclear BrdU incorporation, which revealed increased rate of cell proliferation in tumors generated in conditional-$STAT3^{\Delta/\Delta}$ hosts (Figure 3.3B). Further analysis by flow cytometry revealed that macrophages represented a similar percentage of total cells between $STAT3^{fl/fl}$ and $STAT3^{\Delta/\Delta}$ tumors, suggesting that myeloid cell function was affected by the lack of STAT3 signaling but not macrophage recruitment (Figure 3.3C).

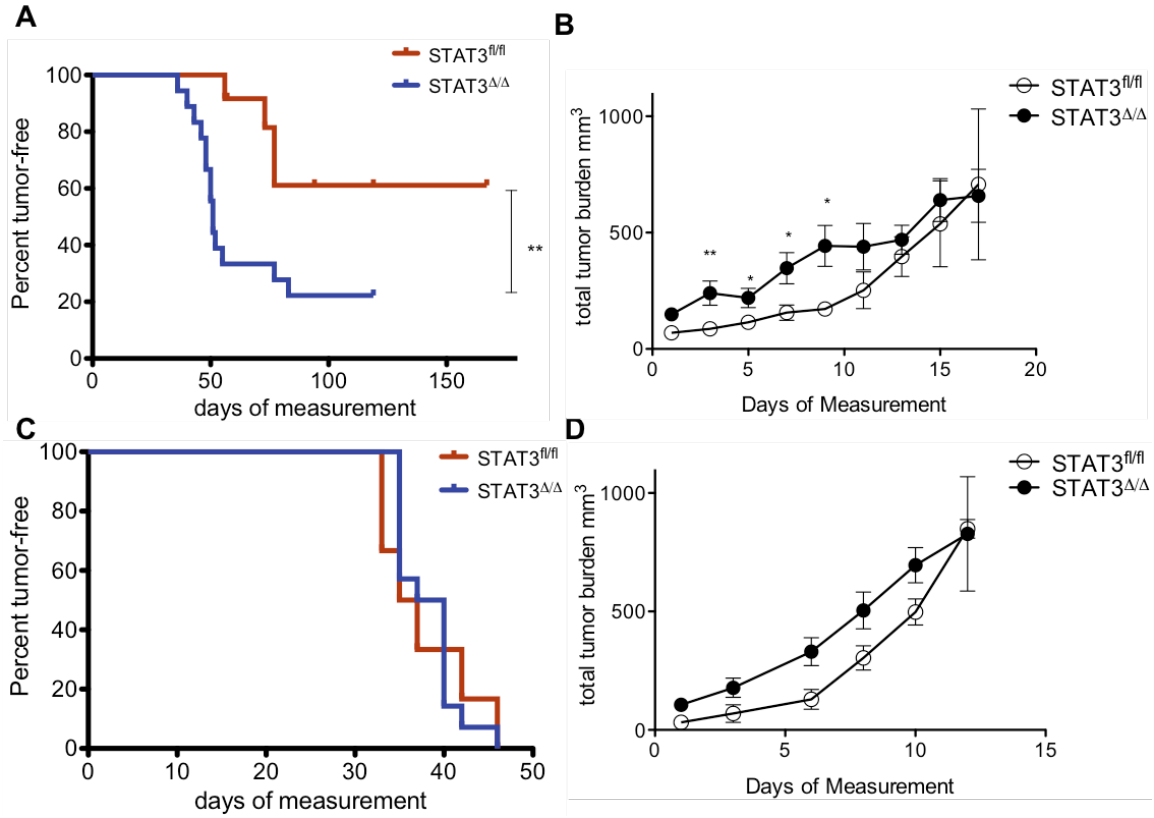

Figure 3.2. Tumor-associated myeloid cells deficient in STAT3 promote growth in FGFR1 dependent tumors. 6-week-old STAT3$^{fl/fl}$ (n=6) or conditional-STAT3$^{\Delta/\Delta}$ (n=9) Balb/c mice were orthotopically injected with 1x10^6 HC-11/R1 cells in each inguinal mammary gland. Mice were examined by palpation for tumor development twice weekly (**A**), and once tumors reached 100mm^3, they were measured every day by caliper (**B**). 6-week-old STAT3$^{fl/fl}$ (n=3) or conditional-STAT3$^{\Delta/\Delta}$ (n=7) FVB mice were orthotopically injected with 0.5x10^6 PyMT cells in each inguinal mammary gland. Tumor measurements were conducted as described in **A** and **B**.

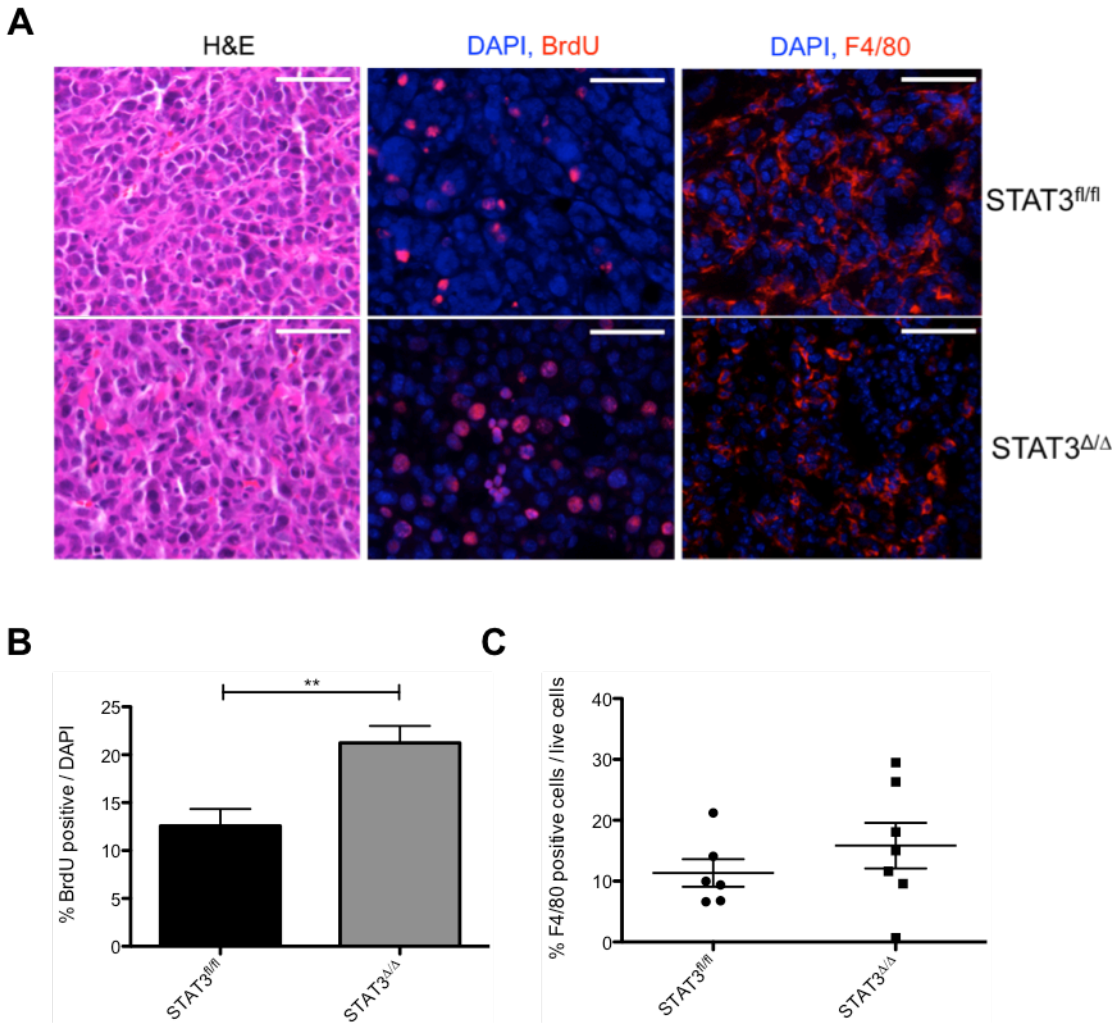

Figure 3.3. Tumor myeloid cells deficient in STAT3 promote tumor cell proliferation *in vivo*. A. 5μm-thick paraffin-embedded sections of the HC-11/R1 tumors generated in Figure 3.2A were stained with hematoxylin and eosin (H&E, left panel), BrdU (red, middle panel), or F4/80 (red, right panel). Scale bars represent 50μm. **B.** $BrdU^{+}$ cells were counted across at least five images in three mice per genotype, and their percentage of total DAPI stained nuclei was calculated. Means were compared using unpaired Student *t*-test. **C.** The percentage of $F4/80^{+}$ cells among all single live cells within control and $STAT3^{\Delta/\Delta}$ HC-11/R1 tumors were calculated using flow cytometry as described in the Methods section. Means were not statistically different.

STAT3-deficient macrophages display an enhanced pro-inflammatory phenotype in the presence of M1 stimuli. STAT3 has a well-defined role in regulating the anti-inflammatory response downstream of IL-10 [161]. However, the mechanisms of STAT3 activation and function in the induction of the M1 phenotype have not been thoroughly investigated. Therefore, we sought to examine primary macrophage responses to the canonical M1 and M2 stimuli. We differentiated macrophages from the bone marrow of $STAT3^{fl/fl}$ and conditional-$STAT3^{\Delta/\Delta}$ mice (Figure 3.4A) and treated them with LPS/IFNγ (M1) and IL-4/IL-13 (M2). We examined the levels of several well-defined M1 and M2 markers by qRT-PCR (Figure 3.4B,C). As expected, expression of canonical M2 markers such as IL-10, arginase I (ArgI), and mannose receptor 1 (Mrc1/CD206) were reduced in BMDM lacking STAT3 compared to $STAT3^{fl/fl}$ cells (Figure 3.4C). Conversely, expression of several M1 chemokines and cytokines exhibited significantly higher expression in $STAT3^{\Delta/\Delta}$ macrophages compared to $STAT3^{fl/fl}$ cells (Figure 3.4B). Specifically, increased gene expression levels of the chemokines *Ccl2* and *Ccl5*, as well as increased levels of the inflammatory cytokines *Ptgs2* and *Il-12* were observed. Expression levels of *Tnfα* and *Il-1β* were not significantly different in conditional-$STAT3^{\Delta/\Delta}$ macrophages compared to $STAT3^{fl/fl}$ macrophages, suggesting that only a subset of M1 markers are affected by loss of STAT3 (data not shown). Additional studies were performed to assess macrophage responsiveness to IL-6, a key tumor cell-derived cytokine that activates STAT3 in macrophages. $STAT3^{fl/fl}$ and $STAT3^{\Delta/\Delta}$ BMDM were treated with rIL-6, and the expression levels of the previously described panel of M1/M2 molecules were examined by qRT-PCR. Among the IL-6 regulated molecules, *Ccl2* showed a significant increase, and *Il-10* showed significant decrease in expression in the $STAT3^{\Delta/\Delta}$ BMDM compared to the $STAT3^{fl/fl}$ (Figure 3.4D, E). These findings indicate that

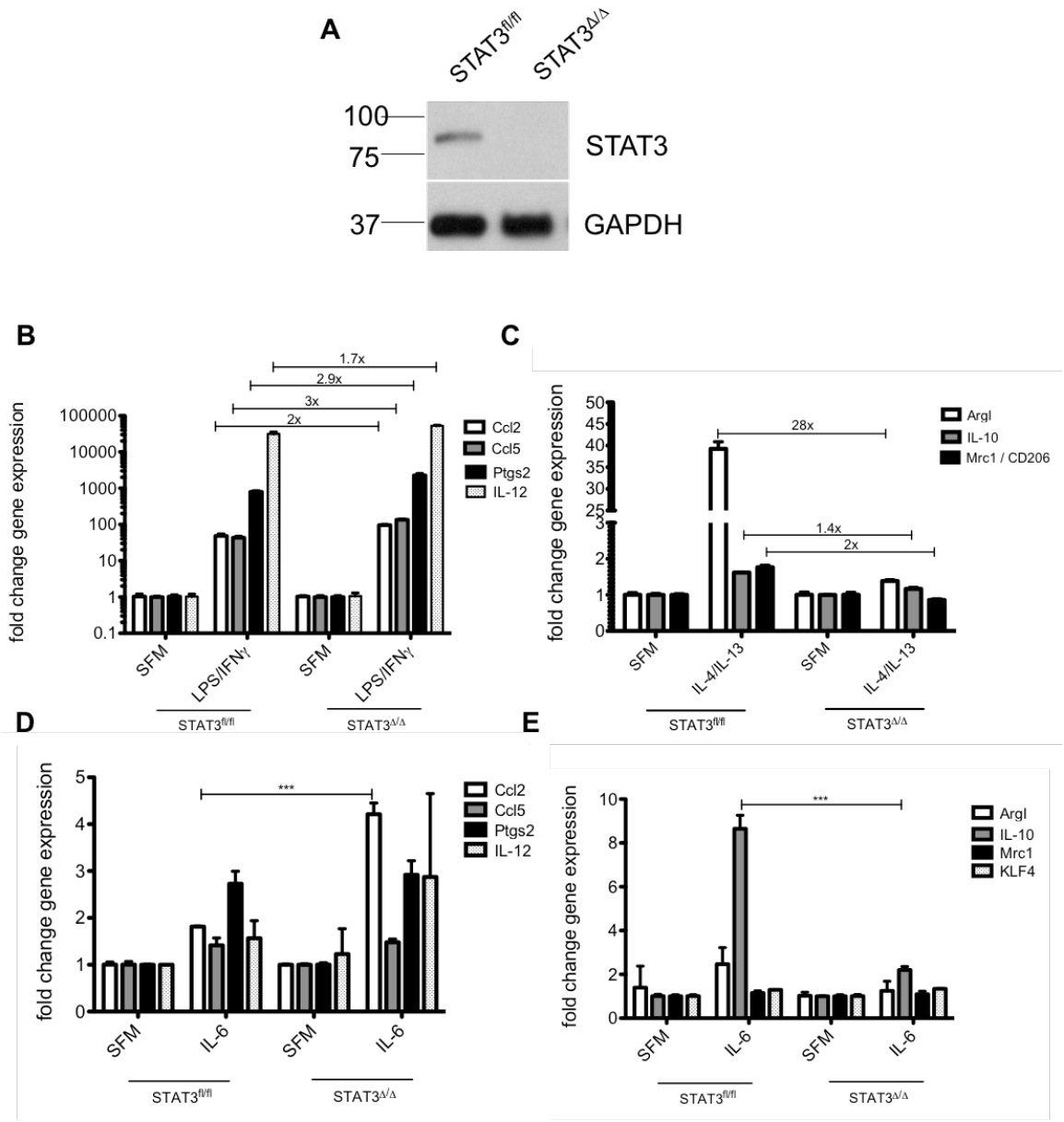

Figure 3.4. STAT3-deficient macrophages display an enhanced pro-inflammatory phenotype. A. BMDM were isolated from STAT3$^{fl/fl}$ and conditional-STAT3$^{\Delta/\Delta}$ mice, as described in the Methods section, and protein lysates were analysed by immunoblot for levels of STAT3 expression. Levels of the housekeeping protein GAPDH are presented as loading control. BMDM were serum-starved and treated with (**B**) 20ng/ml IFNγ + 20ng/ml LPS, (**C**) 20ngml IL-4 + 20ng/ml IL-13, or (**D, E**) 100ng/ml rIL-6 and gene expression levels of M1/M2 markers were determined by qRT-PCR. All gene levels are normalized to the expression of the housekeeping gene *Cyclophilin B*. Expression levels were compared between genotypes in each experiment using one-way ANOVA. Graphs are representative of 3 separate experiments.

in the absence of STAT3 signaling, macrophages display an enhanced pro-inflammatory phenotype in response to pro-inflammatory stimuli.

STAT1 activation is enhanced in STAT3-deficient macrophages. Previously published studies have suggested a role for STAT3 in attenuating the functions of another STAT family member STAT1 [162, 163]. STAT1 is phosphorylated in response to IFNγ and orchestrates a potent inflammatory response in macrophages [164]. Therefore, further studies were performed to assess STAT1 activity in STAT3 deleted macrophages. $STAT3^{fl/fl}$ and $STAT3^{\Delta/\Delta}$ BMDMs were treated with rIL-6 in a time course experiment and levels of phosphorylated STAT1 (pSTAT1) were examined by immunoblot analysis (Figure 3.5A). As previously reported, STAT1 was weakly but transiently activated at 30 minutes in $STAT3^{fl/fl}$ cells [38, 162]. In contrast, rIL-6 treatment led to enhanced and sustained pSTAT1 levels in $STAT3^{\Delta/\Delta}$ BMDMs (Figure 3.5A). To examine the ability of tumor cell derived factors to regulate macrophage STAT signaling in a similar manner, $STAT3^{fl/fl}$ and $STAT3^{\Delta/\Delta}$ BMDMs were treated with conditioned media derived from the human breast cancer line MDA-MB-231. The levels of pSTAT3 and pSTAT1 were examined by immunoblot analysis. As shown in Figure 3.5B, tumor cell secreted factors activated preferentially activated STAT3 over STAT1 in macrophages. However, in the absence of STAT3, exposure of $STAT3^{\Delta/\Delta}$ BMDMs to MDA-MB-231-derived factors resulted in enhanced phosphorylation of STAT1, similar to the findings described above.

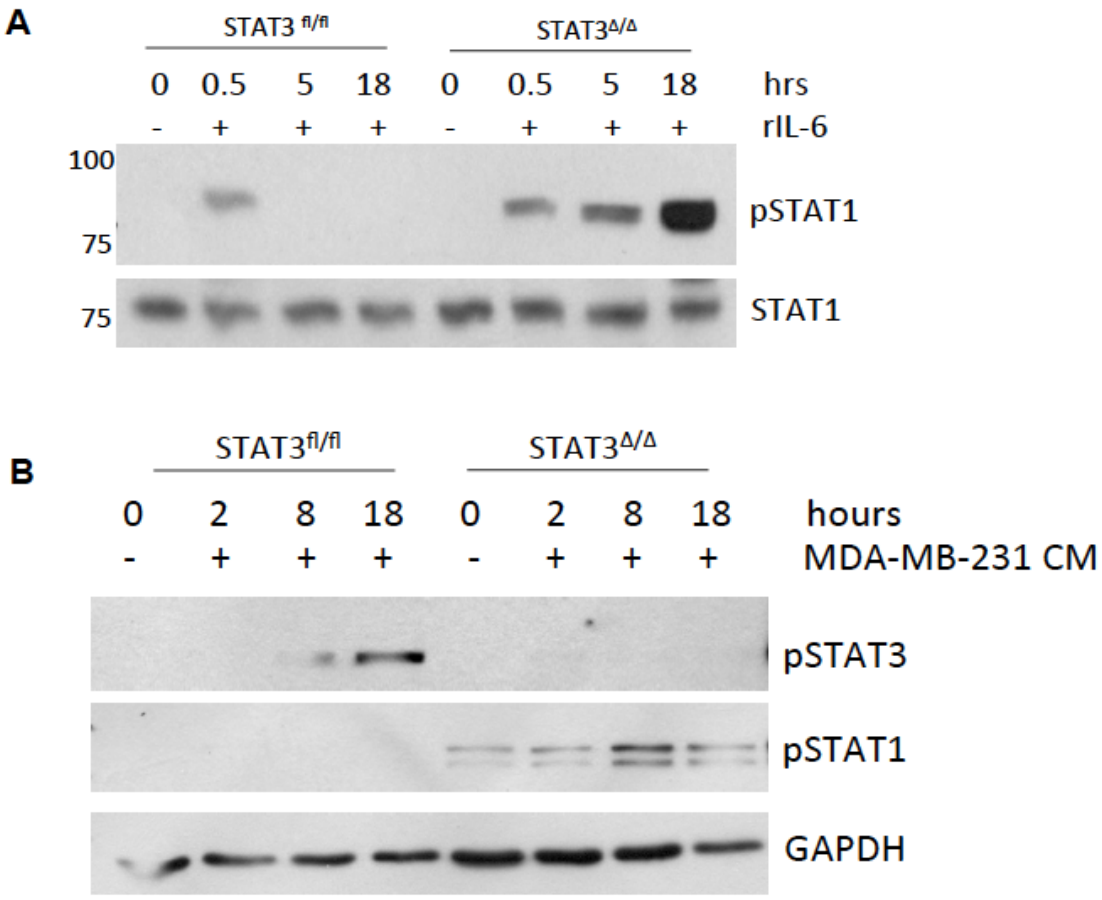

Figure 3.5. STAT1 activation is enhanced in STAT3-deficient macrophages. A. STAT3$^{fl/fl}$ or STAT3$^{\Delta/\Delta}$ BMDM were serum-starved and treated with 100ng/ml rIL-6 for 30 minutes, 5 hours or 18 hours. Protein lysates were analyzed for pSTAT1 and total STAT1 by immunoblot. **B.** Human MDA-MB-231 cells were grown to confluence and serum-starved overnight. Secreted factors were collected and used to treat STAT3$^{fl/fl}$ or STAT3$^{\Delta/\Delta}$ BMDM for 2 hours, 8 hours, or 18 hours. Protein lysates were analyzed for levels of pSTAT3 and pSTAT1. Levels of GAPDH are shown as a loading control.

Expression of downstream STAT1-target genes is upregulated in STAT3$^{\Delta/\Delta}$ macrophages. Further studies were performed to determine whether STAT3 deletion in macrophages led to enhanced expression of STAT1 target genes. *Cxcl9* and *Cxcl10,* which are canonical STAT1 target genes, were examined by qRT-PCR in STAT3$^{fl/fl}$ and STAT3$^{\Delta/\Delta}$ cells following rIL-6 treatment. A significant increase in gene expression levels of both chemokines was observed in the STAT3$^{\Delta/\Delta}$ cells (Figure 3.6A). These results suggest that in the absence of STAT3, IL-6 activates STAT1 and induces expression of STAT1 downstream transcriptional targets. *Pd-l1* is another STAT1-dependent gene expressed by most antigen-presenting immune cells, including macrophages, in response to pro-inflammatory stimuli [165]. Therefore, we examined the levels of PD-L1 in STAT3$^{fl/fl}$ and STAT3$^{\Delta/\Delta}$ BMDMs treated with rIL-6. A significant upregulation of *Pd-l1* gene expression was observed in rIL-6-treated STAT3$^{\Delta/\Delta}$ BMDMs compared to rIL-6-treated control cells (Figure 3.6A). Furthermore, when PD-L1 surface expression was examined by flow cytometry, STAT3$^{\Delta/\Delta}$ BMDMs treated with rIL-6 displayed significantly higher MFI levels than STAT3$^{fl/fl}$ BMDMs (Figure 3.6B). As the pro-tumor effects of PD-L1 expression are well documented in a variety of tumor types, we assessed the levels of PD-L1 on the surface of TAMs from STAT3$^{fl/fl}$ and conditional-STAT3$^{\Delta/\Delta}$ tumors. Significantly higher expression of PD-L1 was observed on F4/80^{+} macrophages isolated from iFGFR1-driven tumors in conditional-STAT3$^{\Delta/\Delta}$ mice when compared to controls (Figure 3.6C). Next, we sought to determine whether the observed increase of *Pd-l1* expression in STAT3$^{\Delta/\Delta}$ BMDMs was dependent on activation of STAT1. As STAT1 phosphorylation relies on the activation of JAK1, we treated cells with JAK1/2 selective inhibitor ruxolitinib (Figure 3.6D). *Pd-l1* increase in STAT3$^{\Delta/\Delta}$ BMDM treated with rIL-6 was abolished in the presence of ruxolitinib, but not the solvent control DMSO, suggesting that *Pd-l1* expression depends on JAK/STAT signaling. These findings

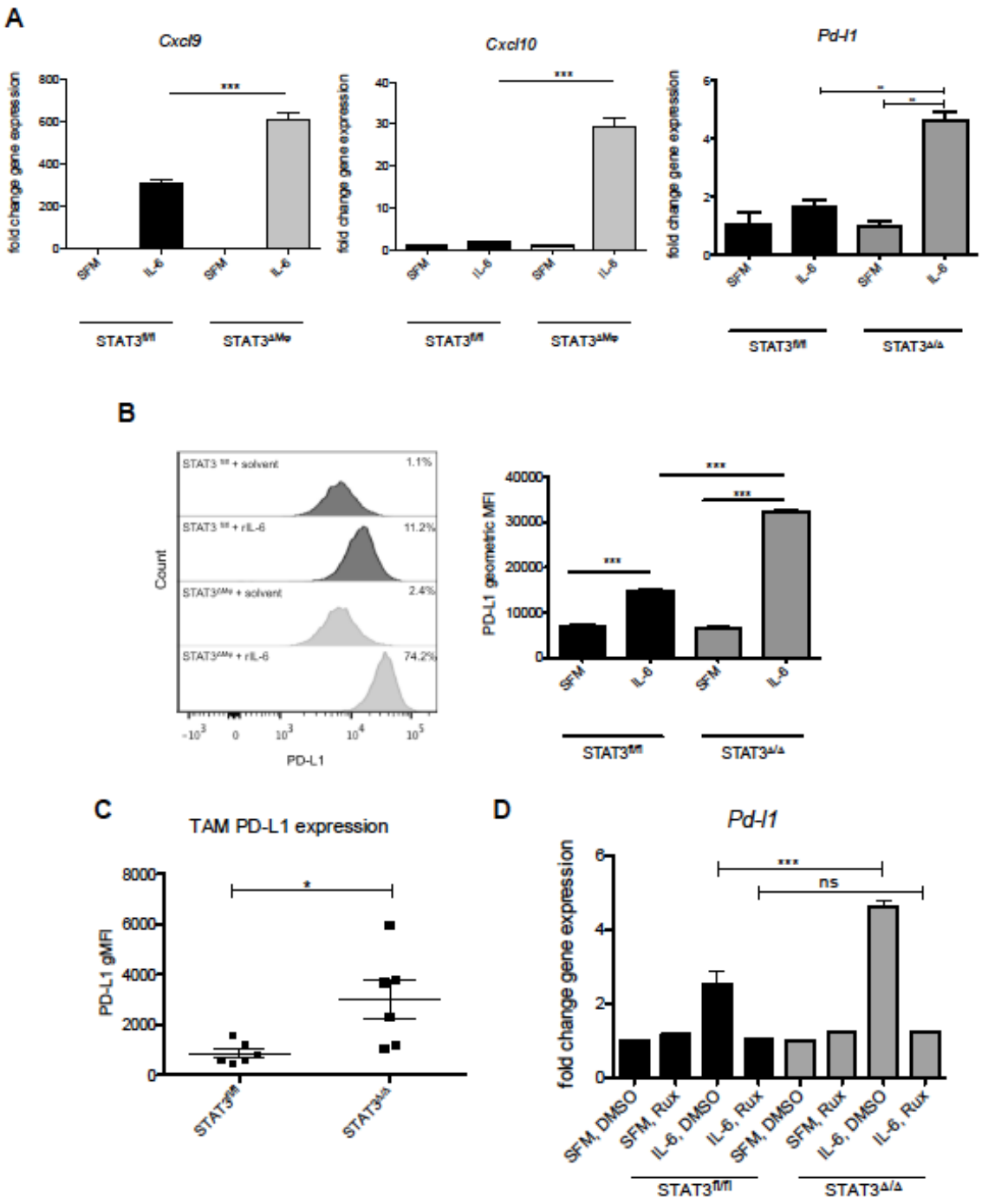

Figure 3.6. Expression of downstream STAT1-target genes is upregulated in STAT3$^{\Delta/\Delta}$ macrophages. A. STAT3$^{fl/fl}$ or STAT3$^{\Delta/\Delta}$ BMDM were serum-starved and treated with 100ng/ml rIL-6 for 2 hours. *Cxcl9, Cxcl10,* and *Pd-l1* mRNA levels were examined by qRT-PCR. **B.** BMDM were treated with 100ng/ml rIL-6 for 18 hours and surface expression of PD-L1 was examined by flow cytometry. Flow plots shown are representative images. **C.** PD-L1 expression on single, live, F4/80^{+} cells within

(*Figure 3.6* continued)

HC-11/R1-derived tumors was examined by flow cytometry. **D.** $STAT3^{fl/fl}$ or $STAT3^{\Delta/\Delta}$ BMDM were treated with pre-treated with 1μM ruxolitinib or the solvent control DMSO for 1 hour. Following pre-treatment, cells were treated with 100ng/ml rIL-6 and/or 1μM ruxolitinib for 2 hours. Levels of *Pd-l1* expression were determined by qRT-CPR. Changes in means were examined using a Student *t*-test in **A, B,** and **C**, or by one-way ANOVA in **D.**

suggest that although STAT3$^{\Delta/\Delta}$ BMDM display an enhanced pro-inflammatory phenotype, their ability to mount an effective anti-tumor immune response might be compromised due to concurrent upregulation of pro-tumor molecules, such as PD-L1.

Discussion

STAT3 activation has been implicated in suppressing the pro-inflammatory response and enhancing M2 polarization in macrophages [158]. However, previous studies have demonstrated that STAT3 function in myeloid cells in the context of cancer is complex. Numerous studies have linked constitutively activated STAT3 with blocking maturation of dendritic cells and enhancing pro-tumor activity in myeloid cells [99-101, 166]. In a mouse model of colon carcinoma, Nefedova *et al.* demonstrated that dendritic cells isolated from tumor-bearing animals exhibited higher levels of pSTAT3 and stimulated T cell activation less efficiently than those isolated from control mice [99]. Additional studies have reported increased anti-tumor immune response following *Mx-cre* mediated hematopoietic STAT3 ablation in subcutaneous mouse models of melanoma and urothelial carcinoma [100]. In contrast, other studies have indicated that STAT3 activation in immune cells might serve an anti-tumor function as well. Deng et al. reported development of spontaneous colon tumors in STAT3^{fl} *Csf1r-iCre* mice, establishing a role for myeloid cell-specific STAT3 in protecting intestinal epithelial cells from the effects of excessive inflammation [103]. Furthermore, in a recent study by Kumar et al., the authors observed reduced STAT3 activity in both MDSC and macrophage populations in several tumor models [104]. Closer examination revealed that STAT3 downregulation was required for TAM accumulation within mammary tumors, and expression of constitutively active myeloid STAT3 together with depletion of

polymorphonuclear-MDSCs inhibited tumor growth [104]. These findings are consistent with data from a mouse medulloblastoma model where STAT3^{fl}*LyzM-cre* conditional deletion of myeloid STAT3 reversed the accumulation of granulocyte-MDSCs and enhanced the ratio of effector : regulatory T cells, but overall failed to affect tumor growth [105]. Finally, in a recent study by Bottos *et al*., systemic JAK inhibition resulted in increased metastasis of mammary tumors due to ineffective maturation of natural killer cells. The authors observed no change in metastasis rate in immunocompromised mice, providing evidence that the effect of JAK inhibition was due to an impaired immune response [167]. Together, these studies highlight the complexities of STAT3 activity in immune cells and suggest that the cell type specificity of genetic deletion may have important consequences for functional outcomes.

Our studies are the first to report the effects of STAT3 deletion in myeloid cells on mammary tumor growth. Our findings are consistent with STAT3 deficiency in myeloid cell populations leading to enhanced tumor formation. Notably, the extent of phenotype observed correlated with the amount of activated STAT3 in macrophages in the tumor microenvironment. These findings would suggest that identifying the levels of STAT3 activity in the tumor microenvironment may be critical for determining how a tumor might respond to STAT3 inhibition. The broad spectrum of tumor phenotypes published previously following STAT3 deletion also points to the need for detailed analysis of all cell populations affected by the particular genetic drivers of *cre* expression. *Csf1r-iCre* is expressed in all cells that at a certain developmental timepoint require CSF-1 signaling. This population consists primarily of monocytes, tissue-resident macrophages and granulocytes; however certain populations of dendritic cells and lymphocytes are also affected by CSF-1 signaling, albeit to a much lower extent [103, 168, 169]. The studies presented here focused primarily on the effects of STAT3

deletion in tumor myeloid cells due to the large number of tumor-infiltrating macrophages. Nonetheless, further studies are warranted to elucidate the contributions of additional CSF1-R-dependent immune populations to tumor growth and development.

Consistent with published studies, we found that loss of STAT3 in macrophages led to enhanced expression of pro-inflammatory mediators in response to canonical M1 stimuli [103, 158]. To better mimic the factors found within the tumor microenvironment that activate STAT3 in macrophages, we examined the levels of inflammatory mediators produced by $STAT3^{\Delta/\Delta}$ BMDM in response to the pro-tumor cytokine IL-6. IL-6 induced expression of a subset of M1/M2 markers in a STAT3 dependent manner, several of which are known to contribute to mammary tumor growth and progression, including Cox-2, CCL2 and PD-L1 [26, 170-173]. Therefore, the pro-tumor effects of STAT3 deletion in myeloid cells could potentially be due to a combination of factors and defining which of these factors functionally contribute to the enhanced tumor formation in the conditional-$STAT3^{\Delta/\Delta}$ animals requires further investigation.

In an effort to delineate the mechanism leading to upregulation of inflammatory molecules in the absence of STAT3, we examined the activation of STAT1, a well-known mediator of inflammation [174]. Previously reported studies have shown that mouse embryonic fibroblasts (MEFs) lacking STAT3 exhibit enhanced STAT1 signaling in response to IL-6 stimulation, leading to an IFNγ-like response [162]. We show here that $STAT3^{\Delta/\Delta}$ BMDM, similarly to $STAT3^{\Delta/\Delta}$ MEFs, upregulate STAT1 signaling in response to IL-6 and express significantly higher levels of STAT1 target genes, including *Cxcl9*, *Cxcl10* and *Pd-l1*, than $STAT3^{fl/fl}$ controls. The precise mechanism that guides this switch is unknown, and several hypotheses have been proposed. IL-6 signaling is known to phosphorylate JAK1, JAK2, and Tyk2, which are all able to recruit and activate STAT1 and STAT3 [175]. It is possible that the relative abundance of STAT1 and STAT3 within

the cell as well as their affinity for the phosphorylated JAKs influence the overall outcome and determine the specificity, strength and longevity of STAT activation [175]. This plasticity in STAT regulation suggests that the contribution of STAT signaling to TAM functions is complex and evolves alongside the repertoire of secreted factors in the tumor microenvironment. Previous studies have suggested that STAT1 activation in breast tumors can be beneficial and results in enhanced anti-tumor response; however more recent findings indicate a correlation between *STAT1* expression in macrophage-rich tumors and worse breast cancer patient outcomes [176, 177]. In addition, Kusmarstev and Gabrilovich have shown that TAMs ability to induce T cells apoptosis in a mouse model of colon cancer was dependent on STAT1 signaling [178]. The results we report here further demonstrate a role of STAT1 in the pro-tumor phenotype of tumor-associated myeloid cells.

STAT3 has emerged as an attractive therapeutic target due to its high levels of activity in breast cancer cells [179]. As a result, several clinical trials have begun testing STAT3-specific, as well as broader JAK-targeting, inhibitors in breast cancer patients ([180-182] ClinicalTrails.gov identifier: NCT02876302). Previous studies, such as those outlined above, together with our current findings suggest that targeting JAK/STAT activation alone can lead to unexpected results such as enhancing tumor development or metastasis. Careful analysis of the effects of these inhibitors on non-tumor cells within the tumor microenvironment could provide rationale for combination therapy where potentially harmful effects of JAK/STAT inhibition are reversed through immune therapy, such as exogenous IL-15 [167]. The results presented here reveal the complexity of JAK/STAT signaling in myeloid cells leading to novel mechanisms of tumor immune evasion possible through upregulation of pro-tumor STAT1-target genes. We observed increased expression of several pro-inflammatory mediators, such as Cox-2, *in vitro* and

detected elevated levels of PD-L1 *in vivo*. We have previously demonstrated that inhibition of some of these pro-inflammatory pathways using small molecule inhibitors, such as celecoxib, decreases mammary tumorigenesis. The findings outlined in this report propose a novel therapeutic opportunity, combing targeted small molecule JAK/STAT inhibition with therapies that fine-tune the immune response such as immune checkpoint inhibitors or macrophage-depleting agents.

Supplemental Table 3.1 Mouse primer sequences used in qRT-PCR experiments.

Gene name	Forward 5' - 3'	Reverse 5' - 3'
Arg1	CTC CAA GCC AAA GTC CTT AGA G	AGG AGC TGT CAT TAG GGA CAT C
Ccl2 / MCP-1	TTA AAA ACC TGG ATC GGA ACC AA	GCA TTA GCT TCA GAT TTA CGG GT
Ccl5 / RANTES	TGC TTT GCC TAC CTC TCC CTA G	CGA GTG ACA AAC ACG ACT GCA
Cxcl9	TTT TGG GCA TCA TCT TCC TGG	GAG GTC TTT GAG GGA TTT GTA GTG G
Cxcl10	CCA AGT GCT GCC GTC ATT TTC	GGC TCG CAG GGA TGA TTT CAA
CycB	TGC AGG CAA AGA CAC CAA TG	GTG CTC TCC ACC TTC CGT
Il-10	CTG GAC AAC ATA CTG CTA ACC G	GGG CAT CAC TTC TAC CAG GTA A
Il-12	TGG TTT GCC ATC GTT TTG CTG	ACA GGT GAG GTT CAC TGT TTC T
Klf4	GAC CGA GGA GTT CAA CGA CC	GGG TTA GCG AGT TGG AAA GGA T
Mrc1 / CD206	CAG ATG GAA GGT CTA TGG AAC CAC	TCA AAC TTG AAT GGA AAT GCA CAG A
Pd-l1	GGC GTT TAC TGC TGC ATA ATC AG	ATT CTC TGG TTG ATT TTG CGG TAT G
Ptgs2 / Cox2	TGA GCA ACT ATT CCA AAC CAG C	GCA CGT AGT CTT CGA TCA CTA TC

Chapter 4. Discussion

Overall Summary

The studies presented in this thesis demonstrate a novel link between activation of the FGFR pathway, alterations of the tumor microenvironment and tumor immune response in mammary tumorigenesis. These studies are the first to demonstrate that FGFR signaling in epithelial cells leads to accumulation of the ECM component hyaluronan (HA) through increased production of pro-inflammatory cytokines and activation of the STAT3 pathway. Therapeutic inhibition of STAT3 *in vivo* reduced HA accumulation, which correlated with reduced tumor burden. Nonetheless, STAT3 inhibition did not result in tumor regression, suggesting that additional pro-tumorigenic mechanisms are able to sustain tumor growth. Previous work has shown that FGFR1 activation leads to rapid recruitment of macrophages with pro-tumorigenic functions [25, 27]. We hypothesized that as TAMs differentiate in the presence of FGFR1-driven IL-6 family of cytokines, the STAT3 signaling pathway would be activated and would influence TAM differentiation. Therefore, further studies focused on delineating the STAT3-dependent phenotype and function of mammary TAMs. Utilizing a mouse model of genetic *STAT3* ablation within myeloid cells demonstrated decreased tumor latency and increased tumor growth rate in conditional-STAT3$^{\Delta/\Delta}$ mice compared to control animals. These results provide evidence to the hypothesis that STAT3 activation in different tumor and immune cell populations can result in both pro- and anti-tumor phenotypes, and detailed understanding of these mechanisms is necessary for developing effective therapeutic approaches.

A. FGFR activation leads to increased HA production

Chapter 2 of this thesis investigated the downstream signaling events following FGFR activation in mammary tumor cells. Our studies demonstrated that activation of FGFR in both mouse and human breast cancer cell lines resulted in increased HA production. Inhibition of HA production significantly decreased FGFR1-driven cell proliferation, migration, and resistance to chemotherapy. These data suggest that ECM alterations contribute significantly to tumorigenesis. HA is a vital ECM component of most healthy tissues providing structural support and organization [67]. Therefore, its localization, production, and extracellular modifications are tightly controlled, and dysregulation of any of these processes has been associated with tumor development [67, 71]. In our studies, we demonstrated inhibition of HA accumulation via inhibition of upstream signaling pathways, however we were not able to address the consequences of direct HA depletion on mammary tumorigenesis. *In vivo* studies of HA contributions to tumor development have been hampered by the paucity of HA inhibitors optimized for *in vivo* use. 4-MU is the only currently available inhibitor of HA synthesis, and its short *in vivo* half-life necessitates twice daily oral gavage of experimental animals, which results in labor-intensive, high-cost studies. Further studies of the effects of HA inhibition on mammary tumor development will likely rely on the alternative delivery method of 4-MU incorporated into mouse chow, which has been shown to be effective in long-term *in vivo* experiments of HA depletion [183, 184].

Our studies thus far have examined the final amounts of HA produced in response to FGFR activation *in vitro* and *in vivo*, however we have not investigated the patterns of HA localization and fragmentation in mammary tumor development. Hyaluronidases are enzymes responsible for cleaving high molecular weight HA into

smaller fragments under specific conditions such as tissue damage or disease [185]. Whereas high molecular weight HA (HMW) is known to contribute to healthy tissue architecture, low molecular weight (LMW) fragments have been shown to promote inflammation and contribute to “cancerized stroma” [71]. Preliminary gene expression studies showed increased expression of the Hyaluronidase genes *Hyal1* and *Hyal2* in HC-11/R1 cells after iFGFR1 activation (data not shown). Our lab is currently working to characterize the pattern of HA fragmentation in a progression of breast cancer cell lines, as well as the interaction of those fragments with the HA receptor CD44. Studies in the field of pancreatic ductal adenocarcinoma (PDA) development have demonstrated that HA is a major component of the highly reactive PDA stroma and contributes to the increased interstitial fluid pressure (IFP), which limits the effectiveness of systemic anti-tumor therapies [186]. These findings have lead to the development of modified recombinant hyaluronidase (PEGPH20), which upon intravenous administration was able to efficiently deplete stromal HA in an autochthonous PDA model and restore IFP levels to that of normal pancreatic tissue. This led to increased blood perfusion, more efficient delivery of the chemotherapeutic agent gemcitabine, and significant increase in survival of tumor-bearing animals treated with PEGPH20 and gemcitabine compared to gemcitabine alone [186]. More recent studies of PEGPH20 in clinical trials of advanced PDA patients, showed PEGPH20 is safe as a systemic treatment and had promising efficacy results in combination with the standard of care [187]. These results suggest that PEGPH20 could be utilized as a clinically relevant tool to examine the effects of HA depletion in mammary tumor development. Data from such studies would inform further investigation of the mechanisms through which HA promotes tumor development, progression and therapeutic resistance.

B. Activation of FGFR results in increased levels of STAT3 phosphorylation

Further studies were performed to define the signaling pathway by which FGFR activation results in HA accumulation. Based on the established link between changes in HA and inflammation, our studies focused on potential contributions of inflammatory mediators [71]. Our data demonstrated that FGFR activation in epithelial cells led to increased expression and production of IL-6 family of cytokines, which are pro-inflammatory factors known to activate STAT3 [35]. *In vitro* experiments demonstrated that FGFR-driven STAT3 activation promoted several tumorigenic phenotypes, which were significantly reduced in the presence of the small molecule STAT3 inhibitor Stattic. In addition, we observed decreased production of HA in cells treated with Stattic, suggesting that STAT3 is driving accumulation of HA downstream of FGFR activation. This conclusion was further supported by analysis of tumor tissues from Stattic-treated mice, which revealed that STAT3 inhibition *in vivo* reduced expression of HA synthesis genes and significantly inhibited HA accumulation. These results suggest that FGFR activation might be the initial step of a feed-forward loop that drives accumulation of pro-inflammatory cytokines, such as IL-6, which signal in an autocrine fashion to enhance activation of inflammatory pathways, such as STAT3, which promote ECM remodeling that further accelerates activation and recruitment of inflammatory mediators. In order to disrupt this tumor-promoting cascade, it might be necessary to inhibit or modulate several pathways involved in this network. Our analysis of breast cancer TMA staining revealed a positive correlation between samples with activated FGFR and STAT3 signaling suggesting these pathways are activated together in a subset of human breast tumors. One novel implication of these findings is the existence of breast cancer patient populations that might benefit from therapies targeting both FGFR and STAT3 signaling

in an attempt to disrupt the inflammation-driving network. As FGFR inhibitors advance through clinical trials, it may prove beneficial to stratify patients in groups reflecting the level of STAT3 activation in addition to *FGFR* genomic alterations. Addition of JAK/STAT targeting agents to the treatment of patients exhibiting high levels of STAT3 activation could result in depletion of ECM components, such as HA, which would remove physical barriers allowing for better delivery of additional therapies. Furthermore, inhibition of STAT3 signaling would lower the expression of STAT3-target genes, which have been shown to contribute to tumor cell survival, proliferation, and migration. Alternatively, addition of HA depleting agents, such as PEGPH20, to the treatment of *FGFR*$^{+}$/pSTAT3^{hi} patients, could enhance the efficacy of FGFR targeting inhibitors by alleviating the changes in ECM remodeling which have accumulated as a result of FGFR pathway activation. The mouse models described in this thesis recapitulate the critical components necessary to test these combination therapies *in vivo* and thus represent a valuable tool in improving personalized targeted treatments.

C. Epithelial cell-derived secreted factors activate STAT3 in tumor-associated macrophages

In addition to changes in ECM components, FGFR1 activation leads to alterations in the immune cells compartment of mammary tumors. The studies outlined in Chapter 2 demonstrated that induction of FGFR1 signaling in mammary epithelial cells lead to increased production of IL-6 family of cytokines. Previous work by our lab has shown that macrophages are rapidly recruited to proliferating mammary epithelial lesions following activation of FGFR1 [27]. As IL-6 is a potent inflammatory mediator, we further focused on determining the effects of tumor cell-derived IL-6 on the inflammatory

environment. Analysis of TAMs in HC-11/R1 tumors showed that 20% of recruited macrophages were positive for pSTAT3. Studies in Chapter 2 demonstrated that FGFR signaling in epithelial cells results in the production of several IL-6 family members, such as Lif (in mouse cells) and IL-11 (in human breast cancer cells). We have not yet determined the levels or patterns of expression of STAT3-activating cytokines that are produced by HC-11/R1 cells *in vivo*. Preliminary IL-6 immunofluorescence staining in HC-11/R1-derived tumors revealed positive staining throughout the tumor sections (data not shown). Future studies will need to establish whether the level of STAT3 activation in TAMs is due to ligand sequestration or localized ligand production by a small tumor cell population.

In an effort to examine macrophage STAT3 signaling in another commonly used model of mammary tumorigenesis, we included orthotopic PyMT-derived tumors in our studies. In contrast to the HC-11/R1-derived tumors, only 8% of macrophages recruited to PyMT-derived tumors were positive for pSTAT3. This finding was surprising given previously published studies establishing the importance of the IL-6/STAT3 signaling pathway in the pathogenesis of the transgenic MMTV-PyMT model [157]. Our data point to one of the drawbacks of many mouse tumor models derived through transplantation of primary tumor cells. As cells are transplanted into the mammary fat pad through an injection, this causes injury and inflammation to the surrounding tissue. The contributions of this non-tumor source of inflammation to the process of tumorigenesis are unknown and may account for some of the differences observed among tumor models. An alternative method to transplantation, which avoids the above-described non-tumor inflammation, is the autochthonous tumor model where an oncogene is expressed under the control of a transgenic promoter resulting in tumor formation. Even though this method more accurately reflects some of the mechanisms of tumor growth likely present

in human patients, autochthonous models often fail to recapitulate the "aggressiveness" of human tumors by frequently developing in a time-frame unsuitable to answer questions pertaining to early tumorigenesis. Nevertheless, the studies presented here allowed us to investigate the contributions of myeloid STAT3 signaling in a $STAT3^{hi}$ (HC-11/R1-derived tumors) and a $STAT3^{low}$ (PyMT-derived) model making it possible to delineate phenotype differences based on levels of STAT3 activation.

D. Genetic ablation of *STAT3* in myeloid-derived cells promotes mammary tumorigenesis

In order to determine the contributions of myeloid cell STAT3 signaling to mammary tumor development and progression, we generated *STAT3^{fl}cfms-iCre* (conditional-$STAT3^{\Delta/\Delta}$) mice, in which expression of *iCre* results in *STAT3* deletion within bone marrow derived myeloid cells and a proportion of granulocytes and splenic T cells [103]. We observed increased tumorigenesis in conditional-$STAT3^{\Delta/\Delta}$ mice injected with HC-11/R1 cells compared to wildtype littermate controls. Tumors generated in conditional-$STAT3^{\Delta/\Delta}$ mice were detectable by palpation sooner and displayed significantly higher growth rates at early experimental time points, however final tumor burden was not significantly different between conditional-$STAT3^{\Delta/\Delta}$ mice and controls. These data suggest that the primary effect of myeloid cell STAT3 signaling occurred during early stages of tumorigenesis, and the effect was lost during later stages of tumor growth. Additionally, this effect was abrogated in mice injected with PyMT-derived cells. Tumors in these mice developed at the same time and grew at similar rates in both conditional-$STAT3^{\Delta/\Delta}$ and wildtype animals. Given our earlier observation that this model had a low number of $pSTAT3^{+}$ TAMs, it is possible that STAT3 signaling is not the

primary pathway involved in TAM function, and therefore, disrupting the pathway did not affect tumor growth. Alternatively, this result could be due to the intrinsic differences between the two models. Staining of the PyMT-derived tumors with the luminal and basal keratins K8 and K14 demonstrated that these tumors consist primarily of luminal cells [173]. HC-11/R1 cells express high levels of markers associated with the claudin-low/TNBC breast cancer subtype, and K8/K14 staining did not reveal a consistent pattern of single positive cells within the tumor (data not shown). These two breast cancer subtypes are characterized by different growth rates, immune cell infiltration, and responses to therapy in human patients, and therefore mouse models of similar subtypes may respond differently to changes in immune cell signaling.

E. *STAT3* deletion in BMDM results in an enhanced pro-inflammatory phenotype *in vitro*

In order to investigate the mechanism through which *STAT3* deletion in myeloid cells enhanced tumor formation, we performed *in vitro* studies using primary wildtype or $STAT3^{\Delta/\Delta}$ BMDMs. Initial experiments focused on delineating the changes in BMDM polarization in response to canonical M1/M2 stimuli. Based on previously published studies, we were not surprised that STAT3 signaling was crucial in the induction of the anti-inflammatory M2 phenotype since several M2 markers, such as *Il-10* and *Argl*, are direct STAT3 target genes [158]. In contrast, we observed increased production of pro-inflammatory mediators, such as *Ccl2, Ccl5,* and *Ptgs2*, when $STAT3^{\Delta/\Delta}$ BMDMs were exposed to M1 stimuli. Previous studies involving $STAT3^{\Delta/\Delta}$ BMDM have reported increased production of inflammatory molecules, however the mechanism of this was not established [103, 158]. Interestingly, we were not able to reliably detect differences in

the production of pro-inflammatory mediators by protein, which was a challenge also reported by others [103]. It is possible that the ELISA assays currently available for the measurement of secreted factors are not sensitive enough to detect differences in the ranges of protein expression we observed, most of which were several times higher than the internal assay controls. In addition, all protein concentrations were measured after the cells were stimulated for at least 18 hours, which could be too late to detect differences in the kinetics of protein production. Further assays and experimental optimization would be needed to demonstrate increased protein expression of pro-inflammatory cytokines in M1-treated STAT3$^{\Delta/\Delta}$ BMDM.

Further studies focused on the response of STAT3$^{\Delta/\Delta}$ BMDM to IL-6, as it was previously shown to be a key activator of macrophage STAT3 in tumor cell conditioned media. Interestingly, only a subset of M1 markers were induced in wildtype BMDM in an IL-6-dependent manner, indicating that the subset of inflammatory mediators activated following exposure to infection-associated stimuli (LPS/IFNγ) is different from those induced in response to tumor cell-derived factors, such as IL-6. Among those IL-6-induced pro-inflammatory genes, several were significantly upregulated in IL-6-treated STAT3$^{\Delta/\Delta}$ BMDM suggesting that STAT3$^{\Delta/\Delta}$ myeloid cells exposed to tumor-derived IL-6 *in vivo* could be contributing to development of tumor-promoting inflammation.

F. STAT3$^{\Delta/\Delta}$ macrophages display enhanced activation of STAT1

Previous work has demonstrated that STAT3 signaling can attenuate the pro-inflammatory signals of another STAT family member, STAT1, in mouse embryonic fibroblasts [162]. Therefore, we examined the levels of STAT1 phosphorylation in the absence of STAT3. STAT3$^{\Delta/\Delta}$ BMDM treated with IL-6 showed prolonged activation of

STAT1 and enhanced expression of several STAT1 target genes. This was a novel finding that suggests that in the absence of myeloid STAT3, tumor cell-derived factors may induce STAT1 signaling instead. Further studies will examine the levels of STAT1 activation *in vivo*, as our observations thus far were limited to *in vitro* assays. The precise mechanism that allows for IL-6 to signal through STAT1 instead of STAT3 is unknown and likely involves several receptor downstream signaling alterations (discussed in more detail in Chapter 3). Interestingly, STAT1 activation is indispensable in the downstream signaling cascade of type I and type II IFNs and has been shown to mediate anti-tumor immune responses [176, 188]. However, *STAT1* expression in human breast cancer tissues was reported to be a predictor of worse patient outcome in cases where *STAT1* was co-expressed with the human macrophage markers *CD68* and *CSF1* [177]. This finding would suggest that STAT1 signaling drives the pro-tumor functions of human breast cancer TAMs. A study by Tymoszuk *et al.* showed that STAT1 signaling contributes to the accumulation of immunosuppresive TAMs in a mouse model of $HER2^{+}$ breast tumors [189]. Our data did not indicate a difference in TAM accumulation between controls and conditional-$STAT3^{\Delta/\Delta}$ mice, suggesting that the mechanisms driving TAM proliferation in our claudin-low mouse model and the transgenic MMTV-Neu model used by Tymoszuk *et al.* may be different. Nonetheless, the overall findings of Tymoszuk and colleagues supported our observations that enhanced STAT1 signaling in macrophages may promote tumorigenesis.

G. Deletion of *STAT3* in BMDM results in increased production of pro-tumor factors

As the numbers of TAMs recruited to the mammary tumors remained constant across mouse genotypes, further work focused on examining the levels of pro-tumor STAT1-dependent molecules that were upregulated in STAT3$^{\Delta/\Delta}$ BMDM treated with IL-6. One such gene, which was upregulated in the absence of STAT3, was *Pd-l1*. PD-L1 is one of two PD-1 ligands and is expressed on macrophages, dendritic cells, mast cells, T and B cells, and numerous non-hematopoietic tissues, such as endothelial and epithelial cells [190]. Upon binding to its receptor on T cells, PD-L1 decreases production of cytokines, and inhibits T cell survival and proliferation [190]. The expression of PD-L1 has been shown to increase in response to tissue damage or stress, therefore establishing a potent negative feedback loop to T cell activation aimed at limiting inflammation-related bystander tissue damage [191]. Studies have shown that this pathway is hijacked by cancers, including breast tumors, in an attempt to escape T cell-mediated antitumor immune responses [192]. Macrophages within HC-11/R1-derived tumors exhibited significantly elevated levels of PD-L1 expression in conditional-STAT3$^{\Delta/\Delta}$ mice compared to controls. *In vitro* treatment of STAT3$^{\Delta/\Delta}$ BMDM with a JAK1/2 inhibitor inhibited PD-L1 upregulation suggesting that PD-L1 expression is dependent on JAK/STAT activation. In order to demonstrate that STAT1 is the primary driver of PD-L1 expression, however, future work will need to assess PD-L1 levels in STAT3$^{\Delta/\Delta}$/STAT1$^{\Delta/\Delta}$ macrophages. SiRNA-mediated STAT1 knockdown in STAT3$^{\Delta/\Delta}$ BMDM was difficult to achieve in these studies due to the intrinsic property of macrophages to become activated in the process of transfection. In addition, we attempted siRNA delivery via electroporation, which resulted in efficient STAT1 knockdown but also led to high cell mortality rates rendering this method unsuitable for use in large-scale experiments. Further studies could make use of BMDM derived from *c-fms-iCre*;*STAT3$^{fl/fl}$;STAT1$^{fl/fl}$* (double K/O) mice, which are not commercially available

and would need to be generated in our lab. Currently, experiments are underway to determine whether the use of anti-PD-L1 antibody following HC-11/R1 cell transplantation in conditional STAT3$^{\Delta/\Delta}$ mice will sufficiently restore immune surveillance and return tumor onset and growth rate to those observed in control mice.

Because *Pd-l1* was not the only STAT1 target gene that was upregulated in the IL-6-treated STAT3-deficient macrophages, it is possible that additional factors contribute to the pro-tumor phenotype of STAT3$^{\Delta/\Delta}$ TAMs. We observed increased mRNA expression of the chemokines *Cxcl9* and *Cxcl10*, which promote recruitment of T cells via CXCR3 [193]. As was described in Chapter 1, studies of human breast cancer samples have shown that these tumors are infiltrated by cytotoxic T cells at very low rates [73]. Further analysis of our conditional-STAT3$^{\Delta/\Delta}$ mouse model will test whether absence of STAT3 signaling in myeloid cells results in increased recruitment of T cells to the tumor. In this hypothesis is true, recruited T cells are likely still unable to mount an effective anti-tumor response within the PD-L1^{hi} immunosuppressive tumor microenvironment. Analysis of T cell activation markers can determine if TILs from these tumors are able to respond to tumor-derived antigens or if they present an “exhausted” phenotype [194, 195]. Increasing TIL levels as a result of myeloid STAT3 inhibition could allow for the use of combination therapy employing immune checkpoint inhibitors (such as α-PD-1 or α-PD-L1 antibodies) and inhibitors targeting oncogenic drivers like FGFR. A recent preclinical study by Liu *et al.* demonstrated the synergistic effect of trametinib (MAPK inhibitor) and PD-1/PD-L1 blockade in a model of melanoma [196]. Our mouse models were developed in immunocompetent hosts allowing us to pursue the effects of such combination therapies, including the detailed examination of potential therapy interactions, optimal treatment schedule, and side effects.

H. Conclusions

Increased FGFR signaling has been shown to contribute to the pathogenesis of all clinically relevant breast cancer subtypes. The studies described in this thesis aimed to address the significance of STAT3 signaling downstream of FGFR1 in tumor epithelial cells and STAT3 signaling, activated as a result of paracrine signaling, in infiltrating tumor macrophages. Despite numerous preclinical studies demonstrating the role of STAT3 as an oncogene in the mammary gland, STAT3 activation in human breast cancer tissues has been shown to be a marker of good patient prognosis [56, 197]. Our data suggest that STAT3 has opposing pro- and anti-tumor effects in different tumor cell populations, and it is possible that the integrated signal derived from these heterogeneous populations determines the disease outcome (Figure 4.1). The results of our initial studies using Stattic indicated that systemic STAT3 inhibition can limit the rate of tumor growth but lack the ability to eradicate the tumors completely. In contrast, targeted disruption of STAT3 signaling in myeloid cells enhanced tumorigenesis, suggesting that STAT3 signaling in this context acts to restrain tumor development. Therefore, it is important to determine the consequences of STAT3-targeted therapies in all cell types that constitute the tumor microenvironment. The results of such studies can help guide the development of combination breast cancer therapies that account for the therapy-induced changes in not just tumor cells, but also the tumor stroma and the tumor immune response.

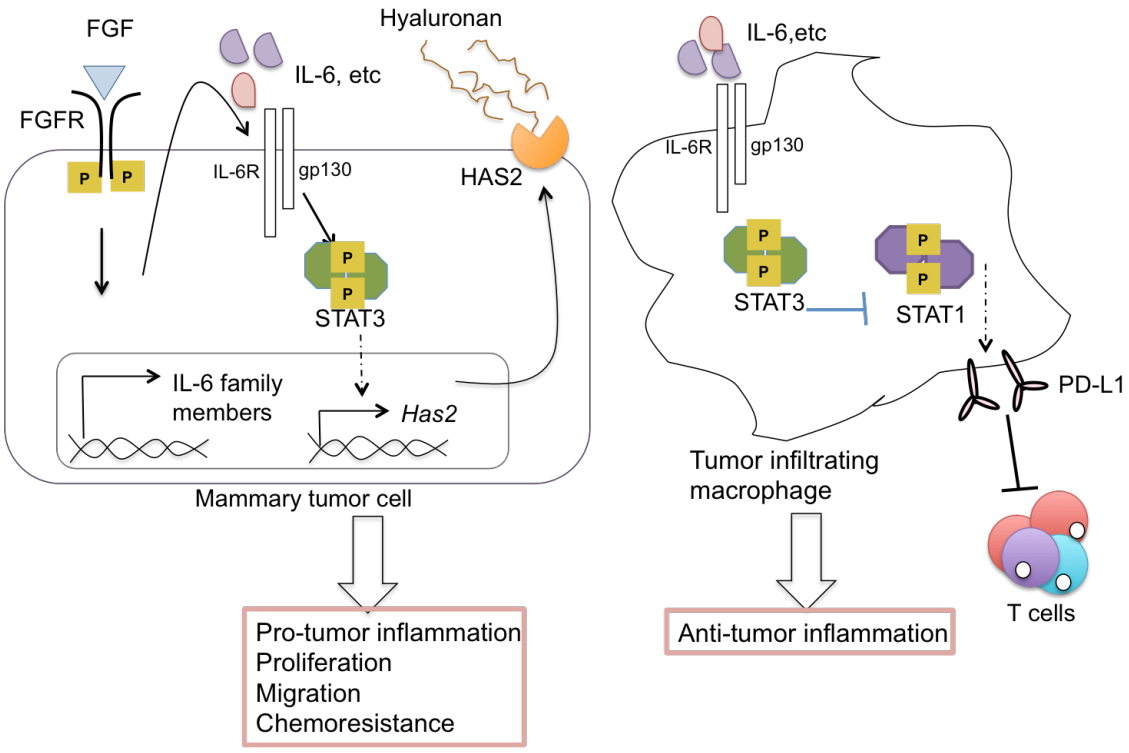

Figure 4.1 Final model. Activation of FGFR results in ECM alterations and STAT3 phosphorylation in tumor and infiltrating myeloid cells through the production of IL-6 family members that act in autocrine and paracrine manner to regulate mammary tumor formation and growth.

References

1. Siegel RL, Miller KD and Jemal A. Cancer statistics, 2016. CA Cancer J Clin. 2016; 66(1):7-30.
2. Bertos NR and Park M. Breast cancer - one term, many entities? The Journal of clinical investigation. 2011; 121(10):3789-3796.
3. Bartlett JM, Brookes CL, Robson T, van de Velde CJ, Billingham LJ, Campbell FM, Grant M, Hasenburg A, Hille ET, Kay C, Kieback DG, Putter H, Markopoulos C, Kranenbarg EM, Mallon EA, Dirix L, et al. Estrogen receptor and progesterone receptor as predictive biomarkers of response to endocrine therapy: a prospectively powered pathology study in the Tamoxifen and Exemestane Adjuvant Multinational trial. J Clin Oncol. 2011; 29(12):1531-1538.
4. Hudis CA. Trastuzumab--mechanism of action and use in clinical practice. The New England journal of medicine. 2007; 357(1):39-51.
5. Dent R, Trudeau M, Pritchard KI, Hanna WM, Kahn HK, Sawka CA, Lickley LA, Rawlinson E, Sun P and Narod SA. Triple-negative breast cancer: clinical features and patterns of recurrence. Clin Cancer Res. 2007; 13(15 Pt 1):4429-4434.
6. Perou CM, Sorlie T, Eisen MB, van de Rijn M, Jeffrey SS, Rees CA, Pollack JR, Ross DT, Johnsen H, Akslen LA, Fluge O, Pergamenschikov A, Williams C, Zhu SX, Lonning PE, Borresen-Dale AL, et al. Molecular portraits of human breast tumours. Nature. 2000; 406(6797):747-752.
7. Lehmann BD, Bauer JA, Chen X, Sanders ME, Chakravarthy AB, Shyr Y and Pietenpol JA. Identification of human triple-negative breast cancer subtypes and preclinical models for selection of targeted therapies. The Journal of clinical investigation. 2011; 121(7):2750-2767.
8. Prat A and Perou CM. Deconstructing the molecular portraits of breast cancer. Mol Oncol. 2011; 5(1):5-23.
9. Cancer Genome Atlas N. Comprehensive molecular portraits of human breast tumours. Nature. 2012; 490(7418):61-70.
10. Eswarakumar VP, Lax I and Schlessinger J. Cellular signaling by fibroblast growth factor receptors. Cytokine Growth Factor Rev. 2005; 16(2):139-149.
11. Turner N and Grose R. Fibroblast growth factor signalling: from development to cancer. Nat Rev Cancer. 2010; 10(2):116-129.
12. Haugsten EM, Wiedlocha A, Olsnes S and Wesche J. Roles of fibroblast growth factor receptors in carcinogenesis. Molecular cancer research : MCR. 2010; 8(11):1439-1452.
13. Fearon AE, Gould CR and Grose RP. FGFR signalling in women's cancers. Int J Biochem Cell Biol. 2013; 45(12):2832-2842.
14. Brady N, Chuntova P, Bade LK and Schwertfeger KL. The FGF/FGFR axis as a therapeutic target in breast cancer. Expert Rev Endocrinol Metab. 2013; 8(4):391-402.
15. Elbauomy Elsheikh S, Green AR, Lambros MB, Turner NC, Grainge MJ, Powe D, Ellis IO and Reis-Filho JS. FGFR1 amplification in breast carcinomas: a chromogenic in situ hybridisation analysis. Breast Cancer Res. 2007; 9(2):R23.
16. Garcia MJ, Pole JC, Chin SF, Teschendorff A, Naderi A, Ozdag H, Vias M, Kranjac T, Subkhankulova T, Paish C, Ellis I, Brenton JD, Edwards PA and Caldas C. A

1 Mb minimal amplicon at 8p11-12 in breast cancer identifies new candidate oncogenes. Oncogene. 2005; 24(33):5235-5245.
17. Turner N, Pearson A, Sharpe R, Lambros M, Geyer F, Lopez-Garcia MA, Natrajan R, Marchio C, Iorns E, Mackay A, Gillett C, Grigoriadis A, Tutt A, Reis-Filho JS and Ashworth A. FGFR1 amplification drives endocrine therapy resistance and is a therapeutic target in breast cancer. Cancer research. 2010; 70(5):2085-2094.
18. Wu YM, Su F, Kalyana-Sundaram S, Khazanov N, Ateeq B, Cao X, Lonigro RJ, Vats P, Wang R, Lin SF, Cheng AJ, Kunju LP, Siddiqui J, Tomlins SA, Wyngaard P, Sadis S, et al. Identification of targetable FGFR gene fusions in diverse cancers. Cancer Discov. 2013; 3(6):636-647.
19. Katoh M. WNT and FGF gene clusters (review). Int J Oncol. 2002; 21(6):1269-1273.
20. Sharpe R, Pearson A, Herrera-Abreu MT, Johnson D, Mackay A, Welti JC, Natrajan R, Reynolds AR, Reis-Filho JS, Ashworth A and Turner NC. FGFR signaling promotes the growth of triple-negative and basal-like breast cancer cell lines both in vitro and in vivo. Clin Cancer Res. 2011; 17(16):5275-5286.
21. Bade LK, Goldberg JE, Dehut HA, Hall MK and Schwertfeger KL. Mammary tumorigenesis induced by fibroblast growth factor receptor 1 requires activation of the epidermal growth factor receptor. J Cell Sci. 2011; 124(Pt 18):3106-3117.
22. Welm BE, Freeman KW, Chen M, Contreras A, Spencer DM and Rosen JM. Inducible dimerization of FGFR1: development of a mouse model to analyze progressive transformation of the mammary gland. J Cell Biol. 2002; 157(4):703-714.
23. Xian W, Schwertfeger KL, Vargo-Gogola T and Rosen JM. Pleiotropic effects of FGFR1 on cell proliferation, survival, and migration in a 3D mammary epithelial cell model. J Cell Biol. 2005; 171(4):663-673.
24. Dey JH, Bianchi F, Voshol J, Bonenfant D, Oakeley EJ and Hynes NE. Targeting fibroblast growth factor receptors blocks PI3K/AKT signaling, induces apoptosis, and impairs mammary tumor outgrowth and metastasis. Cancer research. 2010; 70(10):4151-4162.
25. Bohrer LR and Schwertfeger KL. Macrophages promote fibroblast growth factor receptor-driven tumor cell migration and invasion in a CXCR2-dependent manner. Molecular cancer research : MCR. 2012; 10(10):1294-1305.
26. Reed JR, Leon RP, Hall MK and Schwertfeger KL. Interleukin-1beta and fibroblast growth factor receptor 1 cooperate to induce cyclooxygenase-2 during early mammary tumourigenesis. Breast Cancer Res. 2009; 11(2):R21.
27. Reed JR, Stone MD, Beadnell TC, Ryu Y, Griffin TJ and Schwertfeger KL. Fibroblast growth factor receptor 1 activation in mammary tumor cells promotes macrophage recruitment in a CX3CL1-dependent manner. PLoS One. 2012; 7(9):e45877.
28. Bohrer LR, Chuntova P, Bade LK, Beadnell TC, Leon RP, Brady NJ, Ryu Y, Goldberg JE, Schmechel SC, Koopmeiners JS, McCarthy JB and Schwertfeger KL. Activation of the FGFR-STAT3 pathway in breast cancer cells induces a hyaluronan-rich microenvironment that licenses tumor formation. Cancer research. 2014; 74(1):374-386.
29. Andre F, Bachelot T, Campone M, Dalenc F, Perez-Garcia JM, Hurvitz SA, Turner N, Rugo H, Smith JW, Deudon S, Shi M, Zhang Y, Kay A, Porta DG, Yovine A

and Baselga J. Targeting FGFR with dovitinib (TKI258): preclinical and clinical data in breast cancer. Clin Cancer Res. 2013; 19(13):3693-3702.
30. Sequist LVC, P.; Varga, A. Phase I study of BGJ398, a selective pan-FGFR inhibitor in genetically preselected advanced solid tumors. AACR: Annual Meeting: Abstract CT326. 2014.
31. Beenken A and Mohammadi M. The FGF family: biology, pathophysiology and therapy. Nat Rev Drug Discov. 2009; 8(3):235-253.
32. Dieci MV, Arnedos M, Andre F and Soria JC. Fibroblast growth factor receptor inhibitors as a cancer treatment: from a biologic rationale to medical perspectives. Cancer Discov. 2013; 3(3):264-279.
33. Tomlinson DC, Baxter EW, Loadman PM, Hull MA and Knowles MA. FGFR1-induced epithelial to mesenchymal transition through MAPK/PLCgamma/COX-2-mediated mechanisms. PloS one. 2012; 7(6):e38972.
34. Chikazu D, Hakeda Y, Ogata N, Nemoto K, Itabashi A, Takato T, Kumegawa M, Nakamura K and Kawaguchi H. Fibroblast growth factor (FGF)-2 directly stimulates mature osteoclast function through activation of FGF receptor 1 and p42/p44 MAP kinase. J Biol Chem. 2000; 275(40):31444-31450.
35. Taniguchi K and Karin M. IL-6 and related cytokines as the critical lynchpins between inflammation and cancer. Semin Immunol. 2014; 26(1):54-74.
36. Zhang GJ and Adachi I. Serum interleukin-6 levels correlate to tumor progression and prognosis in metastatic breast carcinoma. Anticancer Res. 1999; 19(2B):1427-1432.
37. Salgado R, Junius S, Benoy I, Van Dam P, Vermeulen P, Van Marck E, Huget P and Dirix LY. Circulating interleukin-6 predicts survival in patients with metastatic breast cancer. Int J Cancer. 2003; 103(5):642-646.
38. Schindler CW. Series introduction. JAK-STAT signaling in human disease. The Journal of clinical investigation. 2002; 109(9):1133-1137.
39. Berishaj M, Gao SP, Ahmed S, Leslie K, Al-Ahmadie H, Gerald WL, Bornmann W and Bromberg JF. Stat3 is tyrosine-phosphorylated through the interleukin-6/glycoprotein 130/Janus kinase pathway in breast cancer. Breast Cancer Res. 2007; 9(3):R32.
40. Heinrich PC, Behrmann I, Haan S, Hermanns HM, Muller-Newen G and Schaper F. Principles of interleukin (IL)-6-type cytokine signalling and its regulation. Biochem J. 2003; 374(Pt 1):1-20.
41. Mullberg J, Schooltink H, Stoyan T, Gunther M, Graeve L, Buse G, Mackiewicz A, Heinrich PC and Rose-John S. The soluble interleukin-6 receptor is generated by shedding. Eur J Immunol. 1993; 23(2):473-480.
42. Scheller J, Chalaris A, Schmidt-Arras D and Rose-John S. The pro- and anti-inflammatory properties of the cytokine interleukin-6. Biochim Biophys Acta. 2011; 1813(5):878-888.
43. Lissilaa R, Buatois V, Magistrelli G, Williams AS, Jones GW, Herren S, Shang L, Malinge P, Guilhot F, Chatel L, Hatterer E, Jones SA, Kosco-Vilbois MH and Ferlin WG. Although IL-6 trans-signaling is sufficient to drive local immune responses, classical IL-6 signaling is obligate for the induction of T cell-mediated autoimmunity. Journal of immunology. 2010; 185(9):5512-5521.

44. Goldberg JE and Schwertfeger KL. Proinflammatory cytokines in breast cancer: mechanisms of action and potential targets for therapeutics. Curr Drug Targets. 2010; 11(9):1133-1146.
45. Mauer J, Denson JL and Bruning JC. Versatile functions for IL-6 in metabolism and cancer. Trends Immunol. 2015; 36(2):92-101.
46. Middleton K, Jones J, Lwin Z and Coward JI. Interleukin-6: an angiogenic target in solid tumours. Crit Rev Oncol Hematol. 2014; 89(1):129-139.
47. Sullivan NJ, Sasser AK, Axel AE, Vesuna F, Raman V, Ramirez N, Oberyszyn TM and Hall BM. Interleukin-6 induces an epithelial-mesenchymal transition phenotype in human breast cancer cells. Oncogene. 2009; 28(33):2940-2947.
48. Matsuda T, Nakamura T, Nakao K, Arai T, Katsuki M, Heike T and Yokota T. STAT3 activation is sufficient to maintain an undifferentiated state of mouse embryonic stem cells. EMBO J. 1999; 18(15):4261-4269.
49. Chapman RS, Lourenco PC, Tonner E, Flint DJ, Selbert S, Takeda K, Akira S, Clarke AR and Watson CJ. Suppression of epithelial apoptosis and delayed mammary gland involution in mice with a conditional knockout of Stat3. Genes Dev. 1999; 13(19):2604-2616.
50. Lin L, Liu A, Peng Z, Lin HJ, Li PK, Li C and Lin J. STAT3 is necessary for proliferation and survival in colon cancer-initiating cells. Cancer research. 2011; 71(23):7226-7237.
51. Ho PL, Lay EJ, Jian W, Parra D and Chan KS. Stat3 activation in urothelial stem cells leads to direct progression to invasive bladder cancer. Cancer research. 2012; 72(13):3135-3142.
52. Diaz N, Minton S, Cox C, Bowman T, Gritsko T, Garcia R, Eweis I, Wloch M, Livingston S, Seijo E, Cantor A, Lee JH, Beam CA, Sullivan D, Jove R and Muro-Cacho CA. Activation of stat3 in primary tumors from high-risk breast cancer patients is associated with elevated levels of activated SRC and survivin expression. Clin Cancer Res. 2006; 12(1):20-28.
53. Hsieh FC, Cheng G and Lin J. Evaluation of potential Stat3-regulated genes in human breast cancer. Biochem Biophys Res Commun. 2005; 335(2):292-299.
54. Wei W, Tweardy DJ, Zhang M, Zhang X, Landua J, Petrovic I, Bu W, Roarty K, Hilsenbeck SG, Rosen JM and Lewis MT. STAT3 signaling is activated preferentially in tumor-initiating cells in claudin-low models of human breast cancer. Stem Cells. 2014; 32(10):2571-2582.
55. Thakur R, Trivedi R, Rastogi N, Singh M and Mishra DP. Inhibition of STAT3, FAK and Src mediated signaling reduces cancer stem cell load, tumorigenic potential and metastasis in breast cancer. Sci Rep. 2015; 5:10194.
56. Sonnenblick A, Shriki A, Galun E, Axelrod JH, Daum H, Rottenberg Y, Hamburger T, Mali B and Peretz T. Tissue microarray-based study of patients with lymph node-positive breast cancer shows tyrosine phosphorylation of signal transducer and activator of transcription 3 (tyrosine705-STAT3) is a marker of good prognosis. Clin Transl Oncol. 2012; 14(3):232-236.
57. Dolled-Filhart M, Camp RL, Kowalski DP, Smith BL and Rimm DL. Tissue microarray analysis of signal transducers and activators of transcription 3 (Stat3) and

phospho-Stat3 (Tyr705) in node-negative breast cancer shows nuclear localization is associated with a better prognosis. Clin Cancer Res. 2003; 9(2):594-600.
58. Wu P, Wu D, Zhao L, Huang L, Shen G, Huang J and Chai Y. Prognostic role of STAT3 in solid tumors: a systematic review and meta-analysis. Oncotarget. 2016; 7(15):19863-19883.
59. Polyak K. Breast cancer: origins and evolution. The Journal of clinical investigation. 2007; 117(11):3155-3163.
60. Maffini MV, Soto AM, Calabro JM, Ucci AA and Sonnenschein C. The stroma as a crucial target in rat mammary gland carcinogenesis. J Cell Sci. 2004; 117(Pt 8):1495-1502.
61. Howlett AR and Bissell MJ. The influence of tissue microenvironment (stroma and extracellular matrix) on the development and function of mammary epithelium. Epithelial Cell Biol. 1993; 2(2):79-89.
62. Allinen M, Beroukhim R, Cai L, Brennan C, Lahti-Domenici J, Huang H, Porter D, Hu M, Chin L, Richardson A, Schnitt S, Sellers WR and Polyak K. Molecular characterization of the tumor microenvironment in breast cancer. Cancer Cell. 2004; 6(1):17-32.
63. Chabottaux V and Noel A. Breast cancer progression: insights into multifaceted matrix metalloproteinases. Clin Exp Metastasis. 2007; 24(8):647-656.
64. Levental KR, Yu H, Kass L, Lakins JN, Egeblad M, Erler JT, Fong SF, Csiszar K, Giaccia A, Weninger W, Yamauchi M, Gasser DL and Weaver VM. Matrix crosslinking forces tumor progression by enhancing integrin signaling. Cell. 2009; 139(5):891-906.
65. Saavalainen K, Pasonen-Seppanen S, Dunlop TW, Tammi R, Tammi MI and Carlberg C. The human hyaluronan synthase 2 gene is a primary retinoic acid and epidermal growth factor responding gene. J Biol Chem. 2005; 280(15):14636-14644.
66. Tammi RH, Passi AG, Rilla K, Karousou E, Vigetti D, Makkonen K and Tammi MI. Transcriptional and post-translational regulation of hyaluronan synthesis. FEBS J. 2011; 278(9):1419-1428.
67. Toole BP. Hyaluronan: from extracellular glue to pericellular cue. Nat Rev Cancer. 2004; 4(7):528-539.
68. Li Y, Li L, Brown TJ and Heldin P. Silencing of hyaluronan synthase 2 suppresses the malignant phenotype of invasive breast cancer cells. Int J Cancer. 2007; 120(12):2557-2567.
69. Auvinen P, Tammi R, Parkkinen J, Tammi M, Agren U, Johansson R, Hirvikoski P, Eskelinen M and Kosma VM. Hyaluronan in peritumoral stroma and malignant cells associates with breast cancer spreading and predicts survival. Am J Pathol. 2000; 156(2):529-536.
70. Urakawa H, Nishida Y, Wasa J, Arai E, Zhuo L, Kimata K, Kozawa E, Futamura N and Ishiguro N. Inhibition of hyaluronan synthesis in breast cancer cells by 4-methylumbelliferone suppresses tumorigenicity in vitro and metastatic lesions of bone in vivo. Int J Cancer. 2012; 130(2):454-466.
71. Schwertfeger KL, Cowman MK, Telmer PG, Turley EA and McCarthy JB. Hyaluronan, Inflammation, and Breast Cancer Progression. Front Immunol. 2015; 6:236.

72. Corte MD, Gonzalez LO, Junquera S, Bongera M, Allende MT and Vizoso FJ. Analysis of the expression of hyaluronan in intraductal and invasive carcinomas of the breast. J Cancer Res Clin Oncol. 2010; 136(5):745-750.
73. Loi S, Sirtaine N, Piette F, Salgado R, Viale G, Van Eenoo F, Rouas G, Francis P, Crown JP, Hitre E, de Azambuja E, Quinaux E, Di Leo A, Michiels S, Piccart MJ and Sotiriou C. Prognostic and predictive value of tumor-infiltrating lymphocytes in a phase III randomized adjuvant breast cancer trial in node-positive breast cancer comparing the addition of docetaxel to doxorubicin with doxorubicin-based chemotherapy: BIG 02-98. J Clin Oncol. 2013; 31(7):860-867.
74. Denkert C. The immunogenicity of breast cancer--molecular subtypes matter. Ann Oncol. 2014; 25(8):1453-1455.
75. Denkert C, Loibl S, Noske A, Roller M, Muller BM, Komor M, Budczies J, Darb-Esfahani S, Kronenwett R, Hanusch C, von Torne C, Weichert W, Engels K, Solbach C, Schrader I, Dietel M, et al. Tumor-associated lymphocytes as an independent predictor of response to neoadjuvant chemotherapy in breast cancer. J Clin Oncol. 2010; 28(1):105-113.
76. Bingle L, Brown NJ and Lewis CE. The role of tumour-associated macrophages in tumour progression: implications for new anticancer therapies. The Journal of pathology. 2002; 196(3):254-265.
77. Leek RD, Lewis CE, Whitehouse R, Greenall M, Clarke J and Harris AL. Association of macrophage infiltration with angiogenesis and prognosis in invasive breast carcinoma. Cancer research. 1996; 56(20):4625-4629.
78. Mahmoud SM, Lee AH, Paish EC, Macmillan RD, Ellis IO and Green AR. Tumour-infiltrating macrophages and clinical outcome in breast cancer. Journal of clinical pathology. 2012; 65(2):159-163.
79. Lin EY, Nguyen AV, Russell RG and Pollard JW. Colony-stimulating factor 1 promotes progression of mammary tumors to malignancy. The Journal of experimental medicine. 2001; 193(6):727-740.
80. Wyckoff JB, Wang Y, Lin EY, Li JF, Goswami S, Stanley ER, Segall JE, Pollard JW and Condeelis J. Direct visualization of macrophage-assisted tumor cell intravasation in mammary tumors. Cancer research. 2007; 67(6):2649-2656.
81. Wyckoff J, Wang W, Lin EY, Wang Y, Pixley F, Stanley ER, Graf T, Pollard JW, Segall J and Condeelis J. A paracrine loop between tumor cells and macrophages is required for tumor cell migration in mammary tumors. Cancer research. 2004; 64(19):7022-7029.
82. Lin EY, Li JF, Gnatovskiy L, Deng Y, Zhu L, Grzesik DA, Qian H, Xue XN and Pollard JW. Macrophages regulate the angiogenic switch in a mouse model of breast cancer. Cancer research. 2006; 66(23):11238-11246.
83. Lin EY, Li JF, Bricard G, Wang W, Deng Y, Sellers R, Porcelli SA and Pollard JW. Vascular endothelial growth factor restores delayed tumor progression in tumors depleted of macrophages. Mol Oncol. 2007; 1(3):288-302.
84. Lohela M, Casbon AJ, Olow A, Bonham L, Branstetter D, Weng N, Smith J and Werb Z. Intravital imaging reveals distinct responses of depleting dynamic tumor-

associated macrophage and dendritic cell subpopulations. Proc Natl Acad Sci U S A. 2014; 111(47):E5086-5095.
85. Shree T, Olson OC, Elie BT, Kester JC, Garfall AL, Simpson K, Bell-McGuinn KM, Zabor EC, Brogi E and Joyce JA. Macrophages and cathepsin proteases blunt chemotherapeutic response in breast cancer. Genes Dev. 2011; 25(23):2465-2479.
86. DeNardo DG, Brennan DJ, Rexhepaj E, Ruffell B, Shiao SL, Madden SF, Gallagher WM, Wadhwani N, Keil SD, Junaid SA, Rugo HS, Hwang ES, Jirstrom K, West BL and Coussens LM. Leukocyte complexity predicts breast cancer survival and functionally regulates response to chemotherapy. Cancer Discov. 2011; 1(1):54-67.
87. DeNardo DG, Barreto JB, Andreu P, Vasquez L, Tawfik D, Kolhatkar N and Coussens LM. CD4(+) T cells regulate pulmonary metastasis of mammary carcinomas by enhancing protumor properties of macrophages. Cancer Cell. 2009; 16(2):91-102.
88. Condeelis J and Pollard JW. Macrophages: obligate partners for tumor cell migration, invasion, and metastasis. Cell. 2006; 124(2):263-266.
89. Balkwill F, Charles KA and Mantovani A. Smoldering and polarized inflammation in the initiation and promotion of malignant disease. Cancer Cell. 2005; 7(3):211-217.
90. Qian BZ and Pollard JW. Macrophage diversity enhances tumor progression and metastasis. Cell. 2010; 141(1):39-51.
91. Mills CD, Kincaid K, Alt JM, Heilman MJ and Hill AM. M-1/M-2 macrophages and the Th1/Th2 paradigm. Journal of immunology. 2000; 164(12):6166-6173.
92. Sica A and Mantovani A. Macrophage plasticity and polarization: in vivo veritas. The Journal of clinical investigation. 2012; 122(3):787-795.
93. Mosser DM. The many faces of macrophage activation. J Leukoc Biol. 2003; 73(2):209-212.
94. Mantovani A, Sozzani S, Locati M, Allavena P and Sica A. Macrophage polarization: tumor-associated macrophages as a paradigm for polarized M2 mononuclear phagocytes. Trends Immunol. 2002; 23(11):549-555.
95. Reuter S, Gupta SC, Chaturvedi MM and Aggarwal BB. Oxidative stress, inflammation, and cancer: how are they linked? Free Radic Biol Med. 2010; 49(11):1603-1616.
96. Movahedi K, Laoui D, Gysemans C, Baeten M, Stange G, Van den Bossche J, Mack M, Pipeleers D, In't Veld P, De Baetselier P and Van Ginderachter JA. Different tumor microenvironments contain functionally distinct subsets of macrophages derived from Ly6C(high) monocytes. Cancer research. 2010; 70(14):5728-5739.
97. Buldakov M, Zavyalova M, Krakhmal N, Telegina N, Vtorushin S, Mitrofanova I, Riabov V, Yin S, Song B, Cherdyntseva N and Kzhyshkowska J. CD68+, but not stabilin-1+ tumor associated macrophages in gaps of ductal tumor structures negatively correlate with the lymphatic metastasis in human breast cancer. Immunobiology. 2015.
98. Yu H, Kortylewski M and Pardoll D. Crosstalk between cancer and immune cells: role of STAT3 in the tumour microenvironment. Nat Rev Immunol. 2007; 7(1):41-51.
99. Nefedova Y, Huang M, Kusmartsev S, Bhattacharya R, Cheng P, Salup R, Jove R and Gabrilovich D. Hyperactivation of STAT3 is involved in abnormal differentiation of dendritic cells in cancer. Journal of immunology. 2004; 172(1):464-474.

100. Kortylewski M, Kujawski M, Wang T, Wei S, Zhang S, Pilon-Thomas S, Niu G, Kay H, Mule J, Kerr WG, Jove R, Pardoll D and Yu H. Inhibiting Stat3 signaling in the hematopoietic system elicits multicomponent antitumor immunity. Nat Med. 2005; 11(12):1314-1321.
101. Kujawski M, Kortylewski M, Lee H, Herrmann A, Kay H and Yu H. Stat3 mediates myeloid cell-dependent tumor angiogenesis in mice. The Journal of clinical investigation. 2008; 118(10):3367-3377.
102. Zhang L, Alizadeh D, Van Handel M, Kortylewski M, Yu H and Badie B. Stat3 inhibition activates tumor macrophages and abrogates glioma growth in mice. Glia. 2009; 57(13):1458-1467.
103. Deng L, Zhou JF, Sellers RS, Li JF, Nguyen AV, Wang Y, Orlofsky A, Liu Q, Hume DA, Pollard JW, Augenlicht L and Lin EY. A novel mouse model of inflammatory bowel disease links mammalian target of rapamycin-dependent hyperproliferation of colonic epithelium to inflammation-associated tumorigenesis. Am J Pathol. 2010; 176(2):952-967.
104. Kumar V, Cheng P, Condamine T, Mony S, Languino LR, McCaffrey JC, Hockstein N, Guarino M, Masters G, Penman E, Denstman F, Xu X, Altieri DC, Du H, Yan C and Gabrilovich DI. CD45 Phosphatase Inhibits STAT3 Transcription Factor Activity in Myeloid Cells and Promotes Tumor-Associated Macrophage Differentiation. Immunity. 2016; 44(2):303-315.
105. Abad C, Nobuta H, Li J, Kasai A, Yong WH and Waschek JA. Targeted STAT3 disruption in myeloid cells alters immunosuppressor cell abundance in a murine model of spontaneous medulloblastoma. J Leukoc Biol. 2014; 95(2):357-367.
106. Greenman C, Stephens P, Smith R, Dalgliesh GL, Hunter C, Bignell G, Davies H, Teague J, Butler A, Stevens C, Edkins S, O'Meara S, Vastrik I, Schmidt EE, Avis T, Barthorpe S, et al. Patterns of somatic mutation in human cancer genomes. Nature. 2007; 446(7132):153-158.
107. Schwertfeger KL. Fibroblast growth factors in development and cancer: insights from the mammary and prostate glands. Curr Drug Targets. 2009; 10(7):632-644.
108. Andre F, Bachelot T, Campone M, Dalenc F, Perez-Garcia JM, Hurvitz SA, Turner N, Rugo H, Smith JW, Deudon S, Shi M, Zhang Y, Kay A, Graus Porta D, Yovine A and Baselga J. Targeting FGFR with Dovitinib (TKI258): Preclinical and Clinical Data in Breast Cancer. Clin Cancer Res. 2013; 19(13):3693-3702.
109. Chioni AM and Grose R. FGFR1 cleavage and nuclear translocation regulates breast cancer cell behavior. J Cell Biol. 2012; 197(6):801-817.
110. Hynes NE and Dey JH. Potential for targeting the fibroblast growth factor receptors in breast cancer. Cancer Res. 2010; 70(13):5199-5202.
111. Issa A, Gill JW, Heideman MR, Sahin O, Wiemann S, Dey JH and Hynes NE. Combinatorial targeting of FGF and ErbB receptors blocks growth and metastatic spread of breast cancer models. Breast Cancer Res. 2013; 15(1):R8.
112. Tarkkonen KM, Nilsson EM, Kahkonen TE, Dey JH, Heikkila JE, Tuomela JM, Liu Q, Hynes NE and Harkonen PL. Differential roles of fibroblast growth factor receptors (FGFR) 1, 2 and 3 in the regulation of S115 breast cancer cell growth. PLoS One. 2012; 7(11):e49970.

113. Pond AC, Herschkowitz JI, Schwertfeger KL, Welm B, Zhang Y, York B, Cardiff RD, Hilsenbeck S, Perou CM, Creighton CJ, Lloyd RE and Rosen JM. Fibroblast growth factor receptor signaling dramatically accelerates tumorigenesis and enhances oncoprotein translation in the mouse mammary tumor virus-Wnt-1 mouse model of breast cancer. Cancer Res. 2010; 70(12):4868-4879.
114. Schwertfeger KL, Xian W, Kaplan AM, Burnett SH, Cohen DA and Rosen JM. A critical role for the inflammatory response in a mouse model of preneoplastic progression. Cancer Res. 2006; 66(11):5676-5685.
115. Gotte M and Yip GW. Heparanase, hyaluronan, and CD44 in cancers: a breast carcinoma perspective. Cancer Res. 2006; 66(21):10233-10237.
116. Solis MA, Chen YH, Wong TY, Bittencourt VZ, Lin YC and Huang LL. Hyaluronan regulates cell behavior: a potential niche matrix for stem cells. Biochem Res Int. 2012; 2012:346972.
117. Itano N. Simple primary structure, complex turnover regulation and multiple roles of hyaluronan. J Biochem. 2008; 144(2):131-137.
118. Wagner KU and Schmidt JW. The two faces of Janus kinases and their respective STATs in mammary gland development and cancer. J Carcinog. 2011; 10:32.
119. Lieblein JC, Ball S, Hutzen B, Sasser AK, Lin HJ, Huang TH, Hall BM and Lin J. STAT3 can be activated through paracrine signaling in breast epithelial cells. BMC Cancer. 2008; 8:302.
120. Leslie K, Lang C, Devgan G, Azare J, Berishaj M, Gerald W, Kim YB, Paz K, Darnell JE, Albanese C, Sakamaki T, Pestell R and Bromberg J. Cyclin D1 is transcriptionally regulated by and required for transformation by activated signal transducer and activator of transcription 3. Cancer Res. 2006; 66(5):2544-2552.
121. Xian W, Schwertfeger KL and Rosen JM. Distinct roles of fibroblast growth factor receptor 1 and 2 in regulating cell survival and epithelial-mesenchymal transition. Mol Endocrinol. 2007; 21(4):987-1000.
122. Nakamura T, Funahashi M, Takagaki K, Munakata H, Tanaka K, Saito Y and Endo M. Effect of 4-methylumbelliferone on cell-free synthesis of hyaluronic acid. Biochem Mol Biol Int. 1997; 43(2):263-268.
123. Kakizaki I, Kojima K, Takagaki K, Endo M, Kannagi R, Ito M, Maruo Y, Sato H, Yasuda T, Mita S, Kimata K and Itano N. A novel mechanism for the inhibition of hyaluronan biosynthesis by 4-methylumbelliferone. J Biol Chem. 2004; 279(32):33281-33289.
124. Kultti A, Pasonen-Seppanen S, Jauhiainen M, Rilla KJ, Karna R, Pyoria E, Tammi RH and Tammi MI. 4-Methylumbelliferone inhibits hyaluronan synthesis by depletion of cellular UDP-glucuronic acid and downregulation of hyaluronan synthase 2 and 3. Exp Cell Res. 2009; 315(11):1914-1923.
125. Wang A, de la Motte C, Lauer M and Hascall V. Hyaluronan matrices in pathobiological processes. FEBS J. 2011; 278(9):1412-1418.
126. Dudka AA, Sweet SM and Heath JK. Signal transducers and activators of transcription-3 binding to the fibroblast growth factor receptor is activated by receptor amplification. Cancer Res. 2010; 70(8):3391-3401.

127. Yu H, Pardoll D and Jove R. STATs in cancer inflammation and immunity: a leading role for STAT3. Nat Rev Cancer. 2009; 9(11):798-809.
128. Liu JF, Crepin M, Liu JM, Barritault D and Ledoux D. FGF-2 and TPA induce matrix metalloproteinase-9 secretion in MCF-7 cells through PKC activation of the Ras/ERK pathway. Biochem Biophys Res Commun. 2002; 293(4):1174-1182.
129. Schust J, Sperl B, Hollis A, Mayer TU and Berg T. Stattic: a small-molecule inhibitor of STAT3 activation and dimerization. Chem Biol. 2006; 13(11):1235-1242.
130. Dave B, Landis MD, Tweardy DJ, Chang JC, Dobrolecki LE, Wu MF, Zhang X, Westbrook TF, Hilsenbeck SG, Liu D and Lewis MT. Selective small molecule Stat3 inhibitor reduces breast cancer tumor-initiating cells and improves recurrence free survival in a human-xenograft model. PLoS One. 2012; 7(8):e30207.
131. Debnath J and Brugge JS. Modelling glandular epithelial cancers in three-dimensional cultures. Nat Rev Cancer. 2005; 5(9):675-688.
132. Veiseh M and Turley EA. Hyaluronan metabolism in remodeling extracellular matrix: probes for imaging and therapy of breast cancer. Integr Biol (Camb). 2011; 3(4):304-315.
133. Sironen RK, Tammi M, Tammi R, Auvinen PK, Anttila M and Kosma VM. Hyaluronan in human malignancies. Exp Cell Res. 2011; 317(4):383-391.
134. Auvinen P, Tammi R, Kosma VM, Sironen R, Soini Y, Mannermaa A, Tumelius R, Uljas E and Tammi M. Increased hyaluronan content and stromal cell CD44 associate with HER2 positivity and poor prognosis in human breast cancer. Int J Cancer. 2013; 132(3):531-539.
135. Karihtala P, Soini Y, Auvinen P, Tammi R, Tammi M and Kosma VM. Hyaluronan in breast cancer: correlations with nitric oxide synthases and tyrosine nitrosylation. J Histochem Cytochem. 2007; 55(12):1191-1198.
136. Heldin P, Karousou E, Bernert B, Porsch H, Nishitsuka K and Skandalis SS. Importance of hyaluronan-CD44 interactions in inflammation and tumorigenesis. Connect Tissue Res. 2008; 49(3):215-218.
137. Monzon ME, Fregien N, Schmid N, Falcon NS, Campos M, Casalino-Matsuda SM and Forteza RM. Reactive oxygen species and hyaluronidase 2 regulate airway epithelial hyaluronan fragmentation. J Biol Chem. 2010; 285(34):26126-26134.
138. Eberlein M, Scheibner KA, Black KE, Collins SL, Chan-Li Y, Powell JD and Horton MR. Anti-oxidant inhibition of hyaluronan fragment-induced inflammatory gene expression. J Inflamm (Lond). 2008; 5:20.
139. Tian X, Azpurua J, Hine C, Vaidya A, Myakishev-Rempel M, Ablaeva J, Mao Z, Nevo E, Gorbunova V and Seluanov A. High-molecular-mass hyaluronan mediates the cancer resistance of the naked mole rat. Nature. 2013; 499(7458):346-349.
140. Tolg C, Hamilton SR, Zalinska E, McCulloch L, Amin R, Akentieva N, Winnik F, Savani R, Bagli DJ, Luyt LG, Cowman MK, McCarthy JB and Turley EA. A RHAMM mimetic peptide blocks hyaluronan signaling and reduces inflammation and fibrogenesis in excisional skin wounds. Am J Pathol. 2012; 181(4):1250-1270.
141. Sakaguchi M, Oka M, Iwasaki T, Fukami Y and Nishigori C. Role and regulation of STAT3 phosphorylation at Ser727 in melanocytes and melanoma cells. J Invest Dermatol. 2012; 132(7):1877-1885.

142. Toole BP. Hyaluronan-CD44 Interactions in Cancer: Paradoxes and Possibilities. Clin Cancer Res. 2009; 15(24):7462-7468.
143. Hanahan D and Weinberg RA. Hallmarks of cancer: the next generation. Cell. 2011; 144(5):646-674.
144. Whiteside TL. The tumor microenvironment and its role in promoting tumor growth. Oncogene. 2008; 27(45):5904-5912.
145. Coussens LM and Werb Z. Inflammation and cancer. Nature. 2002; 420(6917):860-867.
146. de Visser KE, Eichten A and Coussens LM. Paradoxical roles of the immune system during cancer development. Nat Rev Cancer. 2006; 6(1):24-37.
147. Mahmoud SM, Paish EC, Powe DG, Macmillan RD, Grainge MJ, Lee AH, Ellis IO and Green AR. Tumor-infiltrating CD8+ lymphocytes predict clinical outcome in breast cancer. J Clin Oncol. 2011; 29(15):1949-1955.
148. Ries CH, Cannarile MA, Hoves S, Benz J, Wartha K, Runza V, Rey-Giraud F, Pradel LP, Feuerhake F, Klaman I, Jones T, Jucknischke U, Scheiblich S, Kaluza K, Gorr IH, Walz A, et al. Targeting tumor-associated macrophages with anti-CSF-1R antibody reveals a strategy for cancer therapy. Cancer Cell. 2014; 25(6):846-859.
149. Highfill SL, Cui Y, Giles AJ, Smith JP, Zhang H, Morse E, Kaplan RN and Mackall CL. Disruption of CXCR2-mediated MDSC tumor trafficking enhances anti-PD1 efficacy. Sci Transl Med. 2014; 6(237):237ra267.
150. Brady NJ, Chuntova P and Schwertfeger KL. Macrophages: Regulators of the Inflammatory Microenvironment during Mammary Gland Development and Breast Cancer. Mediators Inflamm. 2016; 2016:4549676.
151. Pollard JW. Tumour-educated macrophages promote tumour progression and metastasis. Nat Rev Cancer. 2004; 4(1):71-78.
152. Ruffell B and Coussens LM. Macrophages and therapeutic resistance in cancer. Cancer Cell. 2015; 27(4):462-472.
153. Murdoch C, Muthana M, Coffelt SB and Lewis CE. The role of myeloid cells in the promotion of tumour angiogenesis. Nat Rev Cancer. 2008; 8(8):618-631.
154. Liguori M, Solinas G, Germano G, Mantovani A and Allavena P. Tumor-associated macrophages as incessant builders and destroyers of the cancer stroma. Cancers (Basel). 2011; 3(4):3740-3761.
155. Williams CB, Yeh ES and Soloff AC. Tumor-associated macrophages: unwitting accomplices in breast cancer malignancy. NPJ Breast Cancer. 2016; 2.
156. Van Ginderachter JA, Movahedi K, Hassanzadeh Ghassabeh G, Meerschaut S, Beschin A, Raes G and De Baetselier P. Classical and alternative activation of mononuclear phagocytes: picking the best of both worlds for tumor promotion. Immunobiology. 2006; 211(6-8):487-501.
157. Chang Q, Bournazou E, Sansone P, Berishaj M, Gao SP, Daly L, Wels J, Theilen T, Granitto S, Zhang X, Cotari J, Alpaugh ML, de Stanchina E, Manova K, Li M, Bonafe M, et al. The IL-6/JAK/Stat3 feed-forward loop drives tumorigenesis and metastasis. Neoplasia. 2013; 15(7):848-862.
158. Mauer J, Chaurasia B, Goldau J, Vogt MC, Ruud J, Nguyen KD, Theurich S, Hausen AC, Schmitz J, Bronneke HS, Estevez E, Allen TL, Mesaros A, Partridge L,

Febbraio MA, Chawla A, et al. Signaling by IL-6 promotes alternative activation of macrophages to limit endotoxemia and obesity-associated resistance to insulin. Nat Immunol. 2014; 15(5):423-430.
159. Livak KJ and Schmittgen TD. Analysis of relative gene expression data using real-time quantitative PCR and the 2(-Delta Delta C(T)) Method. Methods. 2001; 25(4):402-408.
160. Farooqui M, Bohrer LR, Brady NJ, Chuntova P, Kemp SE, Wardwell CT, Nelson AC and Schwertfeger KL. Epiregulin contributes to breast tumorigenesis through regulating matrix metalloproteinase 1 and promoting cell survival. Mol Cancer. 2015; 14:138.
161. Hutchins AP, Poulain S and Miranda-Saavedra D. Genome-wide analysis of STAT3 binding in vivo predicts effectors of the anti-inflammatory response in macrophages. Blood. 2012; 119(13):e110-119.
162. Costa-Pereira AP, Tininini S, Strobl B, Alonzi T, Schlaak JF, Is'harc H, Gesualdo I, Newman SJ, Kerr IM and Poli V. Mutational switch of an IL-6 response to an interferon-gamma-like response. Proc Natl Acad Sci U S A. 2002; 99(12):8043-8047.
163. Ho HH and Ivashkiv LB. Role of STAT3 in type I interferon responses. Negative regulation of STAT1-dependent inflammatory gene activation. J Biol Chem. 2006; 281(20):14111-14118.
164. Schindler C and Brutsaert S. Interferons as a paradigm for cytokine signal transduction. Cell Mol Life Sci. 1999; 55(12):1509-1522.
165. Sharpe AH, Wherry EJ, Ahmed R and Freeman GJ. The function of programmed cell death 1 and its ligands in regulating autoimmunity and infection. Nat Immunol. 2007; 8(3):239-245.
166. Sun Z, Yao Z, Liu S, Tang H and Yan X. An oligonucleotide decoy for Stat3 activates the immune response of macrophages to breast cancer. Immunobiology. 2006; 211(3):199-209.
167. Bottos A, Gotthardt D, Gill JW, Gattelli A, Frei A, Tzankov A, Sexl V, Wodnar-Filipowicz A and Hynes NE. Decreased NK-cell tumour immunosurveillance consequent to JAK inhibition enhances metastasis in breast cancer models. Nat Commun. 2016; 7:12258.
168. Sasmono RT, Oceandy D, Pollard JW, Tong W, Pavli P, Wainwright BJ, Ostrowski MC, Himes SR and Hume DA. A macrophage colony-stimulating factor receptor-green fluorescent protein transgene is expressed throughout the mononuclear phagocyte system of the mouse. Blood. 2003; 101(3):1155-1163.
169. MacDonald KP, Rowe V, Bofinger HM, Thomas R, Sasmono T, Hume DA and Hill GR. The colony-stimulating factor 1 receptor is expressed on dendritic cells during differentiation and regulates their expansion. Journal of immunology. 2005; 175(3):1399-1405.
170. Lyons TR, O'Brien J, Borges VF, Conklin MW, Keely PJ, Eliceiri KW, Marusyk A, Tan AC and Schedin P. Postpartum mammary gland involution drives progression of ductal carcinoma in situ through collagen and COX-2. Nat Med. 2011; 17(9):1109-1115.

171. Sabatier R, Finetti P, Mamessier E, Adelaide J, Chaffanet M, Ali HR, Viens P, Caldas C, Birnbaum D and Bertucci F. Prognostic and predictive value of PDL1 expression in breast cancer. Oncotarget. 2015; 6(7):5449-5464.
172. Steiner JL and Murphy EA. Importance of chemokine (CC-motif) ligand 2 in breast cancer. Int J Biol Markers. 2012; 27(3):e179-185.
173. Bohrer LRC, T.S.; Chuntova, P.; Brady, N.J.; Witschen, P.M.; Kemp, S.E.; Nelson, A.C.; Walcheck, B.; Schwertfeger, K.L. ADAM17 in tumor associated leukocytes regulates inflammatory mediators and promotes mammary tumor formation. Genes & Cancer. 2016; Advance Online Publications.
174. Villarino AV, Kanno Y, Ferdinand JR and O'Shea JJ. Mechanisms of Jak/STAT signaling in immunity and disease. Journal of immunology. 2015; 194(1):21-27.
175. Avalle L, Pensa S, Regis G, Novelli F and Poli V. STAT1 and STAT3 in tumorigenesis: A matter of balance. JAKSTAT. 2012; 1(2):65-72.
176. Hannesdottir L, Tymoszuk P, Parajuli N, Wasmer MH, Philipp S, Daschil N, Datta S, Koller JB, Tripp CH, Stoitzner P, Muller-Holzner E, Wiegers GJ, Sexl V, Villunger A and Doppler W. Lapatinib and doxorubicin enhance the Stat1-dependent antitumor immune response. Eur J Immunol. 2013; 43(10):2718-2729.
177. Tymoszuk P, Charoentong P, Hackl H, Spilka R, Muller-Holzner E, Trajanoski Z, Obrist P, Revillion F, Peyrat JP, Fiegl H and Doppler W. High STAT1 mRNA levels but not its tyrosine phosphorylation are associated with macrophage infiltration and bad prognosis in breast cancer. BMC Cancer. 2014; 14:257.
178. Kusmartsev S and Gabrilovich DI. STAT1 signaling regulates tumor-associated macrophage-mediated T cell deletion. Journal of immunology. 2005; 174(8):4880-4891.
179. Yu H, Lee H, Herrmann A, Buettner R and Jove R. Revisiting STAT3 signalling in cancer: new and unexpected biological functions. Nat Rev Cancer. 2014; 14(11):736-746.
180. Oh DY, Lee SH, Han SW, Kim MJ, Kim TM, Kim TY, Heo DS, Yuasa M, Yanagihara Y and Bang YJ. Phase I Study of OPB-31121, an Oral STAT3 Inhibitor, in Patients with Advanced Solid Tumors. Cancer Res Treat. 2015; 47(4):607-615.
181. Wong AL, Soo RA, Tan DS, Lee SC, Lim JS, Marban PC, Kong LR, Lee YJ, Wang LZ, Thuya WL, Soong R, Yee MQ, Chin TM, Cordero MT, Asuncion BR, Pang B, et al. Phase I and biomarker study of OPB-51602, a novel signal transducer and activator of transcription (STAT) 3 inhibitor, in patients with refractory solid malignancies. Ann Oncol. 2015; 26(5):998-1005.
182. Bendell JC, Hong DS, Burris HA, 3rd, Naing A, Jones SF, Falchook G, Bricmont P, Elekes A, Rock EP and Kurzrock R. Phase 1, open-label, dose-escalation, and pharmacokinetic study of STAT3 inhibitor OPB-31121 in subjects with advanced solid tumors. Cancer Chemother Pharmacol. 2014; 74(1):125-130.
183. Nagy N, Freudenberger T, Melchior-Becker A, Rock K, Ter Braak M, Jastrow H, Kinzig M, Lucke S, Suvorava T, Kojda G, Weber AA, Sorgel F, Levkau B, Ergun S and Fischer JW. Inhibition of hyaluronan synthesis accelerates murine atherosclerosis: novel insights into the role of hyaluronan synthesis. Circulation. 2010; 122(22):2313-2322.
184. Nagy N, Kaber G, Johnson PY, Gebe JA, Preisinger A, Falk BA, Sunkari VG, Gooden MD, Vernon RB, Bogdani M, Kuipers HF, Day AJ, Campbell DJ, Wight TN and

Bollyky PL. Inhibition of hyaluronan synthesis restores immune tolerance during autoimmune insulitis. The Journal of clinical investigation. 2015; 125(10):3928-3940.
185. Stern R, Asari AA and Sugahara KN. Hyaluronan fragments: an information-rich system. Eur J Cell Biol. 2006; 85(8):699-715.
186. Provenzano PP, Cuevas C, Chang AE, Goel VK, Von Hoff DD and Hingorani SR. Enzymatic targeting of the stroma ablates physical barriers to treatment of pancreatic ductal adenocarcinoma. Cancer Cell. 2012; 21(3):418-429.
187. Hingorani SR, Harris WP, Beck JT, Berdov BA, Wagner SA, Pshevlotsky EM, Tjulandin SA, Gladkov OA, Holcombe RF, Korn R, Raghunand N, Dychter S, Jiang P, Shepard HM and Devoe CE. Phase Ib Study of PEGylated Recombinant Human Hyaluronidase and Gemcitabine in Patients with Advanced Pancreatic Cancer. Clin Cancer Res. 2016; 22(12):2848-2854.
188. Durbin JE, Hackenmiller R, Simon MC and Levy DE. Targeted disruption of the mouse Stat1 gene results in compromised innate immunity to viral disease. Cell. 1996; 84(3):443-450.
189. Tymoszuk P, Evens H, Marzola V, Wachowicz K, Wasmer MH, Datta S, Muller-Holzner E, Fiegl H, Bock G, van Rooijen N, Theurl I and Doppler W. In situ proliferation contributes to accumulation of tumor-associated macrophages in spontaneous mammary tumors. Eur J Immunol. 2014; 44(8):2247-2262.
190. Intlekofer AM and Thompson CB. At the bench: preclinical rationale for CTLA-4 and PD-1 blockade as cancer immunotherapy. J Leukoc Biol. 2013; 94(1):25-39.
191. Jin HT, Ahmed R and Okazaki T. Role of PD-1 in regulating T-cell immunity. Curr Top Microbiol Immunol. 2011; 350:17-37.
192. Ghebeh H, Barhoush E, Tulbah A, Elkum N, Al-Tweigeri T and Dermime S. FOXP3+ Tregs and B7-H1+/PD-1+ T lymphocytes co-infiltrate the tumor tissues of high-risk breast cancer patients: Implication for immunotherapy. BMC Cancer. 2008; 8:57.
193. Chheda ZS, Sharma RK, Jala VR, Luster AD and Haribabu B. Chemoattractant Receptors BLT1 and CXCR3 Regulate Antitumor Immunity by Facilitating CD8+ T Cell Migration into Tumors. Journal of immunology. 2016; 197(5):2016-2026.
194. Pardoll DM. The blockade of immune checkpoints in cancer immunotherapy. Nat Rev Cancer. 2012; 12(4):252-264.
195. Caras I, Grigorescu A, Stavaru C, Radu DL, Mogos I, Szegli G and Salageanu A. Evidence for immune defects in breast and lung cancer patients. Cancer Immunol Immunother. 2004; 53(12):1146-1152.
196. Liu L, Mayes PA, Eastman S, Shi H, Yadavilli S, Zhang T, Yang J, Seestaller-Wehr L, Zhang SY, Hopson C, Tsvetkov L, Jing J, Zhang S, Smothers J and Hoos A. The BRAF and MEK Inhibitors Dabrafenib and Trametinib: Effects on Immune Function and in Combination with Immunomodulatory Antibodies Targeting PD-1, PD-L1, and CTLA-4. Clin Cancer Res. 2015; 21(7):1639-1651.
197. Aleskandarany MA, Agarwal D, Negm OH, Ball G, Elmouna A, Ashankyty I, Nuglozeh E, Fazaludeen MF, Diez-Rodriguez M, Nolan CC, Tighe PJ, Green AR, Ellis IO and Rakha EA. The prognostic significance of STAT3 in invasive breast cancer: analysis of protein and mRNA expressions in large cohorts. Breast Cancer Res Treat. 2016; 156(1):9-20.